INVESTIGATING THE NEPHROGENIC POTENTIAL OF MOUSE EMBRYONIC STEM CELLS AND THEIR DERIVATIVES

Thesis submitted in accordance with the requirements of the University of Liverpool for the degree of Doctor in Philosophy

by

Aleksandra Rak-Raszewska

October 2010

ABSTRACT

The kidneys are important organs that regulate the level of water and salts in the blood, produce hormones that help to control blood pressure, and maintain homeostasis of the organism by filtering waste products. Kidney disease can either be acute or chronic, the latter progressively worsening over time to become end stage renal disease (ESRD) – a stage when kidneys are non-functional. At present, the only treatment options for ESRD are transplantation or dialysis, which both have severe drawbacks in terms of morbidity, mortality and economic cost. Moreover, the incidence of ESRD is rising annually and an alternative therapy is needed. Therefore, in order to regenerate kidney tissue or prevent worsening of the kidney condition, a new therapy should be developed. One approach is to use embryonic stem cells.

CONTENTS

ACKNOWLEDGMENTS

I would like to thank my supervisors Dr. Patricia Murray, Prof. Dave Fernig and Prof. Jerry Turnbull and my assessors Dr. Bettina Wilm and Mr. Simon Kenny for their support during the project.

I would especially like to thank Dr. Patricia Murray, who showed lots of support in the lab - guided me during the project and allowed for freedom in choices of project directions, as well as outside the lab.

I would also like to thank Dr. Georges Lacaud, Patterson Institute for Cancer Research in Manchester, for kind gift of mESC Bry-GFP cell line.

I would like to thank Mathieu Unbekandt, University of Edinburgh, for providing the protocol for kidney re-integration, and all members of the KIDSTEM network, especially those located at University of Liverpool, for their support and constructive discussions during our lab meetings.

I would also like to thank the MolFun Marie Curie Grant for financial support of this work and the Alder Hey Children's Kidney Fund for financial support during final stages of my PhD.

I would especially like to thank my Parents who were the first to induce scientific interest in my heart, and supported me at all education levels and my husband, who put up well with my humours during writing up period of my PhD.

GLOSSARY

ADH – antidiuretic hormone

AFSC – amniotic fluid stem cells

AFP – alpha-fetoprotein

ASC – adult stem cells

ARF – acute renal failure

BFP – blue fluorescent protein

BO – branchio-oto syndrome

BOR – branchio-oto-renal syndrome

BSA – bovine serum albumin

BMP – bone morphogenic protein

BrdU – bromodeoxyuridine

Bry – Brachyury gene

6-CF – 6-carboxyfluorescein

CACUT – congenital anomalies of the kidney and the urinary tract

CCD – cortical collecting duct

DAPI – 4, 6-diamino-2-phenylindole dihydrochloride

DC – dicarboxylates

DMEM – Dulbecco's Modified Eagle Medium

E11.5 – embryonic day 11.5

EB / EBs – embryoid body / embryoid bodies

EDTA – ethylenediaminetetraacetic acid

ESC – embryonic stem cells

ESRD – end stage renal disease

FACS – fluorescence-activated cell sorting

FBS – foetal bovine serum

FCS – foetal calf serum

FGF – fibroblast growth factor

GAPDH – glyceraldehydes 3-phosphate dehydrogenase

GDNF – glial cell-line derived neurotrophic factor

GFP – green fluorescent protein

hESC – human embryonic stem cells

HBSS – Hanks' buffer saline solution

HSC – hematopoietic stem cells

ICM – inner cell mass

ISH – in situ hybridization

IM – intermediate mesoderm

IMCD – inner medullary collecting duct

IMDM – Iscove's modified Dulbecco's medium

iPSC – induced pluripotent stem cells

KSC – kidney stem cells

LIF – leukemia inhibitory factor

LM – lateral plate mesoderm

LTA – lotus tetragonolobus lectin

mESC – mouse embryonic stem cells

MEF – mouse embryonic fibroblasts

MM – metanephric mesenchyme

MSC – mesenchymal stem cells

NTC – no template control

OA – organic anions

OATs – organic anion transporters

OC – organic cations

OMCD – outer medullary collecting duct

ON – over night

PBS – phosphate buffer saline

PCR – polymerase chain reaction

PFA – paraformaldehyde

PM – paraxial mesoderm

PNArh – peanut agglutinin lectin rhodamine

QDs – quantum dots

RFP – red fluorescent protein

RT-PCR – reverse transcriptase polymerase chain reaction

sqRT-PCT – semi quantitative reverse transcriptase polymerase chain reaction

TAE – tris-acetate-EDTA

TBS – tris buffer saline

TGFβ – transforming growth factor beta

THP – tamm-horsfall glycoprotein

UB – ureteric bud

VD – vybrant dye

YFP – yellow fluorescent protein

Chapter 1: Introduction

The incidence of end stage renal disease (ESRD) continues to rise annually, causing an ever increasing burden on society in terms of both human suffering and economic costs. One of the major challenges of the 21st century will be to devise medical interventions that prevent the onset of ESRD. In most cases, ESRD develops from progressive worsening of chronic renal disease and available treatment options are dialysis and transplantations, although both have severe limitations in quality of life. However, there is usually a time-window of several years from the onset of mild/moderate kidney disease to the development of ESRD, which presents an opportunity to design therapies aimed at preventing disease progression by repairing or replacing damaged renal tissue. Such therapy could be directed with the use of stem cells. These cells are known to be pluri- or multipotent and can either differentiate into all cell types of the body or their differentiation potential is limited to a narrow range of cell types, respectively. However, in order to replace damaged kidney cells, the stem cells should be able to differentiate into at least 10 types of highly specialized cells present in the kidney, including the major cell types within the glomerulus and nephron tubules. Moreover, following transplantation, such cells should be competent to respond appropriately to the kidney environment and be able to function normally. Furthermore, following cell transplantation, the migration and incorporation of injected

cells into the host tissue should be easy to monitor. In other words, prior to transplantation, cells should be labelled with a marker that will allow distinguishing them from the host cells, without affecting cell behaviour.

Therefore, in this chapter, kidney development, kidney anatomy and the normal physiological functions of the kidney will be described; following which, the characteristics of different stem cell types with regard to their contribution to kidney regeneration, and the different methods of cell labelling will be introduced.

1.1 Kidney development

1.1.1 Overview of mammalian urogenital systems: pronephros, mesonephros and metanephros

During gastrulation of the mouse embryo, which occurs at embryonic day (E) 6.0-7.5, the three embryonic germ layers are generated; the ectoderm, mesoderm and endoderm (Rivera-Perez, 2005). Following migration through the primitive streak, the mesoderm forms three sub-populations, the lateral plate mesoderm, the paraxial mesoderm and the intermediate mesoderm. Each sub-population gives rise to a specific set of differentiated cell types. The lateral plate mesoderm gives rise to some of the extra-embryonic tissues and the somatic and splanchnic mesoderm. The somatic mesoderm, together with the ectoderm, forms somatopleura, while the splanchnic mesoderm, together with the endoderm, forms the splanchnopleura. The somatopleura give rise to the head musculature, pericardium, and the bones and muscles of limbs and outer body wall, while the splanchnopleura give rise to visceral smooth muscle, cardiac muscle, endocardium, vasculature and blood cells. The paraxial mesoderm gives rise to the remaining head tissues (bones and muscles) and the somites which develop into: 1) the sclerotome, which gives rise to the axial skeleton; 2) the myotome, which gives rise to the musculature of the back and ribs, and limbs; 3) the dermatome, which gives rise to the dermis. The

intermediate mesoderm gives rise to the urogenital system – the kidney and the gonads and their accompanying duct systems (Gilbert, 2006)

All three types of mesoderm, i.e., the lateral plate, the paraxial and the intermediate mesoderm, are present along the entire cranio-caudal axis of the embryo. The intermediate mesoderm gives rise to three separate excretory organs which develop from cranial to caudal end as follows: the pronephros, the mesonephros, and the metanephros. The first two stages (pro- and mesonephros) are simple temporary organs in mammalian development, while the metanephros is the permanent kidney (Fig.1.1).

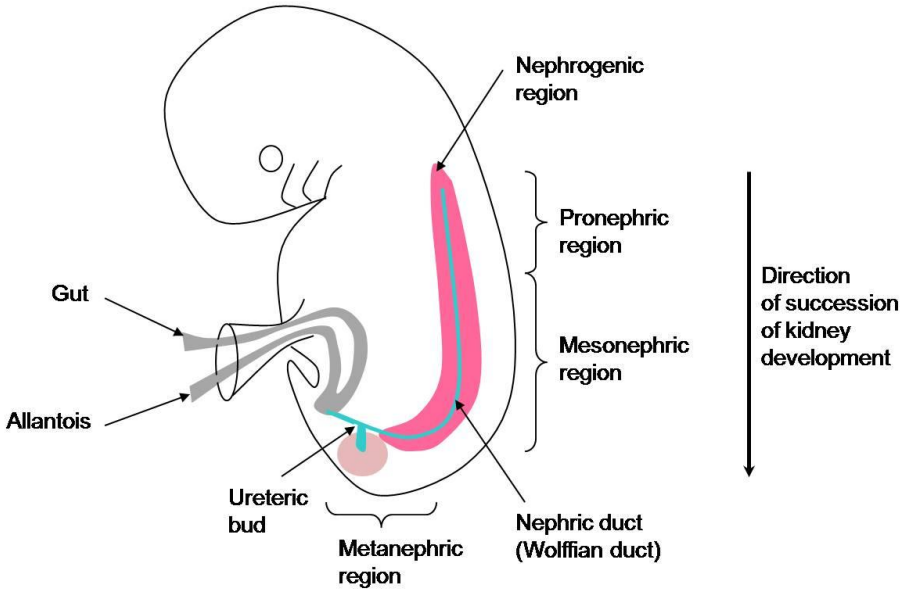

Figure 1.1 Schematic localization of the stages of kidney development in the mouse embryo. Mammalian kidneys develop through three stages: pronephros, mesonephros and metanephros (the permanent kidney), in cranio-caudal direction. Drawing prepared on the basis of Vize 2003 and Gilbert 2006.

The pronephric nephrotomes (single nephrons) are located between the lateral plate mesoderm and paraxial mesoderm. Nephrotomes open into the coelom with the rostrodorsal end equipped with cilia, and the caudal end opens into the cloaca. This is a very important organ for aquatic larvae. Fully-developed pronephroi are found in primitive fish, such as lampreys and hagfish. The pronephric kidney is present during the early development of the embryo, and is a temporary organ for teleost fish, amphibians, reptiles, birds and mammals (Saxen, 1987; Vize, 2003)As soon as the mesonephros develops, the pronephros disintegrates.

The mesonephros is the second stage of kidney development. It is the last stage of kidney organization in teleost fish and amphibians. It consists, therefore, of a large number of nephrons, each having an internal glomerulus, and excretory tubules divided into two kinds: proximal and distal tubules. The mesonephric kidney develops caudal to the pronephros (Vize, 2003).

The metanephros, also called the permanent kidney, is the third stage of kidney development for all amniotes. The elementary unit of the kidney is the nephron and each human kidney contains about $4x10^5$ to $1.2x10^6$ nephrons whereas in the rat kidney there are about $3\text{-}4x10^4$ nephrons (Brenner, 2000). The proximal end of the nephron begins with the renal corpuscle (the Bowman's capsule which surrounds the glomerulus) and continues with the proximal convoluted tubule, proximal straight tubule and thin descending limb, thin ascending limb and thick ascending

limb, all of which form the loop of Henle, and then the distal straight and convoluted tubule, the latter connecting to the collecting (Saxen, 1987; Vize, 1997)

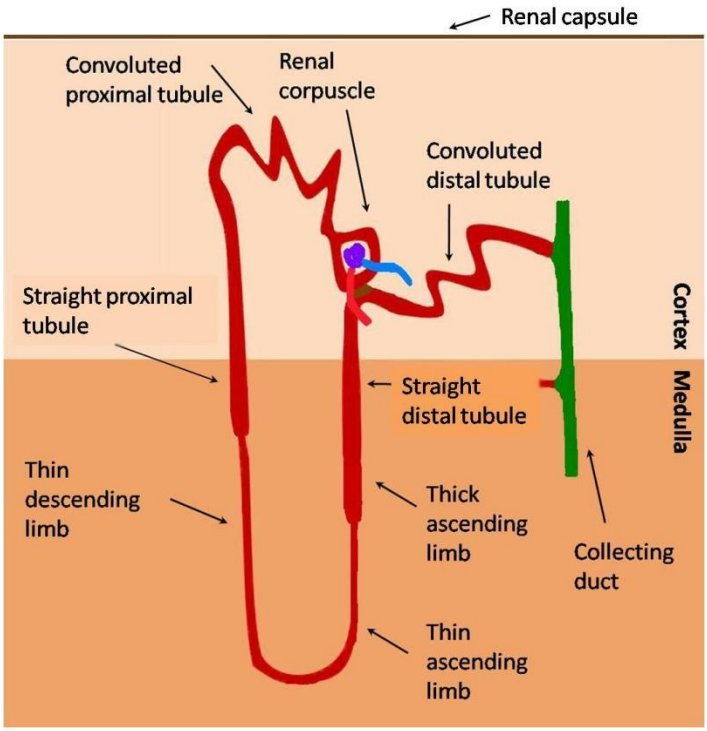

Figure 1.2 Diagram showing the structure of the nephron of the metanephric kidney. Drawing prepared on the basis of Brenner (2000).

1.1.2 Development of the metanephros

Metanephros development comprises of the following stages: development of metanephric mesenchyme, ureteric bud outgrowth and invasion into metanephric mesenchyme, metanephric mesenchyme induction and nephron formation.

Metanephric kidney development begins at E9.5 with the formation of the metanephric mesenchyme, an aggregate of cells derived from the caudal region of the intermediate mesoderm. Specification of the intermediate mesoderm is triggered by signals from the paraxial mesoderm and lateral plate mesoderm; most notably, mediolateral axis gradients of morphogens such as bone morphogenetic protein 4 (BMP4) with its higher concentration in lateral plate mesoderm, and the BMP antagonist, Noggin, with its higher concentration in paraxial mesoderm (Tonegawa, 1998). Later experiments on chicken gastrulae led by Mauch and co-workers (2000) showed that differentiation of intermediate mesoderm depends on signals from paraxial mesoderm (Mauch, 2000). It was also demonstrated that expression of Foxc1 and Foxc2 (fork-head/wing-helix transcription factors) in the paraxial mesoderm is important for somite formation and when they are down-regulated (i.e. in Foxc1-/- and Foxc2-/- mutants), the paraxial mesoderm is converted to an intermediate mesoderm fate (Wilm, 2004). Therefore, intermediate mesoderm differentiation is regulated by morphogens, especially by the BMP4 (James, 2005b) and other paraxial mesoderm-derived signals, and it is characterized by expression of *Lim1*, *Osr1* and *Pax2* genes (Boyle, 2006; Kobayashi, 2005a; Wang, 2005a). The intermediate mesoderm gives rise to the nephric duct and the metanephric mesoderm, the initial development of which is dependent upon the expression of *Wilms' tumour suppressor gene-1* (*Wt1*, a zinc finger transcription factor). In the absence of Wt1, metanephric mesenchyme cells

undergo apoptosis (Bouchard, 2002; Kreidberg, 1993; Pritchard-Jones, 1999; Vize, 2003) causing renal agenesis. However, some studies reported that *Wt1-/-* embryos can generate metanephric mesenchyme-derived renal cells in the presence of *Pax2*, *Six2* and GDNF RNAs (Donovan, 1999), suggesting that the main function of *Wt1* in the early stages of kidney development may be to induce expression of *Pax2*, *Six2* and *GDNF*, Fig. 1.3.

The metanephric mesenchyme induces the nephric duct to form the ureteric bud (UB). One of the signalling molecule required for ureteric bud outgrowth is GDNF (glial cell line derived neurotrophic factor), a member of the TGF β (transforming growth factor) family, which is secreted by the metanephric mesenchyme and binds to the receptor tyrosine kinase, *c-Ret*, which is expressed by the nephric duct epithelium and is required for the induction of ureteric bud outgrowth. *GDNF* expression by the metanephric mesenchyme requires combinatorial action of several transcriptional factors, such as *Osr1, Eya1, Pax2, Six1, Six2, Sall1, Hox11* genes, all of which cause kidney agenesis when not expressed. The genes network mentioned above and described in details below is presented on Fig. 1.3.

The *Osr1* (*Odd skipped related 1*) is a mouse homologue of *Odd1* in *Drosophila melanogaster*. *Osr1* is a zinc finger containing transcriptional factor which plays an essential role during mouse embryogenesis. It is first expressed in the intermediate mesoderm at E8.5, and later during kidney and limb development. *Osr1-/-* mutants show kidney agenesis at an early

stage of development and several heart defects (Stricker, 2006; Wang, 2005a). *Osr1* has a strong influence on kidney development, and was reported to up-regulate expression of other metanephric mesenchyme specific genes; for instance, *Osr1-/-* mutants do not show any expression of: *Eya1*, *Pax2*, *Six1*, *Sall1* and *GDNF*, and have a lower level of expression of *Lim1* (James, 2006).

The first gene to be down-stream of *Osr1* is *Eya1*. *Eya1* is a homologue of *Drosophila melanogaster eyes absent (eya)* gene and lack of its expression causes the syndromes, BOR (Branchio-oto-renal syndrome) and BO (Branchio-oto syndrome) with features of craniofacial abnormalities, hearing loss (BO) and kidney defects (BOR) (Xu, 1999). *Eya1* is expressed in the intermediate mesoderm at E8.5, in the uninduced metanephric mesenchyme (E10.5), and also in the condensed metanephric mesenchyme (E11.0) (Boyle, 2006). *Eya1-/-* mutants have no kidney rudiments or ureter and there is no outgrowth of the ureteric bud. Furthermore, in the *Eya1-/-* mutants the expression of *Six1* and *Pax2* genes was found to be decreased, suggesting that the expression of these genes is regulated by *Eya1* (Sajithlal, 2005).

The *Six1* gene is a homolog of *Drosophila melanogaster sine oculi (so)* gene. It is expressed in the uninduced metanephric mesenchyme (E10.5), in the induced metanephric mesenchyme (E11) and in the ureteric bud (E11.5) (Boyle, 2006; Xu, 1999; Xu, 2003). *Six1-/-* mutants show kidney

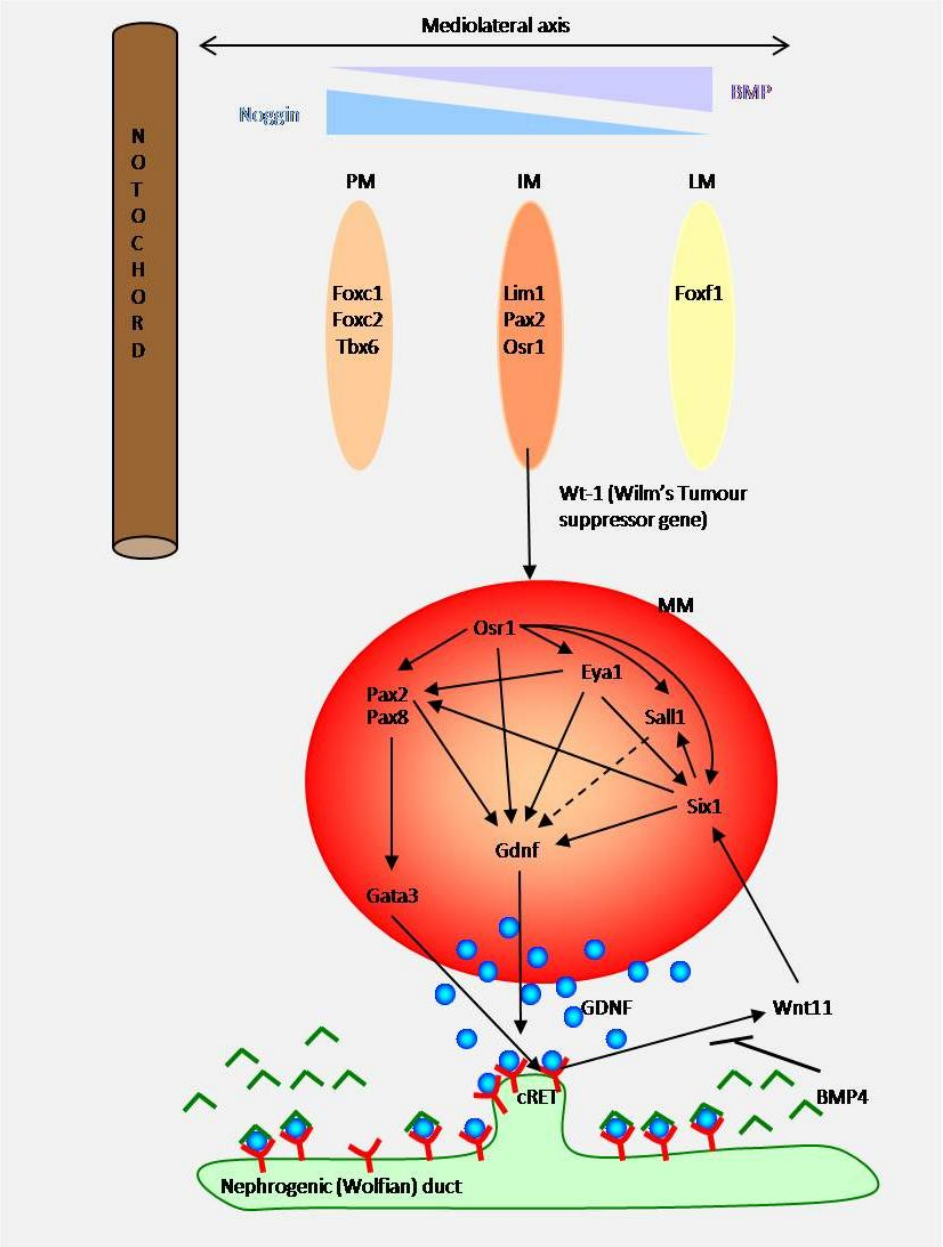

Figure 1.3 Schematic presenting a genes interaction network during metanephric mesenchyme induction. PM – paraxial mesoderm, IM – intermediate mesoderm, LM – lateral plate mesoderm

Table 1 Master regulators of kidney development.

E	Lim1	Wt1	Pax2	Eya1	GDNF	Sall1	Six1
7.5	+	+					
8.5	+	+	+	+			
9.5	+		+	+	+	+	
10.5	+	+	+	+	+	+	+
11.5	+	+	+	+	+	+	+

I, II, III, IV, IV, V, IV, IV

E – embryonic day; I – Shawlot 1999, II – Kobayashi 2003, III – Bouchard 2002, IV – Boyle 2006, V – Bouchard 2004.

agenesis and a lower level of *Pax2* and *Sall1* expression. In other words, *Six1* up-regulates *Pax2* and *Sall1* expression, but it is itself up-regulated by *Eya1* which did not show any changes in its expression level in the *Six1-/-* embryo. Another gene in the Six gene family, *Six2,* is up-regulated by *Six1* (Xu, 2003), but it is playing a similar role to Six1, although its expression is limited to the condensed metanephric mesenchyme (Kobayashi, 2008). Xu (2003) demonstrated that in *Six1-/-* mutants the *Six2* expression level is decreased.

Pax2 expression in the metanephric mesenchyme is upregulated by a few transcription factors but it is first detected in the intermediate mesoderm at E8.5, then in the uninduced metanephric mesenchyme at E10.5 and is strongly expressed in induced metanephric mesenchyme at E11.0, and also in the ureteric bud from E9.5 onwards (Boyle, 2006). Embryonic *Pax2-/-* mutants extend the nephric duct normally, but no ureteric bud formation occurs and no metanephroi form. Another member of the *Pax* gene family

– *Pax8*, also plays a role in kidney development. *Pax8* embryonic mutants seem to have a normal fully-developed excretory system but die because of a defect in thyroid gland development. Interestingly, in double mutants (*Pax2-/- Pax8-/-)*, kidney development fails at the pronephros stage (Bouchard, 2002). Therefore, *Pax2* and *Pax8* have an important role in directing intermediate mesoderm cells to a renal cell fate. *Pax2* and *Pax8* are also important for *Gata3* expression as *Pax2-/-; Pax8-/-* mutants do not show any *Gata3* expression. Thus, *Gata3* seems to have a specific influence on kidney development, especially in terms of CACUT (congenital anomalies of the kidney and the urinary tract) diseases. It was reported by Grote (2005), that in *Gata3-/-* mutants, the c-Ret receptor (tyrosine kinase) and Wnt11 expression is lost, which leads to defects in nephric duct development such as ectopia of the ureteric bud and/or multiple disorganized ducts (Grote, 2005).

The *Sall1 (Sal-like1)* gene is a mouse homologue of *Drosophila melanogaster Sal1* gene. *Sall1* gene is expressed in the nephric duct and in the mesonephros at E9.5, in the uninduced metanephric mesenchyme at E10.5 and in the induced metanephric mesenchyme at E11.0 (Boyle, 2006). It is upregulated by Six1 (Yu, 2004). *Sall1* +/- mutants shows Townes-Brocks syndrome which is characterized by dysplastic ears, preaxial polydactyly and kidney and heart anomalies (Takasato, 2004). *Sall1-/-* deficient mutants die due to kidney agenesis in the perinatal period. These mutants fail in the ureteric bud outgrowth and as a consequence, the

metanephric mesenchyme remains uninduced and undergoes apoptosis (Nishinakamura, 2001; Takasato, 2004). Thus, *Sall1* is important for ureteric bud formation in kidney development.

The paralogous group of *Hox11* genes contains *Hoxa11, Hoxc11 and Hoxd11* and play an important role during kidney development through the regulation of *GDNF* expression. These genes are expressed at E10.5 in uninduced metanephric mesenchyme and at E11.0 in metanephric mesenchymal stromal cells (Boyle, 2006). Single mutations in *Hox11* genes (*Hoxa11-/-* or *Hoxd11-/-*) show discernible kidney abnormalities; double mutants (*Hoxa11-/- Hoxd11-/-*) show kidney hypoplasia; removal of the *Hoxc11* gene results in complete loss of metanephric kidney induction. Furthermore, although *Pax2* expression is normal in triple mutants (*Hoxa11-/- Hoxd11-/- Hoxc11-/-*) there is no *GDNF* expression and the ureteric bud does not form (Wellik, 2002).

Therefore, this large complicated GDNF stimulation network of at least 7 groups of genes is playing an important role in inducing renal development by stimulating GDNF secretion and therefore preventing renal agenesis. However, apart from positive inducers of *GDNF* expression, several transcription factors are present to repress overexpression and/or oversecretion of GDNF. These factors are: *Foxc1*, *Foxc2*, *Slit2* and its receptor *Robo2*, and *BMP4*. *Foxc1* and *Foxc2* are expressed in the paraxial mesoderm at E8.5 and in uninduced metanephric mesenchyme at E10.5, while *Slit2/Robo2* are expressed in the nephric duct and in the metanephric

mesenchyme, respectively. These proteins negatively regulate GDNF secretion, probably by affecting Eya1 and/or Pax2 translation or their activity in the anterior part of the metanephric mesenchyme as suggested by Grieshammer and co-workers (Grieshammer, 2004; Kume, 2000b). On the other hand, BMP4 acts indirectly as an inhibitor of budding after GDNF has bound to the c-Ret receptor (Ichikawa, 2002), and therefore blocks further signalling by Wnt11 expression (Fig.1.3) (Vize, 2003). Moreover, reduced expression of BMP4 in *BMP4*+/- heterozygous mice results in polycystic kidneys (Vize, 2003). Therefore, all these signals are preventing overexpression or oversecretion of GDNF are playing an important role in avoiding ectopic ureteric bud outgrowth, thus helping to avoid the formation of a double ureter as well as polycystic kidney development.

Once the UB is induced by GDNF to grow out from the Wolfian duct in an appropriate site, it extends to reach metanephric mesenchyme (MM). When the UB invades the MM, the cells at the bud tip start to secrete FGF2 and BMP7 to prevent the metanephric mesenchyme from undergoing apoptosis (Dudley, 1999). GDNF also induces the cells at the tip of the ureteric bud to express *Wnt11*, which is required for ureteric bud branching (Vize, 2003). In *Wnt11-/-* mutants, kidney hypoplasia was observed, with the kidneys appearing much smaller in the mutants compared to the wild type (Majumdar, 2003). Other signals from the tips of the branching ureteric bud induce the areas of adjacent metanephric mesenchyme to

aggregate and undergo a mesenchymal–to–epithelial transition. The first signal that makes metanephric mesenchymal cells to condense around the tip of the UB is LIF (leukaemia inhibitory factor) (Barasch, 1999). Under LIF action, cells up-regulate *E-cadherin*, *Pax2*, *Wnt9B* and *Wnt4*, triggering nephron formation (Barasch, 1999; Park, 2007). *Wnt4* plays a crucial role in nephron formation; in *Wnt4-/-* mutants the mesenchyme condenses but does not form an epithelium (Stark, 1994). Although many transcriptional factors involved in the initial differentiation of the metanephric mesenchyme have been identified, it is as yet unclear how the

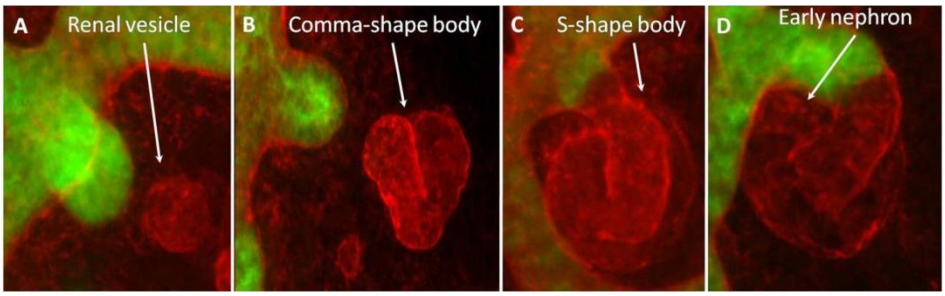

Figure 1.4 Fluorescent microscope photomicrograph presenting stages of nephron formation *ex vivo*. Calbindin (green) staining of UB and laminin (red) staining of the basement membrane of developing nephron in cultured kidney: A) Renal vesicle; B) Comma-shape body; C) S-shape body; D) Early nephron.

terminal nephron differentiation is regulated. However, a few steps of nephron formation have been identified:

- condensation of mesenchymal cells adjacent to the bud tips into aggregates;
- cavitations of these aggregates to form the renal vesicles;
- elongation to comma- and then S-shaped tubules;
- the production of new epithelial cells and further elongation and maturation to form a functional nephron (Fig. 1.4)

In general, during kidney development the ureteric bud forms the ureter and collecting duct system of the mature kidney whereas the metanephric mesenchyme gives rise to the nephrons from the renal corpuscle to the distal tubule (Saxen, 1987) (Fig. 1.2).

1.2 Anatomy of the kidney

Kidneys are bean-shape organs that are located symmetrically on both sides of the body in the retroperitoneal space (Fig. 1.1A). Kidneys are surrounded by connective tissue – the capsule, and have a few characteristic regions that can be easily distinguished on a coronal section (Fig.1.5B). The outer part is the cortex, which contains many capillaries and has reddish-brown colour appearance, whereas the inner part – the medulla is composed of renal pyramids separated by renal columns. Renal pyramids connect at the renal papilla to form a minor calyx. Minor calyces then merge to form a major calyx, and a few major calyces connect together to form the pelvis – which contains the entrance to the ureter. The

ureter connects the kidney with the bladder – an elastic sack that collects the urine and under pressure, allows it to drain by the urethra (Fox, 2008).

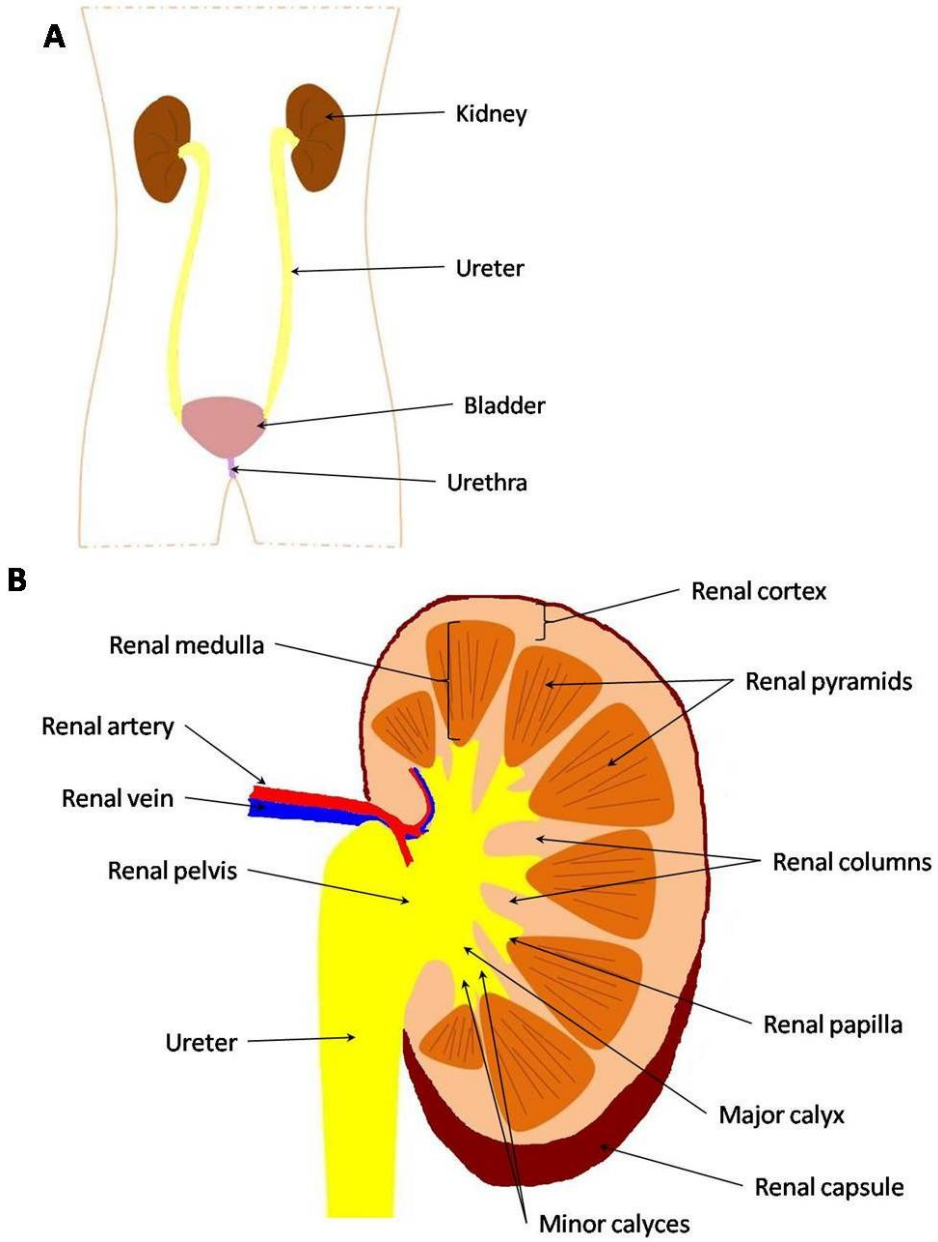

Figure 1.5 Diagram showing location of human kidney (A) and its structure (B). Drawings prepared on the basis of Brenner 2000.

The kidney has two major units, which differ in their origin; the nephron, which develops from the metanephric mesenchyme, and the collecting duct, which develops from the ureteric bud. Both are surrounded by interstitial cells and loose extracellular matrix.

1.2.1 Cell types of the nephron

The smallest functional unit of the kidney is the nephron. It consists of the glomerulus, proximal convoluted tubule, proximal straight tubule, loop of Henle, which consists of thin descending limb, thin and thick
ascending limbs, and the straight and convoluted distal tubule which is connected to the collecting duct (Fox, 2008; Valtin, 1995) (Fig.1.2). All parts of the nephron are characterized by different cell types that are specialized to participate in various functions. Apart from the large number of nephrons and blood vessel networks, kidneys also have a lymphatic and nerve system.

The renal corpuscle is composed of the glomerulus and Bowman's capsule. The glomerulus is a capillary network that supplies the blood via the afferent arteriole and leads away filtered blood via the efferent arteriole. The glomerular capillaries are composed of endothelial cells which line the inner walls of all capillaries thus forming the glomerular basement membrane with overlying podocyte cells (Fig.1.6B). The podocytes represent the visceral layer of the glomerular capsule; whereas the parietal

layer of the glomerular capsule is formed by simple epithelial cells. Podocytes are the biggest cells within the renal corpuscle, and are characterised by their long cytoplasmic processes, which divide into many individual foot processes (Fig.1.7 C). The space between the capillaries is filled with mesangial cells, which build a glomerular matrix – a structural support for the glomerular capillaries. The space between the visceral and the parietal wall of the Bowman's capsule is forming a free area where the ultrafiltrate is collected (Brenner, 2000; Fox, 2008) (Fig. 1.7 B).

At the urinary pole of the glomerulus, the proximal tubule of the nephron begins. It consists of two parts: convoluted and straight proximal tubules, which are divided onto three segments, S1, S2 and S3. The first segment (S1) includes two thirds of the convoluted tubule and cells are characterised by having a very tall brush border, many big mitochondria and many well-developed lysosomes. The second segment (S2) consists of the rest of the convoluted tubule and the initial part of the straight tubule. Cells of this segment possess a medium length brush-border, smaller mitochondria and numerous large lysosomes. The third segment (S3) includes the remaining part of the straight tubule. The brush border length in cells of this segment varies between species; however cells tend to have small and randomly distributed mitochondria and small lysosomes (Brenner, 2000). In the kidney cross section, these tubules have a size similar to distal tubules but due to the brush border, the lumen may not be

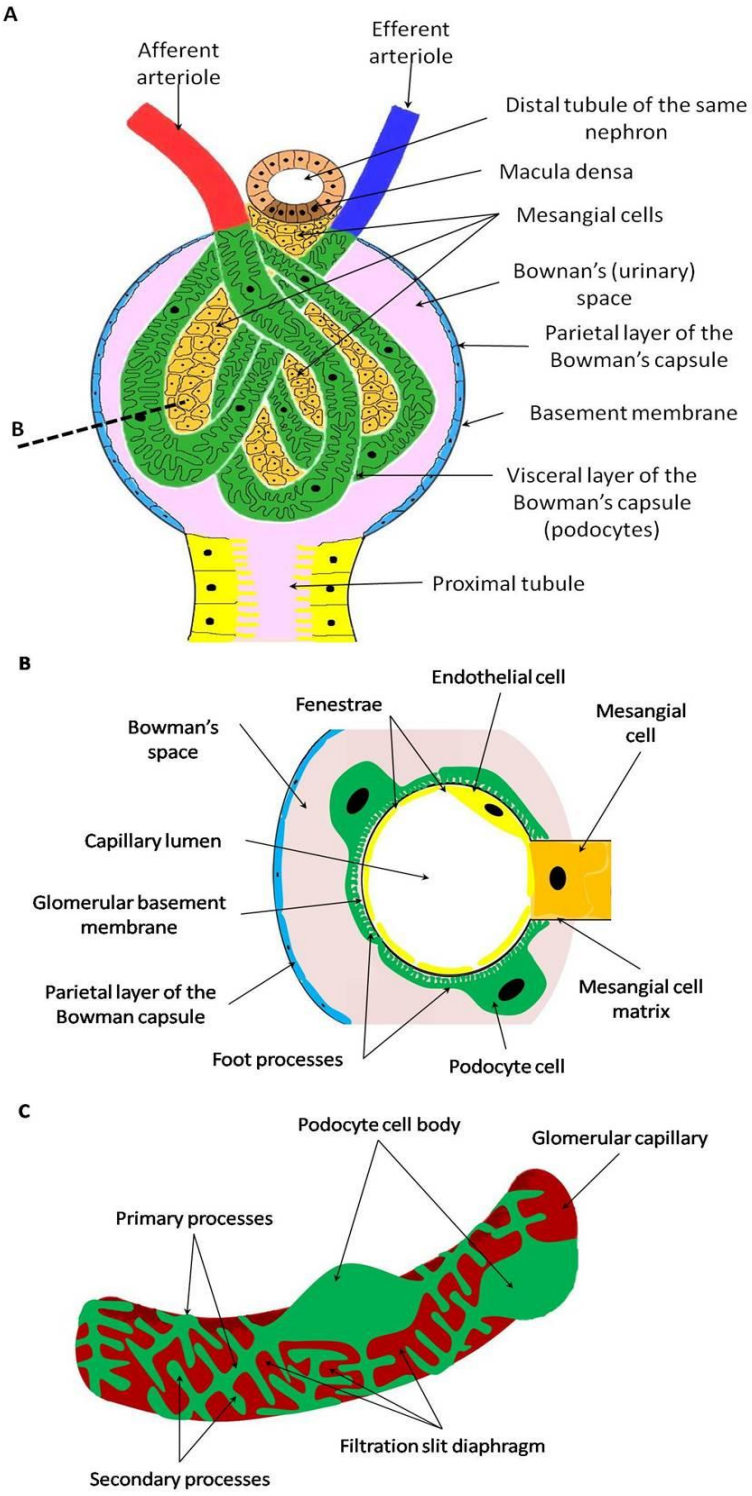

Figure 1.6 Schematic structure of the glomerulus (A), schematic section through glomerular capillary (B) and interactions between podocytes (C). Drawings prepared on the basis of Brenner (2000).

visible or is very small in diameter and irregular in shape (Fig. 1.7 C). At the end of the proximal tubule, the thin descending limb of the loop of Henle begins the third part of the nephron.

The epithelium of the thin descending and thin ascending limbs of the loop of Henle is flatter than in the proximal tubule and lacks microvilli. The epithelium of the thick ascending limb of the loop of Henle is thicker in comparison to the thin limbs and is more similar to distal tubules, and

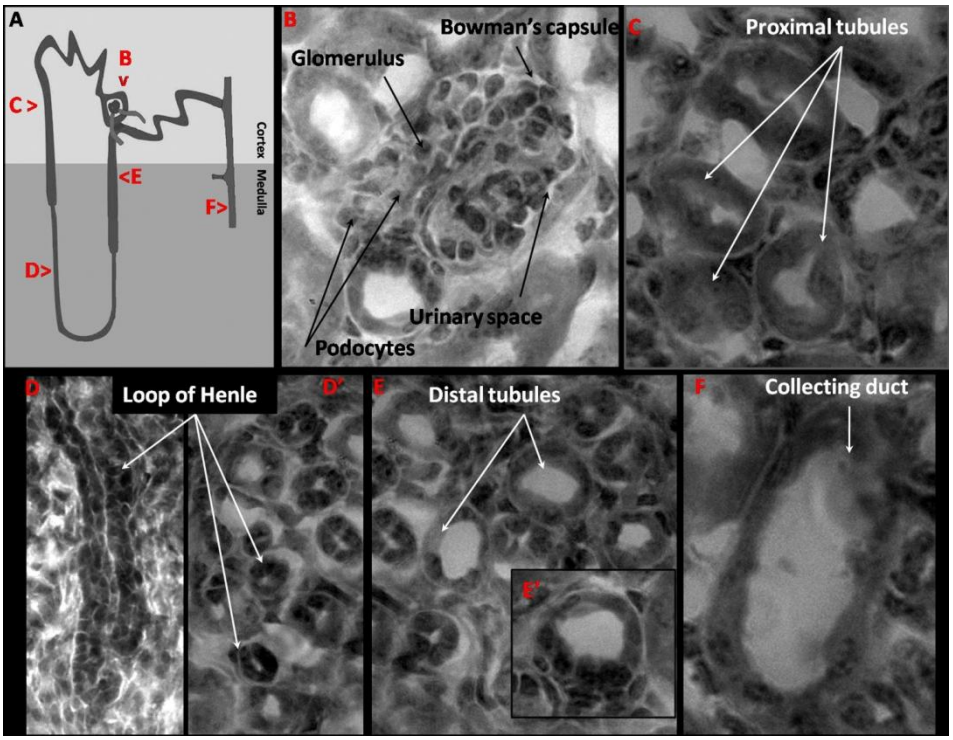

Figure 1.7 Localisation and structure of the different parts of the nephron. A) Schematic location of the nephron parts; B-F) haematoxylin and eosin staining of a cross section of the adult kidney: B – glomerulus, C – proximal tubule, D – hairpin of the loop of Henle, D' – thin limbs of the loop of Henle, E – distal tubule, E' – the macula densa cells in the distal tubule, F – collecting duct.

therefore, is sometimes considered as a part of the straight distal tubule (Brenner, 2000). In the cross section of the kidney it is possible to observe the hairpin of the loop of Henle as well as the easily distinguishable thin limbs of the loop of Henle, characterised by their very small diameter (Fig 1.7 D and D', respectively).

The distal tubule consists of the straight ascending tubule, the specialised region of the macula densa and the convoluted tubule. The straight tubule cells do not have microvilli but most cells possess one or two cilia. These cells have large elongated mitochondria and from the scanning electron microscopy, some cells have a rough surface pattern and some a smooth-surface pattern (Brenner, 2000). The straight distal tubule ends at the specialised region of the macula densa, which is adjacent to the hilium of the glomerulus. Macula densa cells are taller than other cells of the distal tubule, and have an apically located nucleus (Fig. 1.7 E'). At some distance behind the macula densa, the convoluted tubule begins. These cells are very similar to those of the straight distal tubule but are taller, have very small microvilli and long cilia as well as numerous mitochondria (Brenner, 2000). The distal tubules have a similar diameter size as proximal tubules but the distal tubule lumen is clear and wide unlike in the proximal tubules (Fig. 1.7 E). The distal tubules constitute the last part of the nephron and connect to the collecting duct.

1.2.2 Cell types of the collecting duct

The collecting ducts can be divided into three parts, depending on their location: the cortical collecting duct (CCD), which is located in the renal cortex, the outer medullary collecting duct (OMCD) located in the outer medulla and inner medullary collecting duct (IMCD) which is located in the inner medulla. These three segments consist only of two cell types: principal cells (light cells) and intercalated cells (dark cells), but the contribution of those cells differ in each segment. The principal cells have a light cytoplasm staining and fewer organelles whereas intercalated cells have more organelles and numerous cytoplasmic ribosomes which cause the cytoplasm to be more darkly stained. About one third of the CCD and OMCD is built by intercalated cells whereas in the IMCD, intercalated cells constitute only about 10% of all cells. As the duct extends, the diameter expands, from about 10μm at the beginning of the collecting duct to up to 50μm at the papillary tip (Brenner, 2000). The collecting duct has a distinctively wider diameter than the nephron tubules (Fig.1.7 F).

1.3 Kidney functions

The kidneys play an important role in maintaining the homeostasis of the organism by producing hormones regulating the blood pressure, volume of body fluids, performing selective reabsorption of important molecules and excreting toxins via selective secretion. During all these processes the body

metabolites are transferred into the urine. This liquid is first formed in the Bowman's capsule as an ultrafiltrate and undergoes modifications during the flow through different nephron parts and down the collecting duct to become urine.

1.3.1 Renal corpuscle

In the glomerulus, the difference in the diameter between the afferent arteriole (bigger diameter) and the efferent arteriole (smaller diameter), results in raised intraglomerular pressure, which causes many blood components to be filtered through the permselective vessels walls and enter Bowman's space to form the ultrafiltrate (Brenner, 2000). The capillary walls are generated by a triple filtration barrier, the fenestrae, glomerular basement membrane, and podocyte foot processes. The fenestrae are small gaps in the endothelial cell layer, which form a barrier for blood cells such as erythrocytes and leukocytes. The second filtration barrier is determined by the glomerular basement membrane which is a barrier for positively charged plasma macromolecules, and the third filtration barrier is provided by the podocyte foot processes which form a barrier for protein (Brenner, 2000). Therefore, the ultrafiltrate is mainly composed of plasma water and its non-protein constituents (glucose, negatively charged micromolecules). Such liquid enters the proximal tubule.

The role of the glomerulus does not end at ultrafiltrate production. Due to close contact of the glomerulus with its own distal tubule region of the

macula densa, there is a tubulo-glomerular feedback loop that regulates the blood pressure and water balance through the rennin-angiotensin-aldosterone system (Valtin, 1995). Depending on the urate flow (low) through the distal tubule, the macula densa cells produce nitric oxide that induces granular cells of the glomerulus to produce renin (high). Renin induces angiotensin production which stimulates the blood vessel walls to contract and increase the blood pressure. Moreover, angiotensin induces aldosterone production which increases the reabsorption of water and salts. This increases the volume of the body fluids which results in the increase of the blood pressure as well (Brenner, 2000; Valtin, 1995).

1.3.2 Proximal tubule

The first part of the proximal tubule, the convoluted proximal tubule, takes part in active and passive reabsorption of water, organic solutes such as glucose and amino acids, and electrolytes: Na^+, K^+, Ca^{2+}, Cl^-, HCO_3^-, PO_4^{3}, whereas the straight proximal tubule is mainly reabsorbing water and Na^+ ions. The transport of the aforementioned substances can be either active, taking place against the electrochemical potential gradient via Na^+/K^+ ATP pumps, Na^+-cotransporters (glucose) and specialized transporters (glucose), or passive, taking place down the electrochemical potential gradient (urea). Small amounts of proteins that leaked into the ultrafiltrate at the

glomerulus are reabsorbed by endocytosis (Brenner, 2000; Valtin, 1995) (Fig. 1.8).

Another function of the proximal tubule is secretion of endo- and exogenous toxins (such as drugs in the body that form weak acids (anions) and weak bases (cations)), which could not be filtered at the glomerulus due to their being bound to proteins. The secretion mechanism involves active transport with use of specific transporters, usually related to Na^+-cotransporters (Brenner, 2000; Valtin, 1995).

1.3.3 Loop of Henle

The first part of the loop of Henle, the thin descending limb, is the only one permeable to water, and this is where the water is mainly reabsorbed. There is also secretion of urea, Na^+ and Cl^- ions observed, and it is an effect of passive transport down the gradient. The thin ascending limb is passively reabsorbing Na^+ and Cl^- ions, whereas the thick ascending limb is actively reabsorbing Na^+ ions through Na^+/K^+ ATP pumps and Na:K:2Cl cotransporters, that allows the transport of one ion of Na^+ and K^+ each into the cell and 2 ions of Cl^- (Brenner, 2000; Valtin, 1995) (Fig.1.8).

1.3.4 Distal tubule

The distal tubule has two distinct regions in regard to water and sodium ion transport. The early distal tubule is characterized by passive transport

(reabsorption) of Na^+ and Cl^-. This part is, similarly to the most distal part of the loop of Henle, not permeable to water. In the convoluted part

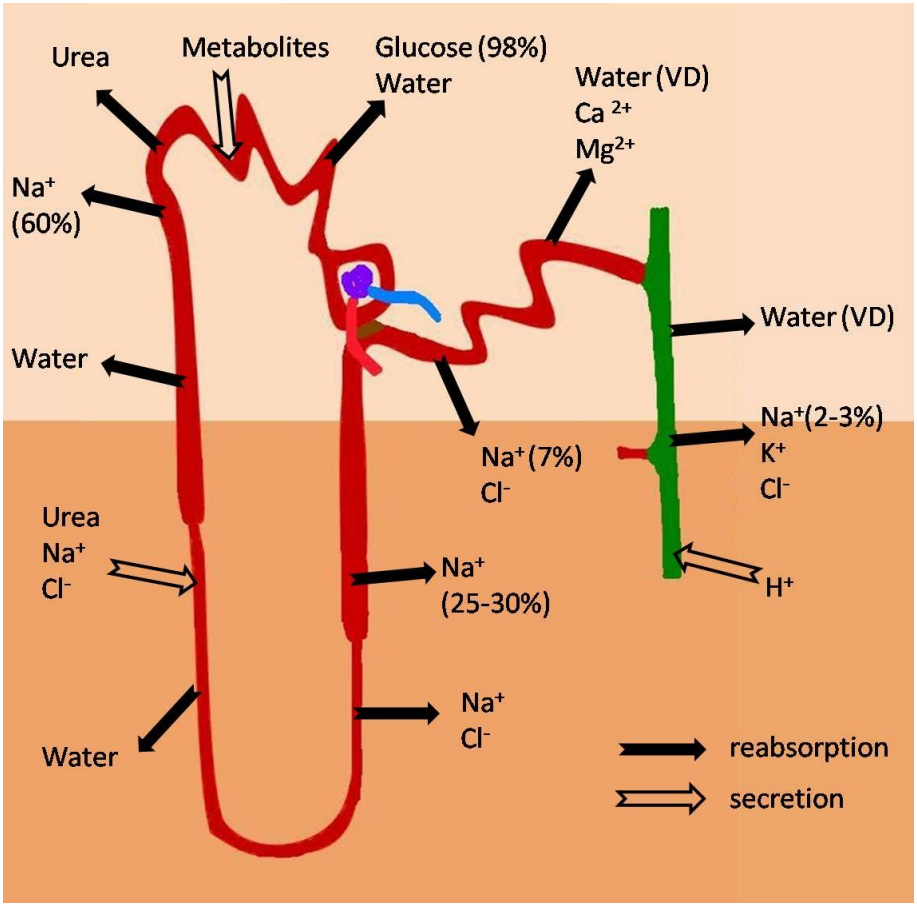

Figure 1.8 Schematic presenting functions of the nephron (red) and the collecting duct (green). The ultrafiltrate produced by the glomerulus is undergoing changes during the process of urine production. In the proximal tubule about 98% of the glucose is reabsorbed as well about 60% of the Na^+ ions and quite high amounts of water and urea. In the proximal tubule, secretion of different metabolites takes place. In the loop of Henle the urea and Na^+ and Cl^- ions are secreted to be reabsorbed in the later parts of the loop of Henle. In the late distal tubule the active reabsorption of Ca^{2+} and Mg^{2+} is taking place and vasopressin dependent (VD) reabsorption of water, the latter is similar to the action taken by collecting duct.

of the distal tubule the reabsorption of Na^+ ions is passive, but this part is presenting active reabsorption of the Mg^{2+} and Ca^{2+} ions. The water reabsorption/secretion depends on the presence/absence of vasopressin, the antidiuretic hormone (ADH) secreted by the hypothalamus. This hormonal regulation of body fluids ensures the right water balance (Brenner, 2000; Valtin, 1995) (Fig.1.8).

1.3.5 Collecting duct

The collecting duct is similar in its functions to the late distal tubule. The principal cells are taking part in the passive reabsorption of Na^+ and K^+ ions and H^+ ions secretion. These cells of the collecting duct are also vasopressin sensitive to regulate the reabsorption/secretion of water depending on the actual fluid level in the body (Brenner, 2000; Valtin, 1995) (Fig. 1.8).

1.4 Stem cells in kidney regeneration

Stem cells are unspecialised cells that have the ability to self-renew, and under the appropriate conditions, differentiate to generate a range of specialised cell types. Depending on their source, stem cells are classified as either adult stem cells or embryonic stem cells.

1.4.1 Adult stem cells

Although adult stem cells (ASC) are present in many adult tissues: skin, hair follicle, corneal epithelium, respiratory system, dental pulp, digestive system, liver, salivary gland, kidney, mammary gland, prostate gland, endometrium, bone marrow, adipose tissue, pituitary gland, and brain (Diaz-Flores Jr. L., 2006), they are not very common and their location is restricted to specialized regions – *the niches* (Oliver, 2004). They are able to self-renew and keep their plasticity for long periods. Most adult stem cells are thought to be either unipotent, meaning that they can give rise to just one cell type, or multipotent, meaning they can give rise to a limited range of differentiated cell types. Within ASC, several types can be distinguished, including kidney stem cells (KSC) and bone marrow derived stem cells: mesenchymal stem cells (MSC) and hematopoietic stem cells (HSC), and amniotic fluid stem cells (AFSC).

Kidney stem cells

Localization of embryonic kidney progenitor cells within metanephroi (Oliver, 2002) gave hope to find adult kidney stem cells. Shortly afterwards, it was reported that adult stem cells were localized within the adult mouse kidney papilla and identified by BrdU staining. A population of these cells were able to divide and generate tubular epithelial cells in response to ischemic injury (Oliver, 2004). Adult kidney stem cells or so-called multipotent renal progenitor cells were isolated from mouse kidney

and characterized by Gupta et al. (2006) as cells able to self-renew and expressing adult stem cell pluripotency markers: Oct4 and Pax2. These cells, supported by specific nephrogenic induction medium, were able to form cell aggregates *in vitro.* Undifferentiated cells injected into rat kidneys were able to integrate into injured tubules (Gupta, 2006). A tubular integration into rat embryonic kidneys *ex vivo* was obtained with use of BrdU positive cells isolated from adult rats' kidneys (Maeshima, 2006) and with Sca-1^{+}Lin^{-} cells from adult mouse kidney (Dekel, 2006b). It was also possible to isolate human adult kidney stem cells using CD133 antibodies. These cells were Pax2 positive and underwent tubulogenesis following subcutaneous implantation into SCID mice (Bussolati, 2005). Following Bussolati's findings, Romagnani's group have isolated and characterised multipotent progenitor cells (CD133+CD24+) (Sagrinati, 2006), and demonstrated that these cells are able to regenerate injured podocytes and tubules (Ronconi, 2009).

Although scientists have been successful in isolating adult kidney stem/progenitor cells and proved their potential to integrate into damaged kidney, most of these cells only integrate into tubules and form only tubular-like structures and only one type was shown to integrate into glomeruli (Ronconi, 2009). Nevertheless, KSC could be a good source of cells for stem cell therapies as they can be derived from the patient and hence the risk of graft rejection would be minimised. Moreover, there would be no need for administration of immunosuppressants. However,

KSC-based therapies might not be a feasible approach for many patients because if large proportion of renal tissue is already damaged, it might not be possible to isolate stem cells from biopsy samples. Furthermore, it is important to note that all of the human KSC lines that have been isolated to date have been derived from the unaffected areas of kidney containing malignant tumours. Therefore, it is possible that these KCS are actually tumour cells that have migrated from the main tumour mass. Therefore, other stem cell types are under investigation.

Bone marrow-derived stem cells

Adult bone marrow cells contain two populations of stem cells: mesenchymal stem cells (MSC) and hematopoietic stem cells (HSC). Both have been tested in the context of their potential to promote renal repair after injury. Renal repair was demonstrated after transplantation of mouse male bone marrow cells into mouse female kidneys; however it was not clear if the beneficial effect came from MSC or HSC (Poulsom, 2001). Later, it was shown that murine HSC ($Rh^{lo}Lin^{-}Sca1^{+}c\text{-}kit^{+}$ and $CD45^{+}$ - hematopoietic marker) transplanted into mouse kidneys after ischemic/reperfusion injury can contribute to renal tubular regeneration (Lin, 2003) and possibly improve renal function by repopulation of glomerular podocytes in a mouse model of Alport Syndrome (Prodromidi, 2006). However, in contrast with this study, Dekel showed HSC to have

only vasculogenic potential and could not contribute to the formation of renal tubules (Dekel, 2006a).

MSC ($CD45^-$) were shown to promote tubular regeneration in acute renal failure (ARF) in a mouse model of cisplatin nephrotoxity (Morigi, 2004) and following the injection of hypertonic glycerol into muscle to induce rhabdomyolysis (Herrera, 2004). MSC were shown to protect animals from renal function impairment and prolong their lifespan (Morigi, 2010) probably by their paracrine effect, as they do not integrate into damaged tubules (Humphreys, 2008; Kunter, 2007).

Bone marrow cells from transgenic rats carrying an EGFP cassette (enhanced green fluorescent protein) transplanted into rats with induced glomerulonephritis showed integration into host tissue: it was reported that 60-70% of intraglomerularly integrated cells were of MSC origin ($CD45^-$), while the remainder were of HSC ($CD45^+$) origin. Therefore, MSC cells can also produce renal epithelial and glomerular mesanglial cells, but not podocyte cells (Ito, 2001). However, although in the short term post injury, MSC ameliorated renal functions, in the longer term, MSC that integrated into glomeruli maldifferentiated into adipocytes (Kunter, 2007).

In one study, it has been shown that in the right environment, MSC do have the ability to be reprogrammed to generate renal cell types. Yokoo and co-workers showed that in a combination of whole-embryo culture followed by organ culture, human MSC ($CD105^+$, $CD166^+$, $CD29^+$, $CD44^+$

and $CD14^-$, $CD34^-$, $CD45^-$) were able to generate functional nephrons when injected into a developing rat embryo *ex vivo* (Yokoo, 2005).

The advantages of using mesenchymal stem cells are that these stem cells can be derived from patients, therefore minimizing the possibility of transplant immunorejection. However, although MSC were shown to generate all kidney cell types if introduced into the embryo at the site of the presumptive kidney (Yokoo, 2005) it would not be possible to perform this procedure with human embryos due to ethical issues. Moreover, although MSC promoted recovery from ARF, this seemed to be due to paracrine effects as they have limited integration abilities. Also, despite integration into glomeruli, these cells underwent maldifferentiation (Kunter, 2007) and therefore, although they could have the potential for promoting renal repair, they would not be able to replace lost nephrons, and would thus be of limited benefit in the treatment of chronic disease.

Amniotic fluid stem cells

A new stem cell source has been confirmed by the Hengstschlager group (Prusa, 2003), who have demonstrated that stem cells expressing Oct-4, a marker of embryonic stem cells and embryonic germ cells, could be isolated from amniotic fluid. Cells obtained from the amniotic cavity are heterogeneous; apart from showing Oct4 expression, they are also positive for mesenchymal stem cell markers such as CD44, CD29, CD105, but are negative for hematopoietic stem cell markers CD45 and CD34

(Bossolasco, 2006; De Coppi, 2007; Tsai, 2004). AFSC have the capacity to differentiate into adipocytes, osteocytes, neuronal, myogenic, endothelial and hepatic cells (Bossolasco, 2006; De Coppi, 2007; Tsai, 2004). More recently, it was shown that AFSC can integrate into kidney rudiments and differentiate into tubular cells (Perin, 2007). However, in this study, the authors showed expression of only one human kidney specific marker expression (GDNF) and two specific for tight junctions (ZO-1, Claudin) which can be found in any epithelium. Therefore, it would be interesting to analyse for the presence of other kidney specific markers: nephrin, podocin, aquaporin 1 and 2, synaptopodin, proximal and distal tubules markers.

Although the potential of AFSC needs to be further investigated, they represent an interesting intermediate stage between embryonic stem cells (ESC) and lineage-restricted adult stem cells. These cells could overcome problems with ethical use of ESC, but also graft rejection in allogeneic transplantations, presenting an opportunity to build an AFSC bank to provide cells for autologous transplants. However, the heterogeneity of cells from amniocentesis is limiting the final number of AFSC to be isolated.

1.4.2 Embryonic stem cells

Embryonic stem cells (ESC) are derived from the inner cell mass (ICM) of blastocyst at stage 4 to 5 days of the developing embryo. First, mouse ES cells were isolated in 1981 independently by Evans and Martin (Evans, 1981; Martin, 1981), and human ESC were isolated in 1998 by Thomson (Thomson, 1998). Although both mouse and human ESC (hESC) are able to self-renew and show pluripotency, it is thought that they are not equivalent. For instance, there are differences in their growth requirements; mouse ESC (mESC) maintain pluripotency in the presence of mouse leukaemia inhibitory factor (LIF) whereas hESC do not respond to LIF and need to be cultured on mouse embryonic fibroblasts (MEFs) cells (Humphrey, 2004) or on special matrix (Koestenbauer, 2006; Stojkovic, 2005). Furthermore, hESC culture conditions require supplementation with FGF (Xu, 2005), whereas this factor promotes mESC differentiation (Stavridis, 2003). Recently it was shown that hESC are likely to be at a later stage of development than mESC, more closely resembling mouse epiblast stem cells (mEpiSC). In support of this, it has been shown that the growth requirements and expression profile of mouse epiblast stem cells is very similar to that of hESC (Nichols, 2009a; Tesar, 2007).

Unlike ASC, ESC are pluripotent, meaning that they are able to give rise to cells of all three germ layers of the embryo: mesoderm, endoderm and ectoderm, as well as the gametes following transplantation into the mouse

blastocyst (Nagy, 1993). They are also able to generate cells of the three germ layers *in vitro* when cultured as embryoid bodies (EBs) – a cellular aggregate that forms when ESC are cultured in suspension, the development of which resembles that of the early embryo. Furthermore, mESC are immortal cells that do not become senescent or lose their potential (Evans, 1981). It was also reported, that human ES cells form teratomas containing: gut epithelium, cartilage, bone, smooth muscle, neural epithelium nephron-like structures following subcutaneous injection of adult mice (Stojkovic, 2005; Thomson, 1998; Yamamoto, 2006). However, although ESC have the potential to form tumours, they are a good tool to investigate the potency of ES cells *in vivo*.

The first study investigating the potential of mESC to develop kidney structures and integrate with host tissue involved injecting undifferentiated mESC into kidney rudiments *ex vivo*. Injected cells showed tubular integration with the host tissue, but with low efficiency (Steenhard, 2005). Therefore, in an attempt to improve the integration potential, subsequent studies used the EB culture system to differentiate the cells (Kim, 2005; Kramer, 2006; Yamamoto, 2006). mESC differentiated via EBs showed formation of ring-like structures which were positive for podocin, nephrin, podocalyxin and cytokeratin and tamm-horsfall glycoprotein (THP). This implied that these cells were differentiating into proximal and distal tubules of the nephrons; however, this was only investigated *in vitro* (Kramer,

2006). In a different study, following mESC differentiations using the EB system, cells were induced with a nephrogenic cocktail of retinoic acid, activin A and BMP4. Following stimulation with this nephrogenic cocktail, the majority of mESC contributed to tubular epithelia following injection into kidney rudiments *ex vivo* (Kim, 2005).

Yamamoto and co-workers used the ability of mESC to form teratomas in order to investigate mESC potential to differentiate into renal tissue. Following EB differentiation, cells were disaggregated and injected subcutaneously to generate tumours. Following 14 and 28 days of growth, tumours were investigated for the presence of kidney markers such as Pax2, endo A cytokeratin and Ksp-cadherin, which confirmed renal fate of some cells of the tumour. However, many of the injected cells formed other cell types (Yamamoto, 2006). Work by Wilson's group showed integration of pre-differentiated mESC into the proximal tubules of the kidney rudiments in culture and kidneys of newborn mice *in vivo*. Similarly, this study used suspension culture to differentiate mESC to express markers such as Pax2, Wt-1, Wnt4 and cadh-11. By predifferentiating the cells prior to integration, it was possible to obtain renal differentiation of cells without tumour formation (Vigneau, 2007).

1.4.3 Induced pluripotent stem cells (iPSC)

In the 2006 first report informing about possibility of generating induced pluripotent stem cells (iPSC) from mouse embryonic and adult fibroblast cells was published (Takahashi, 2006). These first somatic cells were induced to become pluripotent with use of four defined factors: Oct3/4, Sox2, c-Myc and Klf4. Although those iPSC showed morphology similar to ESC they were not identical as their genes profile was different from ESC and they did not shown full pluripotency due to being unable to form chimeras (Takahashi, 2006). Therefore further modifications were undertaken and instead of using only defined factors, endogenous Nanog (Okita, 2007; Wernig, 2007) or Oct4 (Wernig, 2007) were activated. Both, Nanog-iPSC and Oct4-iPSC showed ability to form embryoid bodies; tumours with ecto-, endo-, and meso-dermal cells structures; contributed into germ layers; formed chimeras and did not become senescent over 26 passages. Their genes expression profile was highly comparable with ESC (Okita, 2007; Wernig, 2007). Also female iPSC displayed the same dynamics of X chromosome inactivation as female ESC (Maherali, 2007). Therefore, in iPSC (Nanog and Oct4) pluripotent state is maintained by endogenous pluripotency genes activation and iPSC show most if not all attributes of ESC. However, iPSC are very similar to ESC considering their behaviour and differentiation abilities, they are also easily accessible as can be derived from patients' skin fibroblast cells. This would significantly

reduce possibility of graft rejection. Nevertheless, the nephrogenic potential of iPSC has not yet been investigated.

Table 2 Summary of in vitro, in vivo and ex vivo studies of ability of different stem cell types to show renal fate.

Stem cell types		Metanephric Mesenchyme derivatives		Ureteric Bud derivatives	Other potential
		Renal Tubules	Glomerulus	Collecting duct	
Kidney Stem Cells		Bussolati 2005 Gupta 2006 Maeshima 2006 Dekel 2006 Sagrinati 2006 Ronconi 2009	Ronconi 2009	?	• Contamination with tumour cells if derived form tumouric kidneys (biopsies)
Bone Marrow derived Stem Cells	MSC	Ito 2001 Morigi 2004 Herrera 2004 Morigi 2010	Ito 2001	?	• paracrine effect only-Humprey 2008 • maldifferentiation into adipocytes-Kunter 2007
	HSC	Lin 2003	Prodromidi 2006	?	• vasculogenic potential only-Dekel 2006
Amniotic Fluid Stem Cells		Perin 2007	?	?	-
Embryonic Stem Cells		Steenhard 2005 Kim 2005 Vigneau 2007	?	Vigneau 2007	• Tumourigenic-Yamamoto 2006

? – not yet reported,

Although the aforementioned studies show that stem cells have the potential to generate some renal specific cell types, at present, it is unknown if any of them are capable of generating the entire range of cell types necessary to constitute a functional nephron. Moreover, following transplantation into embryonic, neonatal kidneys or mouse models of kidney disease, it appears that all of the investigated cell types so far are

unable to generate the entire range of nephron cells. Therefore, although mESC derivatives showed good potential in regard of tubular cell differentiation and integration, it will be important to establish if they are capable of generating podocytes within the kidney environment. Furthermore, it will be important to establish if the ESC-derived renal cell types are functional.

1.5 Cell labelling methods

In regard of cell therapies it is very important to be able to identify a label that enables monitoring of cells following transplantation in *in vivo* studies. A number of labels are already well-established for the aforementioned purpose, and will be described here.

1.5.1 GFP

The most commonly used cell label is GFP (green fluorescent protein) or other fluorescent proteins such as RFP (red), YFP (yellow), BFP (blue). These fluorescent labels are most often delivered to cells using a knock-in strategy (Misteli, 1997): GFP is inserted under the control of a ubiquitously active promoter for ubiquitous expression (Sieberta, 2008) or GFP is inserted under the control of specifically active gene promoter (Fehling, 2003) for regulated expression. This method allows for long term observations of cell/tissue movement and requires the generation of transgenic animals. Following appropriate selection, one can obtain 100%

efficiency of stable integration (Nagy, 2003), however, there are reports of GFP and RFP being toxic for cells (Strack, 2008; Taghizadeh, 2008), and the toxicity can depend on the gene insertion locus, protein concentration and/or cell type, and may lead to kidney defects in transgenic animals (Guo, 2007). Another method of delivery of fluorescent proteins to the cells is via lentiviral transfection. Viral vectors can integrate and stably express fluorescent proteins under the control of either viral or cellular promoters (Blomer, 1997; Zhou, 2009). Although lentiviral transfection is rather simple, the use of primate viruses (Poeschla, 1998) and any other viruses raises safety issues for medical applications.

1.5.2 Vital stains

Vital stains are used to label living cells in order to investigate their motility following transplantation *ex vivo* or *in vivo*. These labels include extracellular lipid dyes such as DiI, intracellular protein dyes such as vybrant dye (VD) and small nanocrystals – quantum dots (QDs).

The lipophilic dye – DiI (red) binds to the outer layer of lipids in the cell membrane. It was used to label cells in culture (Ragnarson, 1992) and post-mortem (von Bartheld, 1990). The strength of the dye strongly depends on the dye concentration and due to cell divisions, diminishes within a couple of days following labelling (Ragnarson, 1992). The DiI binds to the lipids in the outer layer of the plasma membrane, and due to membrane dynamics such as endocytosis, can be internalised by the cell. The dye can also be

transferred between the lipid bilayers of contacting cells (Razinkov, 1999; Zimmerberg, 1999).

The protein dye – VD (CFDA SE – carboxyfluorescein diacetate, succinimidyl ester, Invitrogen) binds to intracellular proteins. It passively diffuses into the cells, when the cell membrane permeability was increased by DMSO. Similarly to DiI, the strength of VD depends on the dye concentration and cell type (Wang, 2005c). During cell divisions, the dye is transferred to all daughter cells, but is diluted by 50% with each division (Lyons, 2000).

Another labelling method of living cells that allows for cell tracking is QD labelling. QDs are small nanocrystals that can be of many colours: green, red, yellow, different shades of blue (Lin, 2007), which are stably located in cytoplasmic vesicles (Rosen, 2007). Although QDs present high labelling efficiency, the label up-take and maintenance depends on the cell type (Lin, 2007; Rosen, 2007). QDs were showed to be resistant for photobleaching (Solanki, 2008) and therefore prolonging the imaging time. Moreover, QDs are up-taken by all cell types, but the coating can be modified with different ligands or antibodies, that would allow targeting specific cells (Gao, 2004; Gao, 2005; Kim, 2008; Koshman, 2008; Lidke, 2004) and therefore presenting potential clinical use. However, due to toxicity of the QD core (CdSe) it is unlikely to happen.

In spite of high efficiency of labelling, DiI, VD and QDs are diluted with every cell division (Parish, 1999) and therefore not suitable for labelling of

rapidly dividing cells (Lin, 2007; Rosen, 2007; Sechrist, 1989; von Bartheld, 1990; Wang, 1989). However, the longevity of each type of label can differ and should be investigated and optimised for the cell types and experimental settings used.

1.6 Hypothesis

Many stem cell types show potential for promoting renal repair and/or regeneration (see chapter 1.4); however, given the ability to generate derivatives of all three germ layers, it is likely that ESC have the greatest potential to generate all cell types of the nephron. Previous work has shown that if ESC are differentiated towards the renal lineage (identified by expression of kidney markers: Pax2, Wt1, Wnt4 and cadherin11), prior to transplantation into embryonic and neonatal kidney, they are able to integrate into kidney tubules without tumour formation (Vigneau, 2007).

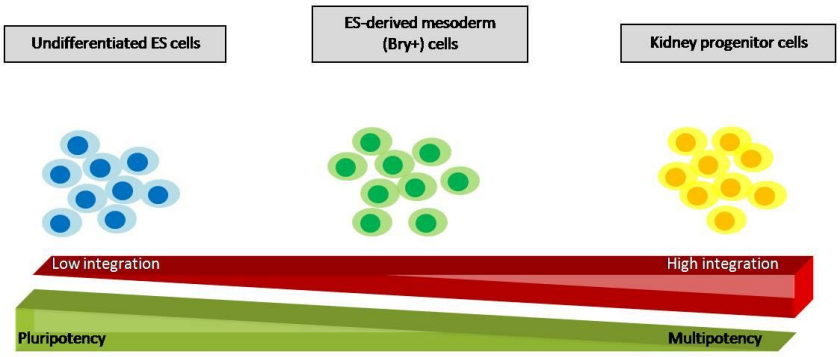

Fig.1.9 Schematic of the hypothesis investigated in the current study. Differentiation of mES cells into mesoderm should give better integration into mouse kidney rudiments than undifferentiated ES cells.

The study of kidney organogenesis revealed that kidneys develop form mesoderm (Saxen, 1987). Mesoderm is recognized as a Brachyury (*T*, Bry) expressing cells (a known mesodermal marker (Rivera-Perez, 2005). Therefore, the hypothesis of the current study was that ESC already differentiated into mesoderm (to express Bry) thus will present a higher potential for kidney cell generation, than undifferentiated ESC.

1.7 Aims

The possibility of healing kidney diseases with stem cell therapy is becomming more feasible, and in the future, could be a useful alternative to dialysis and renal transplantations. Embryonic stem cells have the potential to generate all kinds of cell types of the body (Nagy, 1993), but on the other hand, these cells have tumourigenic potential (Yamamoto, 2006). Nevertheless, Vigneau (2007) showed that the tumourigenic potential of embryonic stem cells could be reduced, or even eliminated by differentiating them into kidney linage. However, this study did not show intraglomerular integration and differentiation into podocytes. There is a lack of studies investigating the effect of exogenous cells on the host tissue and of functional studies, to prove that integrated cells actually function properly to their location.

The aim of this study was to investigate:

- in the first instance, how the differentiation of embryonic stem cells into mesoderm, prior to injection into kidney rudiments, improves their ability to integrate with embryonic kidneys
- if kidney progenitor cells, ESC or their derivatives can have a detrimental effect on kidney development *ex vivo*
- if investigated cells, following integration, would still present a characteristic of undifferentiated cells
- and finally, whether or not the cells display any functionality.

Chapter 2: Materials and methods

2.1 Cell lines

2.1.1 Embryonic stem cells

The E14 mouse embryonic stem cell (mESC) line was originally derived from the inbred mouse strain 129/Ola in 1985 by Martin Hooper in Edinburgh, Scotland, UK. The E14.1a ESC line used here was obtained from the Mark Boyd Laboratory at the University of Liverpool.

Mouse Bry-GFP knock-in ESC were given to our lab by Georges Lacaud (Paterson Institute for Cancer Research, Manchester). All information about the construct can be found in the following paper: Fehling, *et al*., 2003. Fig. 2.1 presents a construct map published in the aforementioned paper (Fehling, 2003).

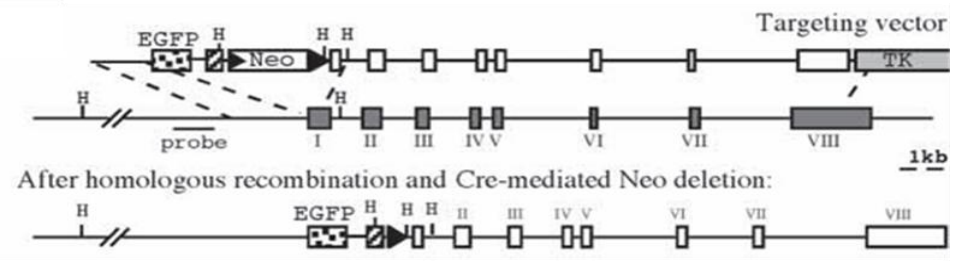

Figure 2.1 Construct of Bry-GFP cell line. EGFP was knocked into the Bry locus, into the first exon of the Bry gene (Fehling, 2003).

2.1.2 Feeder cells

Mouse embryonic fibroblast (MEF) cells were isolated from decapitated and eviscerated mouse embryos at embryonic day E11.5 – E12.5. MEFs

were isolated from mouse embryos at embryonic day E11.5 – E12.5. Embryos were decapitated and eviscerated in PBS^{Ca+Mg+}. Eviscerated embryos were transferred onto fresh petri dish and minced into small pieces, which were then incubated for 20-30 min in 0.25% trypsin/EDTA solution at 37°C. Following incubation, the trypsin reaction was stopped with complete MEF medium (see 2.17 for protocols). Cells were seeded at a density of 1 embryo per 10 cm culture dish (Corning Incorporated) and incubated at 37°C and 5%CO_2. After 3-4 days cells were at ~90% confluence and were either frozen or used for feeder cell preparation.

2.2 Cell freezing protocol

The cell freezing protocol used in this work was as follows. Firstly, cells cultured on 3.5 cm dishes were washed 2x with 2 ml of PBS (Phosphate Buffered Saline) and cells were trypsinized as follows: 2 ml of 1x trypsin/EDTA (Sigma) solution was added to each dish. The cells were then transferred into an incubator at 37°C for 3-5 min. Following incubation, the trypsin reaction was terminated with 2 ml of 10% FCS (Foetal Calf Serum) DMEM medium (see 2.17 for protocol) and cells were transferred into a 15 ml conical tube and centrifuged at 100x *g* for 2.5 min. After spinning, the supernatant was discarded and cells were resuspended in 1 ml of freezing recovery medium (Invitrogen) per trypsinized dish. Then, 0.5 ml of resuspended cells was transferred into cryovials labelled

with cell type, passage number and date. Cryovials were then placed into a freezing chamber, filled with isopropanol, and placed in a -80°C freezer for overnight incubation. This allowed for slow decrease in temperature by 1°C per hour. Following freezing, cells were transferred into liquid nitrogen container.

2.3 Cell thawing protocol

To thaw cells, the following protocol has been used in this work. The cryovials containing frozen cells were rapidly thawed by placing vials into a 37° C water bath. As soon as the cells thawed, they were transferred into a 15 ml conical tube and 2 ml of 10%FCS DMEM medium was added and the cells were centrifuged at 100x *g* for 2.5 min. Pelleted cells were then resuspended in appropriate medium, ESC medium for embryonic stem cells or MEF medium for MEF cells (see 2.17 for protocol). The cells were cultured in the incubator at 37°C and 5% (v/v) CO_2. Medium was changed every other day.

2.4 Gelatinization protocol

To culture MEF cells or ES cells without MEF feeder layer, culture dishes were coated with 0.1% (w/v) gelatine solution in PBS (see 2.17 for protocol). 2 ml of 0.1% (w/v) gelatine was added to the cell culture dish and incubated at room temperature for at least 15 min. Following incubation, the dishes were washed 3x 5min with warm PBS.

2.5 Cell counting

In order to count cells, cells were trypsinized as described in section 2.2 and were collected in 15 ml falcon tube in 5ml of appropriate media. 10µl were collected from the cell suspension and mixed with 10µl of trypan blue (Sigma) in a 0.2ml tube (Eppendorf). 10µl of the cells solution was transferred onto hematocytometer (Hausser Scientific) and cells were observed down the microscope using 10x objective. Cells were counted in four squares and average number (A) of cells per square was calculated. Obtained average number of cells was multiplied by a chamber factor (10^4) and trypan blue dilution factor (2) which gave the number of cells in 1 ml. Required number of cells was calculated using cross-multiplication formula and diluted in appropriate amount of medium.

2.6 Cell culture

2.6.1 MEF culture

MEF (mouse embryonic fibroblast) cells were maintained in gelatinized tissue culture dishes in MEF medium (see 2.17 for protocol) in a humidified atmosphere at 37°C with 5% (v/v) CO_2 in air.

2.6.2 Preparation of MEFs as a feeder layers

MEF cells at passage 1 (P1) were thawed and seeded on a 10 cm dish (Corning Incorporated). After a few days, when cells were ~90% confluent

they were split 1:3 every 3 days on 10 cm gelatinized dishes until passage 4 (P4). Confluent dishes of MEF cells at P4 were treated with Mitomycin C (2mg/ml, Sigma) to arrest cells from further mitotic divisions. To obtain a final concentration of Mitomycin C of 20μg/ml, 5 ml of MEF medium was left in the dish and 100 μl of Mitomycin C added. The dish was gently agitated to ensure that the Mitomycin C was evenly distributed and was incubated for 2-3 hours in humidified incubator at 37ºC and 5% (v/v) CO_2 in air. Following incubation with Mitomycin C, MEF cells were washed twice with 1xPBS (Invitrogen / Gibco) and trypsinized as described in section 2.2. Following trypsinization and centrifugation the supernatant was aspirated and the cell pellet resuspended in appropriate amount of freezing recovery cell medium (Invitrogen) to give a final cell density of $2x10^6$ cells per 1 ml. Cells were then placed in freezing vials (1 ml / vial) and frozen as described in section 2.2. When needed, vial(s) of inactivated MEF cells were thawed using the protocol described in section 2.3 and cells were typically split 1:3 on 3.5cm gelatinized dishes (Nunc). The dishes were gently agitated before replacing in the incubator. MEF cells were ready to use as a feeder for Bry-GFP cells after overnight (ON) incubation.

2.6.3 Routine ES culture

E14 Bry-GFP mESC were maintained in gelatinized tissue culture dishes, coated with MEF feeder cells, in ESC medium (see 2.17 for protocol) in a humidified atmosphere at 37°C with 5% (v/v) CO_2 in air.

Cells were typically cultured on MEFs feeders and split 1:4 every 3 to 4 days. Cells were trypsinized as described in section 2.2. The supernatant was aspirated and the cell pellet resuspended in 6 ml ESC medium and 2 ml of the cell suspension was transferred to each dish. The dishes were gently agitated before replacing in the incubator. Medium was changed every other day.

2.7 Differentiation of mouse embryonic stem cells

2.7.1 Monolayer differentiation protocol

For differentiation of mESC in monolayer culture, Bry-GFP cells were cultured typically for a few passages on MEF feeder cells in ESC medium, then transferred onto 3.5cm gelatinized dishes (Nunc) for 2 passages (in order to deplete the number of MEF cells) before setting up a differentiation experiment. Following the second passage on gelatinized dishes, cells were trypsinized as described in section 2.2 and resuspended in ES monolayer differentiation medium; either 10% FCS DMEM or 10% FCS IMDM both supplemented with 2ng/ml Activin A (R&D Systems) and 0.25ng/ml BMP4 (R&D Systems) (see 2.17 for protocols) and plated

on 3.5cm dishes (Nunc) at 3 different densities: 500 cells cm^{-2}, 1000 cells cm^{-2}, 2500 cells cm^{-2}, counted as described in section 2.5. Medium was changed on a daily basis.

2.7.2 Suspension differentiation protocol

For differentiation of mESC in suspension culture, Bry-GFP ESC were used to make embryoid bodies. For that purpose Bry-GFP cells were cultured typically for a few passages on MEF feeder cells in the ESC medium, then transferred onto 3.5cm gelatinized dishes (Nunc) for 2 passages (in order to deplete number of MEF cells in EB culture) before setting up an embryoid body culture. During the first passage on gelatine cells were cultured in ESC medium, and during second passage, cells were cultured in ES/EB medium (see 2.17 for protocols). Following the second passage on gelatinized dishes, cells were trypsinized as described in section 2.2, and resuspended in the EB medium (see 2.17 for protocols). Cells were seeded onto non-adherent dishes that were treated with detergent, Pluronic (Sigma) to further reduce adhesion. Pluronic was prepared fresh before pouring onto dishes. 2 ml of the pluronic at a concentration of 0.01% (w/v) in PBS was added to 3.5 cm petri dishes (Sarsted) and incubated at room temperature for at least 20 min. Following incubation, dishes were washed 3x 3min with 1x warm PBS and used immediately. Cells were counted as described in section 2.5 and seeded at different densities in suspension: low cell densities: $5x10^3$ cells ml^{-1}, $25x10^3$ cells

ml^{-1}, $50x10^3$ cells ml^{-1}, $75x10^3$ cells ml^{-1}, $1x10^5$ cells ml^{-1}, and high cell densities: $25x10^4$ cells ml^{-1}, $50x10^4$ cells ml^{-1}, $75x10^4$ cells ml^{-1} and $1x10^6$ cells ml^{-1}. Onto each dish treated with Pluronic, 2 ml of cell suspension were added and kept in culture for up to 20 days. Culture medium was changed every 2 days and if necessary, EBs were transferred to new petri dishes prepared as described above.

2.7.3 Preparation of embryoid bodies for FACS sorting

EBs at day 4 or 6 of development were disaggregated using 1x trypsin (Sigma) in PBS (Invitrogen) solution. For that purpose, EBs were transferred into a 15 ml conical tube and allowed to settle under gravity. Medium was aspirated and EBs were washed with 1x PBS and 3 ml of 1x trypsin solution was added to the EBs pellet and incubated in 37°C (in the water bath) for 3-5 min. Following incubation EBs were vigorously pipetted and incubated for 10 min in 3 ml of 10%FCS DMEM medium to stop trypsin reaction, and again vigorously pipetted to give single cell suspension.

In order to prepare cells for FACS sorting analysis, cells were centrifuged for 2.5 min at 100x *g*, following which, medium was discarded and replaced with 0.1% bovine serum albumin (BSA; Sigma) in $PBS^{Ca+\ Mg+}$ solution and vigorously pipetted to single cell suspension. Cells were counted as described in section 2.5 and diluted to obtain a final

concentration of $1x10^6$ cells ml^{-1}. Such prepared cells were ready to be sorted.

2.7.4 FACS sorting

Firstly GFP-positive (GFP+) cells number was established by counting using BD Calibur FACS machine, and obtained data were analysed with *WinMDI* software.

The FACS Ventage SE (BD Biosciences) was used to sort GFP+ and GFP- cells. Before sorting FACS machine was cleaned to ensure sterile conditions for sorting. After alignments and calibrations conducted with fluorescent three colour beads (BD Biosciences), the FACS machine was ready to count cells. Before sorting, more optimisations were done to establish the best drop off point and align side streams to be smooth, after which FACS was ready to sort. First, a solution of negative control of non-fluorescent cells (treated the same way as those to be sorted, but not transfected with GFP) was used to establish the level of cell auto fluorescence. Following this final alignment, cells prepared as described above (see section 2.6.3), were sorted into polystyrene tubes (Falcon) filled with 1ml 10%FCS DMEM medium to prevent cell adhesion to the tube walls. Sorted cells (GFP+ and GFP-) were kept in the incubator at 37°C until the required number of cells was sorted. FACS data obtained from

FACS Ventage SE machine were analysed with use of Cell Quest PRO software.

2.7.5 Cytospin of cells

EBs at day 14 of culture were disaggregated as described above (see section 2.6.3). Cells were counted and density was adjusted to give a final concentration of $1x10^5$ cells ml^{-1} in PBS and cytospinned using Cytospin3 (Shandon Scientific Limited). Glass slides were subbed prior to use (see section 2.12) and cells were fixed following the spin.

2.8 Organ dissection

2.8.1 Dissection of embryonic kidney rudiments

Mouse embryos at embryonic day (E) 11.5 and 13.5 were dissected from timed mated CD1 mice (Charles River) as follows. Firstly, mice were sacrificed as stated in Schedule 1 procedure (Home Office Regulations) by cervical dislocation. The uterine horns were dissected at room temperature and placed into L-15 medium (Invitrogen / Gibco) supplemented with 1% (v/v) FCS and embryos were then removed from extraembryonic membranes and placed into the same medium on ice.

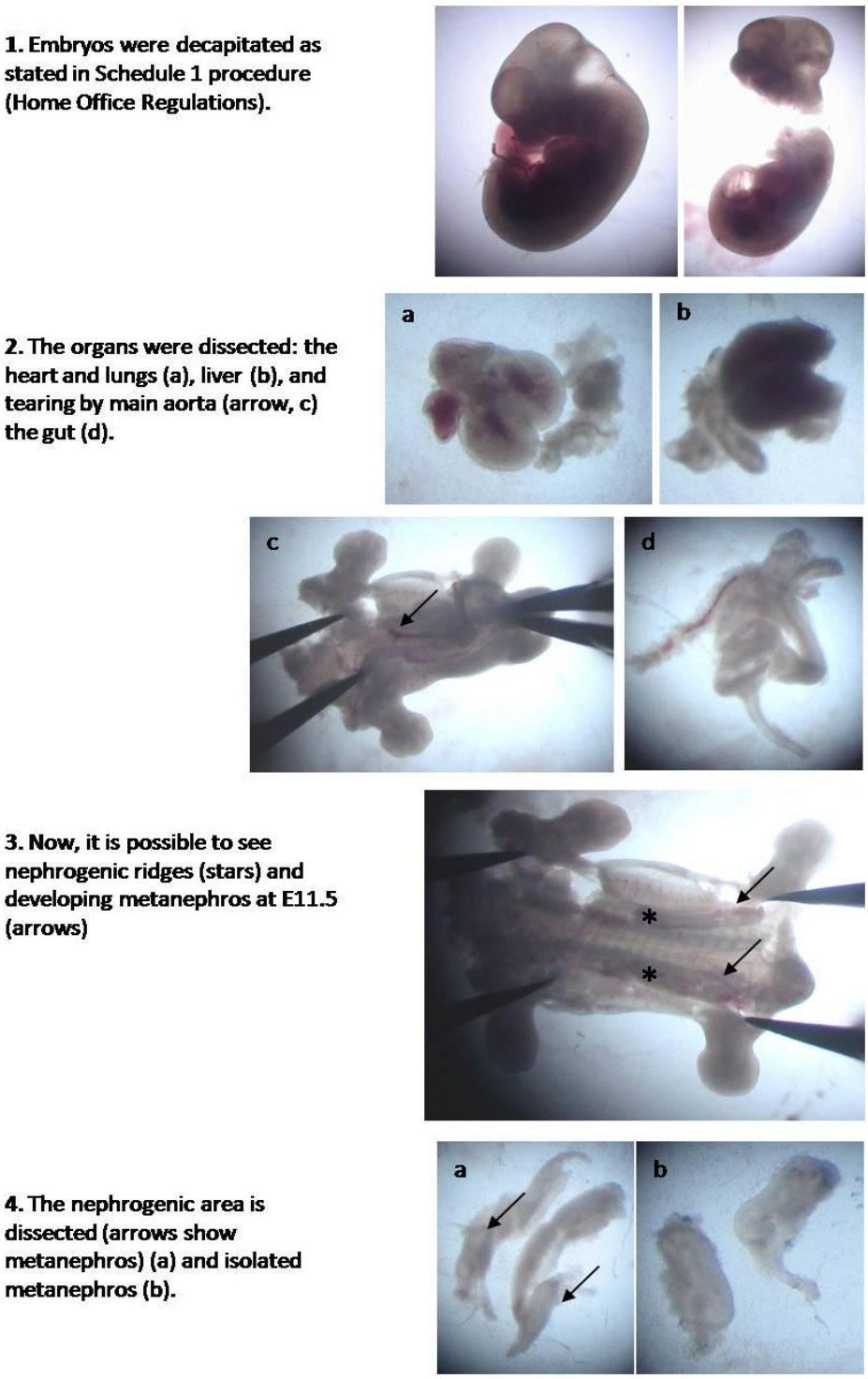

Figure 2.2 Kidney rudiment dissection from mouse embryos at embryonic day (E) 11.5.

Kidney rudiments were dissected using a stereoscopic microscope (LEICA *MZFLIII*) from the mouse embryos as follows. Firstly, the embryos were decapitated as stated in Schedule 1 procedure (Home Office Regulations). Following the decapitation all organs were removed starting from the heart and lungs through the liver and gut. The nephrogenic ridge of mesonephros and early developing metanephros could now be observed. Before dissecting the metanephros, the dorsal aorta was carefully removed. At E11.5 the kidney rudiments have a characteristic morphology (Fig. 2.2).

Following dissection, the kidney rudiments were transferred onto isopore (1.2μm) membrane filters (Millipore) placed on a metal grid (Fig. 2.3) and filled with kidney culture medium (see section 2.17 for protocols) just below the level of metal grid.

Kidney rudiments were then transferred and cultured in a humidified atmosphere at 37°C with 5% (v/v) CO_2 in air.

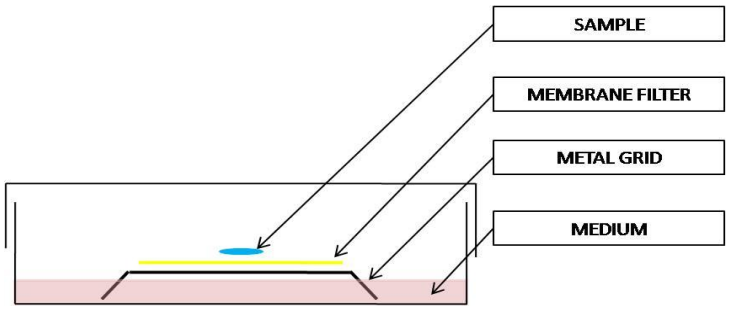

Figure 2.3 Kidney rudiment culture conditions.

2.8.2 Dissection and disaggregation of neonatal kidney

Neonatal mice were sacrificed using increasing concentrations of CO_2 in air as described in Schedule 1 procedure of Home Office Regulations. The neonatal kidneys were dissected from 6-10 day old mice (CD1) (University of Liverpool) and transferred into 1x PBS (Invitrogen).

The kidneys were disaggregated as follows: first, kidneys were cut into ~1mm^2 pieces and transferred into a 15 ml conical tube containing PBS. After the tissue fragments had settled at the bottom of the tube the PBS was aspirated and replaced with Hank's buffered saline solution (1x HBSS with Ca^{2+} and Mg^{2+}) (Invitrogen). After the tissue fragments had settled at the bottom of the tube, the HBSS buffer was then removed and replaced with 5 ml of warm (37ºC) Collagenase I (Sigma) in HBSS buffer solution and incubated at 37ºC for 20 min. After incubation, the digested kidney tissue was aspirated into the syringe and passed through a 23-gauge needle twice. The procedure was repeated with a 26-gauge needle. Following disaggregation, the cell suspension was centrifuged at 100x *g* for 2.5 min. The supernatant was then aspirated and renal cells were resuspended in a kidney culture medium and placed into gelatinized cell culture dishes. The samples were incubated in a humidified atmosphere at 37°C with 5% (v/v) CO_2 in the air. The renal cells were fixed with 4% PFA for immunostaining after 24h of culture.

2.9 Integration of cells into developing kidney

Cell of interest (Bry^+ cells sorted from EB day 4; Bry^- cells sorted from EB day 4; ESC, embryonic kidney cells) were labelled with Quantum Dots (Sigma) as described in chapter 2.9.1 and mixed with disaggregated embryonic kidneys. The cell integration method was developed in Davis Lab (University of Edinburgh) (Unbekandt, 2010) and a slightly modified version was used here. Embryonic kidneys were isolated from mouse embryos at E13.5 as described in chapter 2.8, collected in 1.5 ml microcentrifuge tubes, washed once with 1x PBS and trypsinized in 1x trypsin/EDTA solution for 5-7 min at 37°C. After 4 min of incubation kidneys were pipetted and left at 37°C for the remaining incubation time (until kidneys formed single cell suspension). The trypsin reaction was stopped using 10% FCS DMEM medium and cells were incubated at 37°C for 10 min. Cells were then pipetted and centrifuged at 1400x *g* for 1 min. The supernatant was discarded and pelleted cells resuspended in kidney culture medium (see chapter 2.17 for protocols).

QDs-labelled cells and kidney cells were counted as describe n section 2.5 and mixed in a ratio of 1:8 (one labelled cell for eight unlabelled kidney cells) in 0.5 ml microcentrifuge tubes (Fig. 2.4). Cells were centrifuged at 1400x *g* for 3min, and pellets were transferred onto isopore membrane filters (Millipore) and cultured for up to 7 days as shown on figure 2.3, in a humidified incubator at 37°C and 5% CO_2. For the first 24h of incubation a Rho kinase (ROCK) inhibitor (Y27632, 5mM, Sigma) was applied to

obtain final concentration of 5µl ml^{-1}. Medium was changed every second day. Samples were collected for fixation in cold methanol and immunostaining after 3h (day0), 24h (day1), 48h (day2), 72h (day3), 120h (day5) or 168h (day7) of culture.

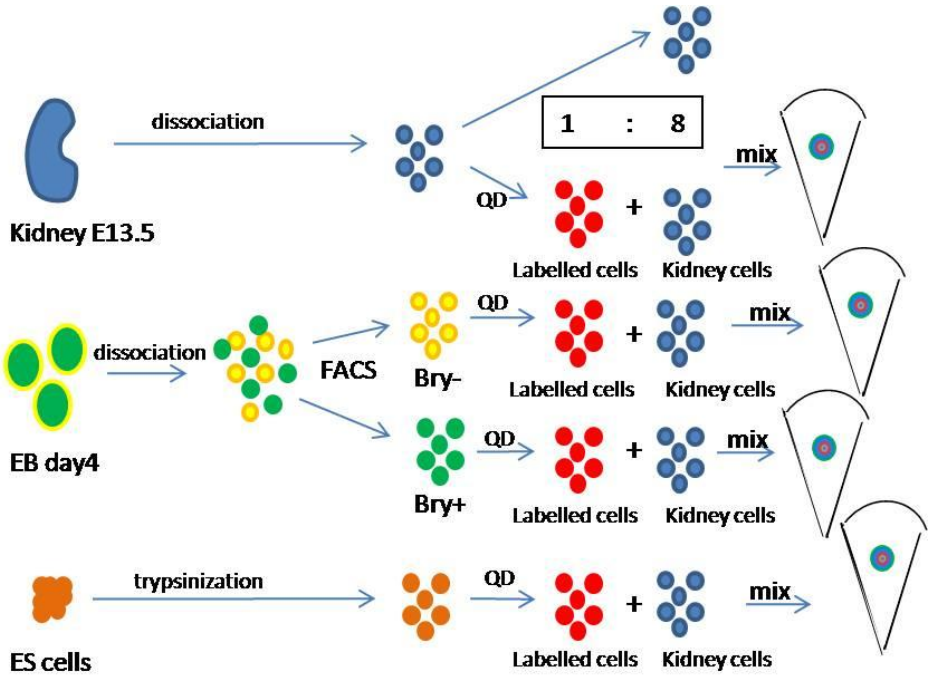

Figure 2.4 Preparation of nephrogenic chimeras.

2.10 Cell labelling

2.10.1 Quantum dots labelling

Cells of interest were labelled with Quantum Dots (QDs) (Invitrogen, Qtracker® Cell Labelling Kit (Q25021MP)) in order to enable localization

of the cells within cultured kidney chimeras. Cells were labelled with QDs as recommended by supplier. Briefly, component A and component B of QDs (1µl of each component) were pipetted into a microcentrifuge tube and incubated for 5 min at room temperature. Following incubation, 200 µl of complete growth medium (kidney culture medium), was added to the QDs solution to obtain concentration of QDs at 10nM, and vortexed for 30 sec. Such prepared QDs-medium was applied to cells growing in a monolayer (adherent cells) or to trypsinized cells (suspension cells) and incubated for 45-60 min in the incubator at 37°C and 5% CO_2. Following incubation time, cells were washed 4x with complete growth medium and cultured for 1, 3 and 7 days.

2.10.2 Vybrant dye labelling

Cells of interest were labelled with Vybrant dye (Invitrogen, Vybrant® CFDA SE Cell Tracer Kit (V12883)) in order to compare the labelling efficiency and dye retention to quantum dots. Cells were labelled as recommended by supplier. Briefly, following the preparation of Vybrant dye (VD) stock by dissolving component A (VD) with component B (DMSO), 1µl of the stock was added to 1ml of prewarmed PBS (37°C) (to obtain a concentration of 10nM). Such prepared dye was added to the cells and incubated for a 15 min in the incubator at 37°C and 5% CO_2. Following incubation with dye, cells were incubated for further 30 min at

37°C in the culture medium to ensure complete modification of the probe. Next, cells were seeded on the culture dishes at a density of 500 cells cm^{-2} and cultured for 1, 3 and 7 days.

2.10.3 Lentivirus transduction

KSC clonal line H6 was transduced with a pHR-SFFV-GFP lentiviral-derived vector constitutively expressing green fluorescent protein (GFP) under the control of spleen focus-forming virus (SFFV) promoter. On the day of transfection KSC-H6 cells were trypsinized and seeded into a fresh tissue culture dish, then 110μl of lentivirus supernatant, was added to the culture medium (final volume 3ml). The cells were incubated with the supernatant for 6 hours at 37°C and 5% CO_2. Following the incubation time the medium was completely replaced with fresh culture medium. The presence of H6 GFP-expressing cells (KSC-H6/GFP^+) was verified by observing the cells under a Leica DMIL fluorescent microscope (Leica, Heidelberg, Germany) and by FACS (FACS Ventage SE; BD Biosciences) and was first found 96h post transduction. KSC-H6/GFP^+ cells were transduced by E. Ranghini (University of Liverpool) and used to determine the transfer of QDs from KSC-H6/GFP^+ cells to kidney GFP- cells.

2.11 Functionality assay

Cells used to form kidney chimeras were investigated for their functionality. This was achieved by investigating the function of the

organic anion transporters (OATs) of the proximal tubules. A slightly modified method of that described by Sweet (2006) and Rosines (2007) was used (Rosines, 2007; Sweet, 2006). Briefly, chimeras grown for 4, 5 and 6 days in culture, were washed twice in 1x PBS^{Ca+Mg+} for 5 min. Following washes, samples were transferred into 1 μM 6-carboxyfluorescein (6-CF) solution (Sigma) in PBS^{Ca+Mg+} and PNA rhodamine (Peanut Agglutinin Lectin, PNArh) (20μg/ml) (Vector Lab.) and incubated at 25°C for 1 hour in the dark. Control samples were incubated in OATs blocking solution composed of 2 mM probenecid (Sigma) in PBS^{Ca+Mg+}, 1 μM 6-CF and PNArh (20μg/ml). Following incubation, samples were washed twice in ice-cold PBS^{Ca+Mg+} to remove background staining. In order to block further OAT function, samples were blocked in 8 mM probenecid in PBS^{Ca+Mg+} solution for 15 min. After blocking, samples were transferred onto glass slip and covered with 80% (v/v) glycerol and cover slip. Such prepared samples were immediately imaged using confocal fluorescent microscope (LEICA AOBS SP2).

2.12 Subbing slides protocol

Slides were soaked in 100% ethanol for 15 min, and then washed 5x in distilled water. Following final wash slides were transferred for 25 sec into subbing solution (see section 2.17 for protocols) consisting of 0.5% (w/v) gelatine and 0.05% (w/v) chromium potassium solution in distilled water.

After incubation slides were allowed to dry in a dust-free environment and were ready to use for collection of frozen tissues sections or cytospinned cells.

2.13 Fixation

2.13.1 Fixation of cells

Embryonic stem cells and cytospinned cells were fixed in 4% (w/v) PFA (paraformaldehyde) (see section 2.17 for protocols) for 10 min in the dark at room temperature. Following fixation, samples were washed 3x 5 min in PBS and stored in PBS at 4°C until they were used for immunostaining.

2.13.2 Fixation of embryoid bodies and sectioning

Embryoid bodies (EB) were collected in a 15 ml conical tube and allowed to settle under gravity, the supernatant was discarded and EBs were fixed in 4% PFA in the dark at room temperature. The timing of fixation depended on the age of EBs (see Tab. 2.1). Following fixation, EBs were washed 3x 10 min in PBS and soaked in 15% (w/v) sucrose solution (see section 2.17 for protocols) for overnight incubation at 4°C. On the next day, the sucrose solution was aspirated and EBs were transferred into the middle of small freezing cubes (Polysciences Ltd.) containing embedding medium (Bright Instrument Company Ltd.), and frozen in cold isopentane (isopentane on dry ice). Following freezing, EBs were stored at -20°C until used for sectioning.

Frozen sections of 8-10µm were prepared using the cryostat set to -20°C (MICROM HM505 N). EBs sections were transferred to subbed slides (see section 2.12), and stored at -20°C until used for immunostaining.

Table 2.1 Embryoid body fixation times.

EBs age (days in culture)	Fixation time (4% PFA incubation time)
1-6	10 min
7-12	15 min
13-20	20 min

2.13.3 Fixation of kidney rudiment and kidney chimeras

Kidney rudiments and kidney chimeras were fixed in cold methanol at room temperature for 10 min and stored in fresh methanol at -20°C until ready for staining (max. 1 month) or washed immediately 3x 5 min in 1xPBS and immunostained. Following long storage in methanol at -20°C, samples were washed in 1x PBS for 1-2 hours at room temperature prior to staining.

2.14 Immunostaining

2.14.1 Haematoxylin and eosin staining

Frozen sections were incubated in 1x PBS at room temperature for 15 min in order to remove mounting medium from the sample. Samples were placed in staining rack and submerged in a haematoxylin solution for 6 min. After haematoxylin (Sigma) staining, samples were briefly washed in a bowl of tap water and immediately placed in acid-alcohol for 2 sec to differentiate. Following differentiation, samples were washed well (~5-10 min) in tap water until blue colour. Next, samples were stained for 1 min in eosin solution (Sigma), briefly washed in tap water and dehydrated by short washes in alcohol solutions (see table 2.2). Following dehydration, samples were mounted with 80% glycerol (see section 2.17 for protocols) and mounted with cover slips.

Table 2.2 Samples dehydration steps during H&E staining.

Alcohol solutions	Incubation time
70% (1st) ethanol	20 sec
70% (2nd) ethanol	20 sec
90% ethanol	40 sec
100% ethanol	40 sec

2.14.2 Lectin staining

Following fixation and storage in methanol, and a 1h wash in PBS, samples were incubated 1h in TBS (Tris Buffered Saline) at room temperature. Following the washes, samples were incubated for 2h at room temperature with lectin (10µg/ml) in TBS solution. After the lectin staining, samples were washed twice in TBS and twice in PBS and the immunostaining protocol continued.

2.14.3 Immunostaining of cells

Following fixation, samples were incubated for 1 hour at room temperature in blocking solution, consisting of 0.1% (v/v) TritonX in PBS and 10% (v/v) serum (Sigma). The serum used in this study to block primary and secondary antibody was chicken or goat, depending on the organism in which the secondary antibody was raised. When possible, the serum used for blocking was from the species in which the secondary antibody was raised. After incubation time, primary antibody solutions were prepared, as follows: 1x PBS supplemented with 1% (v/v) appropriate serum, 0.1% (v/v) TritonX and antibody (see Table 2.3 for concentration); and left for overnight incubation at 4°C or 1.5 h at room temperature for Brachyury antibody, in a humidified chamber.

Table 2.3 List of primary antibodies used for immunostaining in this study

Antigen	Type	Concentration	Supplier
Pax2	Rabbit polyclonal IgG	1:200	Covance #PRB-276P
Six2	Rabbit polyclonal IgG	1:200	Proteintech Europe #11562-1-AP
Bry	Goat polyclonal IgG	1:300	Santa Cruz #sc-17743
Nanog	Rabbit polyclonal IgG	1:300	Abcam #ab 21603
Laminin	Rabbit polyclonal IgG	1:1000	Sigma #L 9393
Synaptopodin	Mouse monoclonal IgG_1	1:4	Fitzgerald #BM 5086
Wt1	Mouse monoclonal IgG_1	1:500	Upstate #05-753
Calbindin	Mouse monoclonal IgG_1	1:500	Abcam #ab 9481
β-Catenin	Mouse monoclonal IgG_1	1:500	Santa Cruz #sc-7963
Oct4	Mouse monoclonal IgG_{2b}	1:500	Santa Cruz #sc-9081

Table 2.4 List of secondary antibodies used for immunostaining in this study

Antibody	Type	Concentration	Supplier
Goat α Mouse	IgG_1 –350	1:800	Invitrogen
Goat α Rabbit	IgG – 350	1:800	Invitrogen
Chicken α Rabbit	IgG – 488	1:500	Invitrogen
Chicken α Goat	IgG – 488	1:500	Invitrogen
Goat α Rabbit	IgG – 488	1:500	Invitrogen
Donkey α Goat	IgG – 488	1:1000	Invitrogen
Goat α Mouse	IgG_1 – 488	1:500	Invitrogen
Goat α Mouse	IgG_{2B} – 488	1:1000	Invitrogen
Goat α Rabbit	IgG – 594	1:500	Invitrogen
Goat α Rabbit	IgG – 594	1:500	Invitrogen
Goat α Mouse	IgG_{2B} – 594	1:2000	Invitrogen

Following incubation of the primary antibody, samples were washed off 3x 5 min with 1xPBS and secondary antibody solutions were prepared as follows: 1xPBS supplemented with 1% (v/v) appropriate serum, 0.1% (v/v) TritonX, and appropriate secondary antibody (see Table 2.4 for concentration); and incubated for 2 hours at room temperature in dark in humidified chamber. After incubation the secondary antibody was washed 2x 5 min in 1xPBS and samples were counter-stained with 1:100,000 DAPI (4,6-diamino-2-phenylindole dihydrochloride) solution in 1xPBS for 5min in the dark at room temperature. The DAPI solution was washed 1X in PBS and samples were covered with DAKO Fluorescent Mounting Medium (Dako Cytomation) and mounted with cover slips. All solutions of primary and secondary antibodies were centrifuged at 13400x *g* for 6 min before use to precipitate protein aggregates.

2.14.4 Immunostaining of frozen sections

The frozen sections, after being removed from -20°C freezer were left at room temperature for 5 min to defrost. Then slides were incubated at room temperature in 1x PBS until embedding solution was removed. Following incubation, samples were immunostained as described above.

2.14.5 Immunostaining of kidney rudiments and kidney chimeras

After fixation kidney rudiment and kidney chimeras were removed from -20°C freezer and placed into 1xPBS for 1-2 hours in order to wash off the

fixative. Following incubation, the immunostaining was performed as described above with a couple of minor changes: firstly, the secondary antibody incubation was performed overnight at 4°C; and secondly, DAPI staining time was prolonged up to 10 min.

2.15 Molecular biology

2.15.1 Primers

Primers used in PCR reactions were individually designed for the respective genes of interest and ordered from Sigma in a quantity of 0.025µmol. Details on primer sequence and product length are given in table 2.5. All primers were reconstituted in nuclease-free water and made up to a working concentration of 6.25pmol/µl for use in PCR reactions. All in house primers were sequenced by the Sequencing Service in School of Life Sciences (MSI/WTB Complex) at the University of Dundee.

2.15.2 RNA extraction

To harvest cells for RNA extraction, all cell culture medium was first aspirated from the culture dish and the cells were immediately collected in 1ml of Trizol® (Invitrogen) and transferred to a 1.5 ml microfuge tube. 200µl of chloroform (Sigma) was then added and the tubes were shaken for 15 sec and centrifuged at 12,000x *g* for 15 min at 4°C. The upper aqueous phase, containing the RNA, was transferred into a new tube

containing 1ul of glycogen (working conc. 1µg/µl) (Boehringer Mannheim; stock conc. 20mg/ml) (to get a visible pellet when small amounts of RNA were being extracted), and an equal volume of isopropanol (Sigma) (approximately 500 µl) added and the solution mixed by inversion 6 times. After incubation at room temperature for 10 min, the precipitated RNA was pelleted by centrifugation at 7000x *g* for 10 min at 4ºC. All the following steps were performed on ice: the supernatant was discarded, the RNA pellet washed in 1ml of 75% (v/v) ethanol in nuclease free water (Sigma) and centrifuged again at 4400x *g* for 5min at 4ºC. The 75% (v/v) ethanol was then removed and the RNA pellet was allowed to air dry for a few minutes before being dissolved in 15 - 20µl nuclease-free water (Sigma) (depending on the size of the pellet).

The quality of RNA after isolation was checked by running on an electrophoresis gels. Two distinguishable bands of rRNA subunits were visible in all cases, the higher band representing the 28S subunit and the lower band representing the 18S subunit (Fig. 2.5). Lack of smears on the gel that indicated that RNA was intact and had not degraded.

Table 2.5 List of primers used in this study

Gene	Primer sequence	Amplicon size (bp)	Temp C/cycle no	Source
MESODERMAL MARKERS				
Bry	F: 5' AACTTTCCTCCATGTGCTGAGAC 3'	532	56/33	Yasunaga, M., et al., 2005
	R: 5' TGACTTCCCAACACAAAAAGCT3'			
Osr1	F: 5' GCAGCGACCCTCACAGAC 3'	169	62/33	In house
	R: 5' GCCATTCACTGCCTGAAGGA 3'			
Foxf1	F: 5' CCTCCTACATCAAGCAACAG 3'	251	58/33	In house
	R: 5' GATAGTAAGATCCTCCGCCT 3'			
Foxc1	F: 5' TCAGAGCGGAAATTGTAGGA 3'	226	58/33	In house
	R: 5' GTATTTGTTCATGTGCCAACTC 3'			
Tbx6	F: 5' GCCTCCTTCCGATTTCCT 3'	141	62/33	In house
	R: 5' CATCCCGCTCCCTCTTAC 3'			
ENDODERMAL MARKERS				
AFP	F: 5' ACATCAGTGTCTGCTGGCAC 3'	461	63/33	Murray P., Edgar D., 2000
	R: 5' AGCGAGTTTCCTTGGCAACAC 3'			
BMP4	F: 5' GCGCCGTCATTCCGGATTAC 3'	402	63/33	Luppen C., et al, 2008
	R: 5' CATTGTGATGGACTAGTCTG 3'			
GATA4	F: 5' GGCCCCTCATTAAGCCTCAG 3'	249	62/33	Roche, E., et a., 2005
	R: 5' CAGGACCTGCTGGCGTCTTA 3'			
GATA5	F: 5' GCGTCTGTCCTCATCCCCGAA 3'	354	62/33	Roche, E., et al., 2005
	R: 5' CTGGAGGCCTGGGAGGTGATA 3'			
Sox17	F: 5' TTTGTGTATAAGCCCGAGATGG 3'	469	62/33	Yasunaga, M., et al., 2005
	R: 5' AAGATTGAGAAAACACGCATGAC 3'			
ECTODERMAL MARKERS				
Pax6	F: 5' GAGAAGAGAAGAGAAACTGAGGAACCAGA 3'	201	63/33	Vigneau, C., et al., 2007
	R: 5' ATGGGTTGGCAAAGCACTGTACG 3'			
KIDNEY MARKERS				
Pax2	F: 5' CCTGGGCAGGTACTACGAGAC 3'	224	62/35	In house
	R: 5' CTTTGGTCCGGATGATCCTG 3'			
GDNF	F: 5' TGCCAGCCCAGAGAATTCCA 3'	216	62/33	In house
	R: 5' AGCCTTCTACTCCGAGACAG 3'			
Wt1	F: 5' CCAGTGTAAAACTTGTCAGCGA 3'	234	60/33	Yamamoto, M. et al., 2006
	R: 5' TGGGATGCTGGACTGTCT 3'			
Sall1	F: 5' GACACTGGGCAACTTCTCGG 3'	121	62/33	In house
	R : 5' GCAGAGCCAGGAGTTGTTCC 3'			
OTHER MARKERS				
Oct4	F: 5' TGGAGACTTTGCAGCCTGAG 3'	188	56/33	In house
	R: 5' CTTCAGCAGCTTGGCAAACTG 3'			
E-cadherin	F: 5' CATGTTTCCCAGCGTGTACC 3'	228	63/33	In house
	R: 5' ACTTTCAGCCAGCCTGTCTC 3'			
GAPDH	F: 5' TGAAGCAGGCATCTGAGGG 3'	102	56/33	In house
	R: 5' CGAAGGTGGAAGAGTGGGAG 3'			

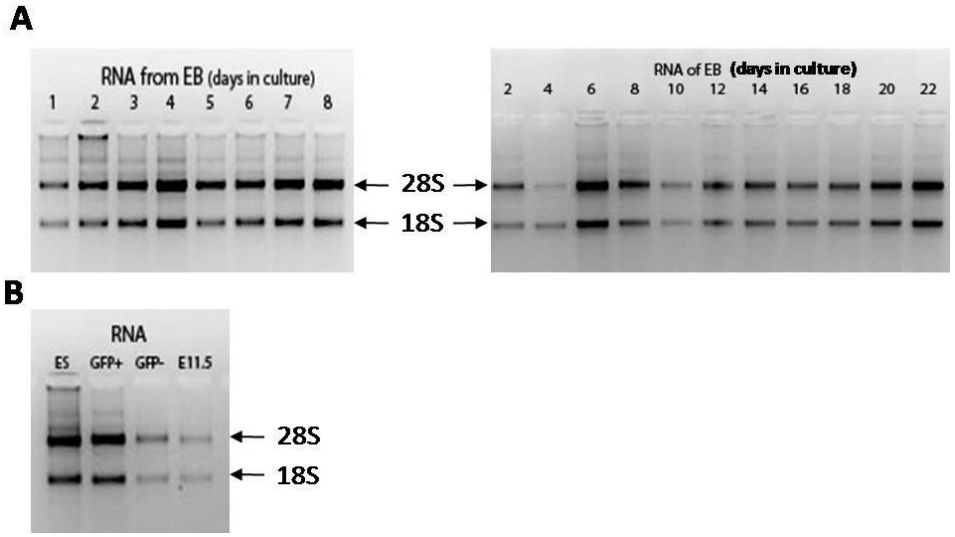

Figure 2.5 Electrophoresis gels of RNA isolated from EBs. A) short-term culture (1-8 days) and long-term culture (2-22 days); B) GFP+ and GFP- cells after FACS sort.

2.15.3 DNase treatment

Before cDNA synthesis, RNA was treated with DNase I (1000U/ml) (Promega) to degrade any contaminating genomic DNA. 8 µl of RNA solution was transferred to a fresh 0.2 ml microfuge tube and 1 µl of DNase buffer (Promega) plus 1 µl of DNase I was added and incubated at 37ºC for 30min. To stop the reaction, 1µl of STOP buffer (Promega) was added and the solution was incubated for a further 15min at 60ºC.

2.15.4 cDNA synthesis

For cDNA synthesis, 5 µl of DNase-treated RNA were mixed with 5µl of Sigma water (Sigma) and 2µl of random hexamers (100ng/µl) (ABgene),

incubated at 80ºC for 3 min to denature RNA secondary structure and any hexamer duplexes, then chilled on ice and pulse centrifuged to collect all the contents. 4 µl of 5x 1st strand buffer (Invitrogen), 2 µl DTT (0.1 M) (Invitrogen) and 1 µl dNTP mix (10 mM) (Bioline) were then added, the final solution gently mixed by pipetting and incubated at 42ºC for 2 min to allow random hexamers to anneal to template RNA. 1µl of reverse transcriptase (SuperScript III) (Invitrogen) (200 U) was added and the reaction was incubated for 50 min at 42ºC for cDNA synthesis. The reaction was stopped by heat inactivation of the reverse transcriptase at 65ºC for 10 min. The solution was then pulse centrifuged to collect all contents and the cDNA diluted with nuclease-free water to a final concentration of 200ng/µl. Amount of DNA was quantified using Nanodrop.

2.15.5 Polymerase chain reaction

PCR reactions were performed in a volume of 25µl comprising: 12.0 µl of nuclease-free water (Sigma), 2.5 µl PCR buffer (10x NH_4 Reaction Buffer) (Bioline), 0.5 µl $MgCl_2$ (25mM stock) (Bioline), 0.5 µl dNTP mix (10mM stock) (Bioline), 5.0 µl cDNA solution (200ng/µl), 2.0 µl forward primer (6.25pmol/µl stock) (see Table 2.3), 2.0 µl reverse primer (6.25pmol/µl stock) (see Table 2.3), 0.5 µl Taq DNA Polymerase (Bioline). The thermal cycler (GeneAmp PCR Systems 9700) was set as follows: 1 cycle of 95^{o} C

for 5min (denaturation), 36 cycles of 95^{o}C for 6 sec (denaturation), annealing temp depends on a primers and was set for 30 sec – see table 2.3, and 72^{o}C for 30 sec (elongation), followed by 1 cycle of 72^{o}C for 5 min (final elongation) and were then held at 4ºC.

2.15.6 Electrophoresis gels

2% (w/v) agarose gels in TAE buffer (see chapter 2.15 for recipes) were used for electrophoresis. Following cooling the gel to ~60ºC, 5µl of ethidium bromide was added to 120ml of TAE buffer before pouring the gel. The Bioline hyperladder IV was used as a DNA molecular weight marker (100 – 1000 bp bands).

2.16 Statistical analysis

For all statistical analysis the same numbers of samples (3) /pictures per sample (6-10) were analysed. Basic functions used were: average (ave), standard deviation (St.dev.), standard error (St. err.), percentage (%) and Student's t-test (tt). Error bars present on all graphs are calculated on the standard error basis.

2.17 List of protocols for solutions

2.17.1 Cell/tissue culture media

10%FCS DMEM

- 10% FCS (PAA Laboratory)
- DMEM (Invitrogen)

MEF medium

- 10% FCS (PAA Laboratory)
- 1% (v/v) 200mM L-glutamine (Invitrogen)
- 1% (v/v) non essential amino acids (Sigma)
- 1% (v/v) penicillin/streptomycin (Sigma)
- 0.01% (v/v) 50mM 2-mercaptoethanol (Invitrogen)
- DMEM (Invitrogen)

ESC medium

- 10% FCS (PAA Laboratories)
- 1% (v/v) 200mM L-glutamine (Invitrogen)
- 0.15% (v/v) 100mM monothioglycerol (Sigma)
- 1% (v/v) penicillin/streptomycin (Sigma)
- 1000U/ml LIF (Chemicon)
- Advanced DMEM (Invitrogen)

ES monolayer differentiation medium

- 10% FCS (PAA Laboratories)
- 1% (v/v) 200mM L-glutamine (Invitrogen)
- 0.15% (v/v) 100mM monothioglycerol (Sigma)
- 1% (v/v) penicillin/streptomycin (Sigma)
- DMEM or IMDM (Invitrogen)
- 2ng/ml Activin A (R&D Systems) - added to the medium just before adding to the cells
- 0.25ng/ml BMP4 (R&D Systems) – added to the medium just before adding to the cells

ES/EB medium

- 10% FCS (PAA Laboratories)
- 1% (v/v) 200mM L-glutamine (Invitrogen)
- 0.15% (v/v) 100mM monothioglycerol (Sigma)
- 1% (v/v) penicillin/streptomycin (Sigma)
- 1000U/ml LIF (Chemicon)
- IMDM (Invitrogen)

EB medium

- 15% FCS (PAA Laboratory)
- 1% (v/v) 200mM L-glutamine (Invitrogen)
- 0.45% (v/v) 100mM monothioglycerol (Sigma)
- 1% (v/v) Interleukin-Transferin-Selenium (Invitrogen)

- 1% (v/v) penicillin/streptomycin (Sigma)
- 0.1% (v/v) 500mM ascorbic acid (Sigma)
- IMDM (Invitrogen)

Kidney culture medium

- 10% FCS (PAA Laboratory)
- 1% (v/v) 200mM L-glutamine (Invitrogen)
- 1% (v/v) penicillin/streptomycin (Sigma)
- MEME (Invitrogen)

2.17.2 Buffers and solutions

Phosphate buffered saline (PBS) 10x

From IHC world, 2009

- 80.0 g NaCl (Normapur)
- 2.0 g KCl (BDH Chemical Ltd.)
- 14.4 g Na_2HPO_4 dibasic (AnalarR)
- 2.4 g KH_2PO_4 monobasic (AnalarR)
- Up to 1L distilled H_2O

pH adjusted to 7.4 – 7.6

Tris Buffered Saline (TBS) 10X

From IHC world, 2009

- 61g Tris base (Sigma)

- 90g NaCl (Novapur)
- Up to 1L distilled water

pH adjusted to 7.4-7.6

0.1%BSA

- 1 ml 10% (w/v) BSA
- 100 ml PBS^{Ca+Mg+} (Sigma)

Sterilised before use

0.1% (w/v) Gelatine

- 1 g porcine gelatine type A (Sigma)
- 1 L H_2O

Autoclaved before use

4% (w/v) Paraformaldehyde (PFA)

- 4 g PFA (Sigma)
- 100 ml PBS

pH adjusted to 7.4-7.6
PFA should be weighted in the fume cupboard as it is toxic. 4% PFA should be stored up to 7 days in the dark at 4°C, then discarded.

15% (w/v) Sucrose

- 15 g sucrose (Sigma)
- 100 ml PBS

Autoclaved before use

80% (v/v) glycerol

- 80 ml glycerol (Sigma)
- 20 ml H_2O

Autoclave before use

Subbing solution

- 2.5g porcine gelatine type 1 (Sigma)
- 500 ml distilled water
- 0.25g $CrKSO_4x12H_2O$

2.17.3 Molecular biology buffers

Tris-acetate- EDTA (TAE) 50X

From IHC world, 2009

- 242 g 40 mM Tris base (Sigma)
- 57.1 ml 20 mM glacial acetic acid (AnalarR)
- 100 ml 0.5M EDTA (Sigma)
- up to 1L distilled H_2O

pH adjusted to 8.0

2% agarose gel

- 2.4 g agarose (Bioline)
- Up to 120 ml TAE

- 5 μl ethidium bromide

Gel loading buffer 6x

- 3 ml glycerol (Sigma)
- 25 mg bromophenol blue (Sigma)
- 10 ml of distilled H_2O

Chapter 3: Directing mesoderm differentiation

3.1 Introduction

In order to test the hypothesis that mESC differentiated towards the mesodermal lineage would have an increased ability to generate functional renal tissue, it was first necessary to optimise conditions for mESC differentiation. It is well known that kidneys develop from mesoderm, the germ layer between ectoderm and endoderm (Saxen, 1987). Mesoderm differentiation in the mouse embryo starts at embryonic day (E) E6.0-7.5 during gastrulation (Rivera-Perez, 2005). During this stage, signaling centres (Spemann's organizer in amphibians or Hensen's node in birds and its equivalent in mammals – primitive streak) develop to regulate the gastrulation processes. Cells migrate through the primitive streak to reach their final location and fate (Gilbert, 2006; Tam, 1997). There are a few types of mesoderm, but the first is formed through cell ingression and gives rise to extraembryonic tissues. Later the primitive streak elongates to the distal end of the embryo and paraxial mesoderm (PM) emerges and is followed by intermediate (IM) and lateral plate mesoderm (LM) formation (Nagy, 2003; Rivera-Perez, 2005), which develop in this particular order (Tam, 1997). Each of these tissues has its own very specific marker(s): Tbx6 and Foxc1 for PM; Osr1 for IM; Foxf1 for LM.

In situ hybridization (ISH) studies on gene expression profiles have shown that one of the first genes expressed in the nascent mesoderm is the pan-

mesoderm marker *brachyury* (*T,* Bry). Its expression occurs at E5.5 in the proximal epiblast and later in the early primitive streak (E6.5) and deteriorates by day E7.5 (Chapman, 1996; Rivera-Perez, 2005). *T* expression is followed by expression of *Foxc1*, a gene which is highly expressed first by PM and later also by IM (Kume, 2000a; Sasaki, 1993) but at lower levels of expression. This signal is immediately followed by *Tbx6*, another PM marker. *Tbx6* shares expression domains with *T* in the primitive streak and tail bud, but only *Tbx6* is found in the mid and late primitive streak in the region of somitic (paraxial) mesoderm of the trunk (Chapman, 1996). Expression of *Tbx6* is followed by expression of the IM marker *Osr1* at E7.5. *Osr1-/-* mutants do not show any signs of metanephric kidney development, suggesting an important role during gastrulation and organogenesis of the kidney (Wang, 2005b). The LM marker, *Foxf1*, was found at day E8.5 of mouse development within the posterior primitive streak mesoderm, where it plays a role in mesenchyme migration (Malin, 2007). *Foxf1* knock-out studies show its importance in the proper development of the embryonic and extraembryonic structures, as all *Foxf1-/-* embryos died by day E10 (Mahlapuu, 2001).

Table 3.1 In situ hybridisation studies identified timing of gene expression for different populations of mesoderm.

E	M-T	PM-FOXC1	PM-TBX6	IM-OSR1	LM-FOXF1
5.0					
5.5	+[1]				
6.0	+[1]				
6.5	+[1]	+[2]			
7.0	+[1]	+[2]	+[1]		
7.5	+[1]	+[2]	+[1]	+[4]	
8.0		+[2]	+[1]	+[4]	
8.5		+[2,3]	+[1]	+[4]	+[5]
9.0		+[2,3]	+[1]	+[4]	+[5]
9.5		+[2,3]	+[1]	+[4]	+[5]

E-embryonic day, M-mesoderm, PM-paraxial mesoderm, IM-intermediate mesoderm, LM-lateral plate mesoderm, T – brachyury, +[1]- Chapman et al. 1996; +[2]- Sasaki et al. 1993; +[3]- Kume et al. 2000, +[4] Wang et al. 2005-, +[5] - Mahlapuu et al. 2001

mESC are derived from 4 to 5-day-old blastocyst. They are pluripotent, meaning that they are able to give rise to all cell types of the body including germ cells (Nagy, 1993) and can self-renew in culture (Evans, 1981; Martin, 1981). Self-renewal and mESC pluripotency are maintained in culture due to the presence of MEFs (mouse embryonic fibroblasts) and/or by supplementation of media with LIF (leukaemia inhibitory factor) (Williams, 1988). During such conditions, mESC express pluripotency markers such as Oct4 and nanog. Upon LIF withdrawal from mESC in monolayer culture, the cells down-regulate expression of Oct4 and nanog, and undergo a dramatic change in shape, from tightly packed rounded cells with high nucleus-to-cytoplasm ratio to flattened, spread cells with lower nucleus-to-cytoplasm ratio (Notariani, 2006). On the other

hand, LIF removal and change of culture conditions from monolayer to suspension (non-adherent dishes) allows for cell aggregation and embryoid body (EB) formation (Murray, 2004). EB development resembles normal mouse development and since the 1980s they have been used as a model system for studying the early stages of mouse embryo development (Robertson, 1987). The first cells that differentiate in EBs are those at the periphery, which down-regulate Oct4 and nanog and become primitive endoderm cells. The primitive endoderm cells deposit a basement membrane between themselves and the inner cells of the EB, and

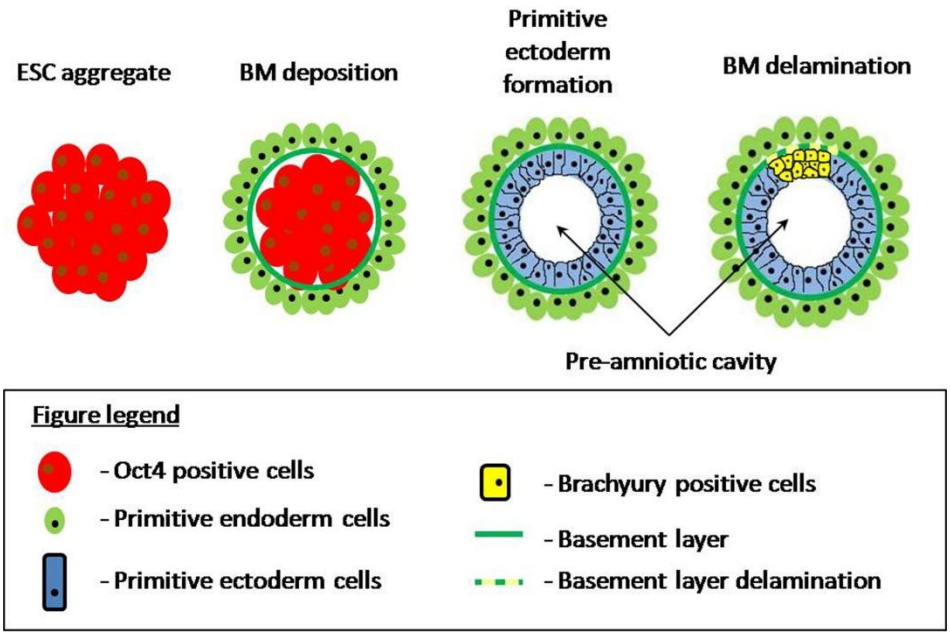

Figure 3.1 Schematic of the embryoid body development based on Murray and Edgar, 2000.

also give rise to parietal and visceral endoderm cells. Inner cells in contact with the basement membrane become polarised to form primitive ectoderm, which produces signals that cause the cells at their apical surface to undergo cell death, giving rise to a proamniotic-like cavity(Murray, 2000). As the EB matures, the primitive ectoderm cells undergo a process that resembles gastrulation (Smyth, 1999), where cells delaminate from the primitive ectodermal epithelium and up-regulate *T* (Fujiwara, 2007) (Fig.3.1).

Several protocols have been developed to differentiate mESC into mesoderm in culture. Some complex protocols involved the use of serum free medium and/or addition of different growth factors to cells in monolayer (Notariani, 2006; Yasunaga, 2005). The first protocol involved the use of SFO3 medium (Sanko Junyaku, Tokyo, Japan), which was not available for overseas customers, and supplemented with activin A (Yasunaga, 2005). A second protocol described in 'Embryonic Stem Cells – practical approach' book required co-culture of mESC with a OP9 feeder cells monolayer and supplementation of media with VEGF and BMP4 (Notariani, 2006). In the first protocol, mesoderm differentiation (recognised as a goosecoid positive (Gsc+) and negative for Sox17 (Sox17-)), was a side product of the differentiation mESC into definitive endoderm (Gsc+ Sox17+), whereas, in the second protocol, mesoderm differentiation was a first step in the differentiation of mESC into

hemangioblasts. Other methods were more simple, involving EB formation in the presence of high concentration of foetal calf serum (FCS) (Fehling, 2003; Johansson, 1995). Mesodermal differentiation of mESC was obtained in cells in suspension culture following 4-5 days in culture, in Iscove's Modified Dulbecco's Medium (IMDM) or Dulbecco's Modified Eagle's Medium (DMEM) supplemented with 15%FCS (Fehling, 2003; Johansson, 1995). In both cases the efficiency of mesodermal differentiation was high (~80%). When EBs were cultured in serum free chemically defined medium, they required additional supplementation of Activin A to support differentiation of dorsoanterior-like mesoderm or BMP4 to support posteroventral-like mesoderm (Johansson 1995). Activin A and BMP4 belong to the TGFβ superfamily, and are known to play important roles during *in vivo* development of the fruit fly (*Drosophila melanogaster*), amphibians (*Xenopus laevis*), birds (*Gallus gallus domesticus*) and mammals (*Mus musculus*) (Asashima, 1990; James, 2005a; Kaufmann, 1996; Kingsley, 1994).

The aim of my work was to first compare the efficiency of the previously published methods for generating mesoderm in the E14 mESC line, in order to establish which method generated the highest number of mesodermal cells and would be reproducible. For that purpose, a brachyury-GFP (Bry-GFP) knock-in ESC line (Fehling, 2003) was used. The GFP was knocked-in to the first exon of the Bry gene locus rendering

one copy of the gene non-functional. These cells have been used previously to establish hemangioblast differentiation (Fehling, 2003) and hepatocyte differentiation (Kubo, 2004).

This chapter will describe:

- the optimisation of culture conditions that lead to efficient mesoderm differentiation
- the purification of mesodermal cells (Bry-GFP+) from EBs
- the characterisation of GFP+ and GFP- cells
- the expression profile of key mesodermal and MM-specific genes during EB development.

3.2 Results

In order to promote mesoderm differentiation from ESC, culture conditions were optimized and expression of the key pan-mesodermal gene – *Brachyury* (*T, Bry*) was investigated. To be able to follow cell differentiation in live cells, Bry-GFP cells (Fehling, 2003) were used. The GFP cassette knocked into the Brachyury locus causes cells to become fluorescent (green) when cells differentiate into mesoderm and express *T*. The Bry-GFP cells were cultured in both monolayer and suspension culture systems for optimisations of the conditions for mesodermal differentiation.

3.2.1 Directing mesoderm differentiation in monolayer culture

Cell densities for the monolayer culture assay were: 500 cells cm^{-2}, 1000 cells cm^{-2}, 2500 cells cm^{-2}. Bry-GFP cells were seeded in 2 different media: 10% FCS DMEM (Dulbecco's Modified Eagle Medium) and 10% FCS IMDM and both were supplemented with Activin A (2ng ml^{-1}) and BMP4 (0.25ng ml^{-1}) (Johansson, 1995). Cells cultured at all three plating densities in 10% FCS DMEM detached from the culture dish by day 5 of culture (data not shown) whereas those cultured in IMDM supplemented with 10% FCS at 500 cells cm^{-2} started to change morphology and many no longer displayed the typical characteristics of undifferentiated mESC. Generally, the cells became more spread and the nuclear-to-cytoplasmic ratio decreased, with cells adopting an epithelial-like morphology (Fig.3.2). However, these conditions did not induce mesodermal differentiation, as no signs of GFP fluorescence were observed at any day of the experiment (data not shown). Moreover, immunostaining of these cells with *T* antibody showed lack of T protein and supported the result obtained with the GFP fluorescence. To verify that the cells had differentiated, immunostaining for the pluripotent markers Nanog and Oct4 was performed. The results showed that although a few cells were still positive for Nanog and Oct4, the majority were negative, showing that most of the cells had differentiated.

In the developing embryo, *T* expression is under the control of Wnt/β-catenin signalling, and thus the presence of nuclear β-catenin, is an early

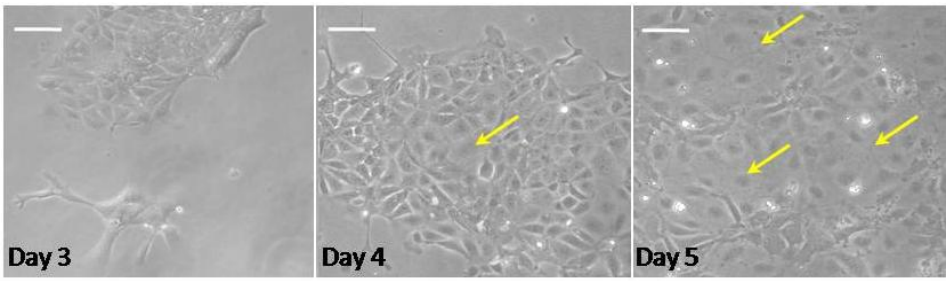

Figure 3.2 Differentiation of mESC in monolayer culture system. Phase contrast pictures showing differentiation at day 3, 4 and 5 of culture at density of 500 cells cm-2 in 10%FCS IMDM and visible changes in cell morphology (epithelial-like cells – yellow arrows); Scale bar 100μm.

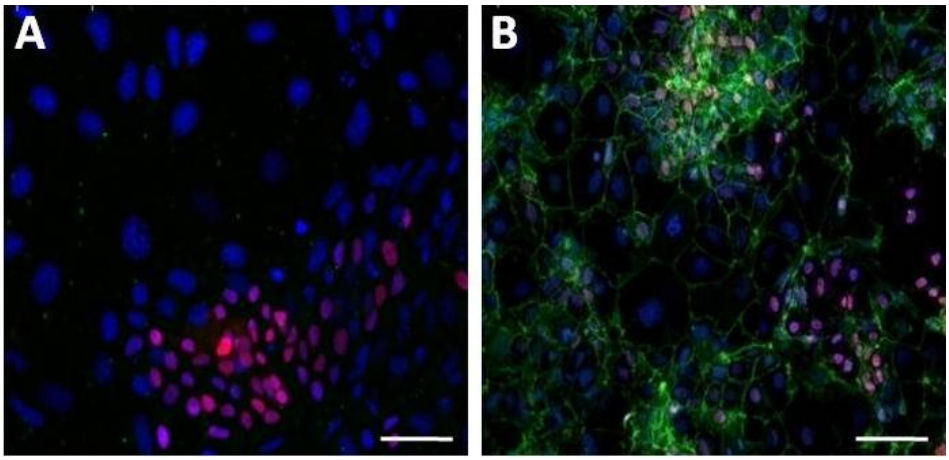

Figure 3.3 Fluorescent staining of BRY-GFP cells cultured for 5 days in 10%FCS IMDM at 500cells cm^{-2}. A) Bry (green) and Nanog (red) fluorescent staining showing lack of Brachyury protein and persistence of some undifferentiated cells. Nuclei were counterstained with DAPI (blue). B) β-catenin (green) and Oct4 (red) fluorescent staining show presence of a few undifferentiated cells and absence of any cells with nuclear β-catenin. β-catenin staining at cell-cell contacts show presence of cells with low nucleus to cytoplasm ratio which had differentiated, but not towards mesoderm. Nuclei counterstained with DAPI – blue. Scale bar: A –50μm; B – 100μm.

marker for nascent mesoderm (Lindsley, 2006). Therefore, immunostaining was performed to determine if the differentiated cells expressed nuclear β-catenin. The results showed, that β-catenin was located in the cell membrane rather than the nucleus, confirming that the cells had not differentiated towards the mesodermal lineage (Fig. 3.3). Cells seeded at densities 1000 cells cm^{-2} and 2500 cells cm^{-2} in 10% FCS IMDM medium grew in a multilayer, becoming overgrown by day 5 and were therefore not analysed further (data not shown). These results showed that using the culture conditions described above, the monolayer system was not effective in directing mesoderm differentiation as neither GFP expression was found, nor Brachyury protein.

3.2.2 Directing mesoderm differentiation in suspension culture

To determine the effect of cell density on mesoderm differentiation in EBs in suspension culture, two ranges of cell densities were tested. The low cell density range included the following seeding densities: $5x10^3$ cells ml^{-1}, $25x10^3$ cells ml^{-1}, $50x10^3$ cells ml^{-1}, $75x10^3$ cells ml^{-1}, $10x10^4$ cells ml^{-1}, and the high cell density range included the following seeding densities: $25x10^4$ cells ml^{-1}, $50x10^4$ cells ml^{-1}, $75x10^4$ cells ml^{-1} and $1x10^6$ cells ml^{-1}. EBs were also cultured in the following four media to determine which condition supported maximal mesodermal differentiation: 10% FCS DMEM, 15% FCS DMEM and 10% FCS IMDM, 15% FCS IMDM. Initial observations showed that in all media types, high cell densities (≥ 250K

cells ml^{-1}) did not induce mesoderm differentiation over the time course of the experiment (8 days). Also, DMEM medium did not induce mesoderm differentiation as effectively as IMDM (Fig. 3.4), irrespective of the concentration of the FCS used (not shown).

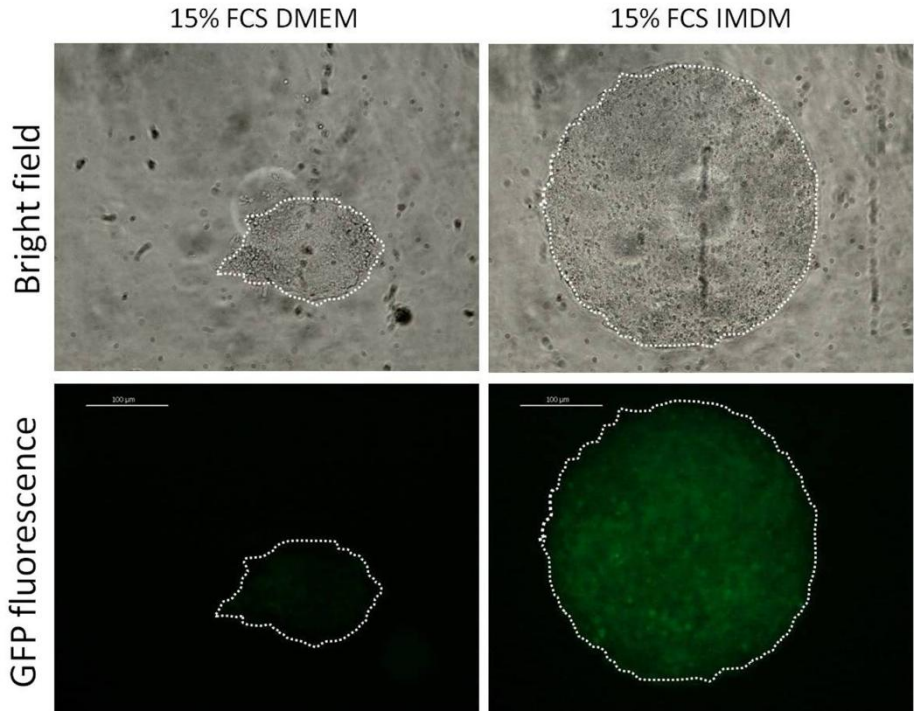

Figure 3.4 Difference in GFP fluorescence in EBs cultured 4 days in DMEM and IMDM medium. Cells differentiating in IMDM medium showed high GFP expression at day 4 in 15% FCS concentration at density of $75x10^3$ cells ml^{-1} in contrast to cells differentiating in DMEM which showed very low GFP expression at day 4 in 15% FCS concentration and $75x10^3$ cells ml^{-1}. Scale bar – 100μm.

Optimal conditions for GFP – brachyury expression

During EB culture, only IMDM medium supported efficient mesoderm differentiation. At day 3 of culture in 15% FCS IMDM medium, EBs at all

lower densities (<100K cells ml^{-1}), showed the first signs of GFP fluorescence, indicating *Bry* expression and mesoderm differentiation. EBs cultured in 10% FCS IMDM also showed signs of mesoderm differentiation, however, it was found that the higher the seeding cell density, the later GFP fluorescence occurred (Tab 3.2).

To confirm that GFP expression in EBs reflected expression of T protein, day 4 EBs cultured in 15% FCS IMDM were immunostained for T protein. The results showed that many cells within the EBs expressed nuclear T (Fig.3.5). To determine the time-course of induction of *T* mRNA, semi-quantitative RT-PCR was performed using RNA derived from ESC and EBs (day1 – day8) cultured at different densities in 10% and 15% FCS IMDM. The reference gene was *Gapdh* (glyceraldehyde 3-phosphate dehydrogenase). RT-PCR analysis showed good correspondence between *T* gene expression and GFP. In other words, *T* was found to show delayed expression in 10% FCS IMDM medium in comparison to 15% FCS IMDM medium, where at all cell seeding densities *T* was expressed at day 3 of culture. Furthermore, in both concentrations of FCS, *T* expression was delayed at higher cell densities, and at the highest density used (250K ml^{-1}) expression levels were dramatically reduced (Fig. 3.6).

These results showed that suspension culture is a good and effective system to direct mesoderm differentiation. Analysis of GFP fluorescence together with RT-PCR results for *T* expression showed that 15% FCS IMDM medium induced efficient differentiation of mesoderm. In cells

Table 3.2 Summary of GFP expression in cells cultured in different conditions

EB day	1	2	3	4	5	6	7	8	1	2	3	4	5	6	7	8
density	10%FCS IMDM								15%FCS IMDM							
5000			√	√	√	√					√	√	√			
25000			√	√	√	√					√	√	√	√		
50000				√	√						√	√	√	√		
75000				√	√						√	√	√	√		
100000				√	√	√						√	√	√		
density	10%FCS DMEM								15%FCS DMEM							
5000											√					
25000				√												
50000				√												
75000				√												
100000				√												

Thick √ means that GFP fluorescence was observed in >50% EBs; thick √ means that GFP fluorescence was observed in <50% EBs

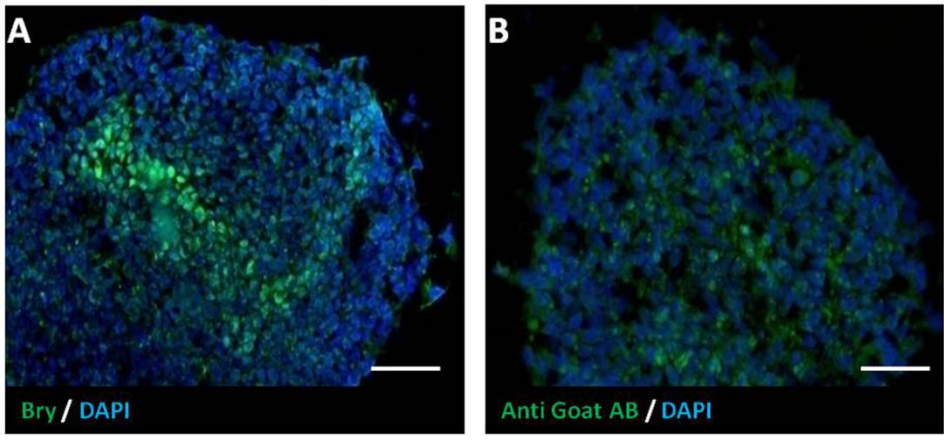

Figure 3.5 Photomicrograph of fluorescent staining of frozen section of EB at day 4 of development. A) Presence of Brachyury (green) positive cells in EB; B) Control of staining where primary antibody was omitted. Scale bar – 50µm.

cultured in low serum concentration *Bry* expression was delayed in higher seeding cell densities, while in high serum concentration cells in all densities showed *T* expression at day 3, meaning that there was no delay in differentiation irrespective of cell seeding density. Therefore, 15% FCS IMDM was chosen as an optimal condition to direct mesoderm differentiation.

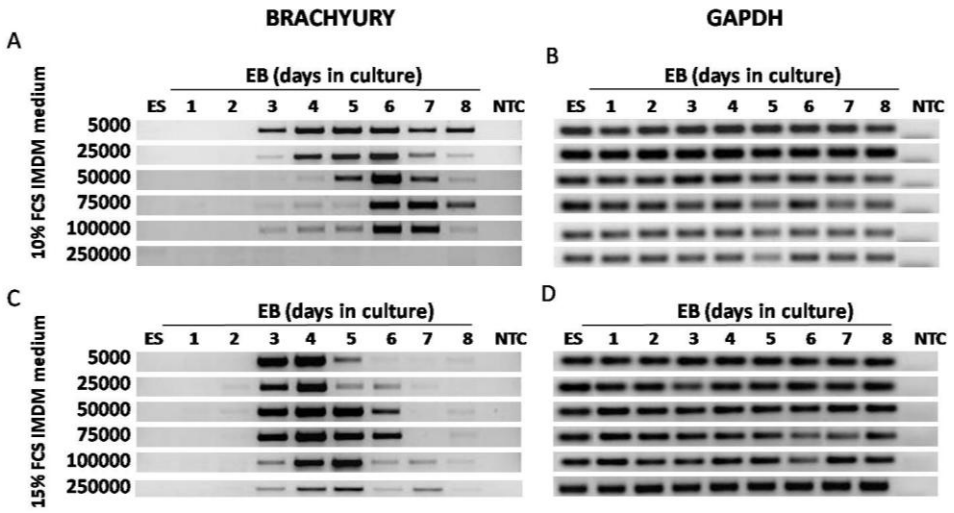

Figure 3.6 Semi-quantitative RT-PCR analysis of brachyury expression in EBs culture. A) EBs cultured in 10% FBS IMDM showed T expression at day 3 at the lowest seeding density and in higher densities Bry expression was delayed to not be present in the 250K cells ml^{-1}; B) housekeeping gene GAPDH levels for 10%FBS IMDM medium; C) EBs cultured in 15%FBS IMDM showed expression at day 3 in all seeding densities, but in higher (≥100K cells ml^{-1}) Bry expression was at lower level; D) housekeeping gene GAPDH levels for 15%FCS IMDM medium. Experiment was performed three times; the results shown being representative of those observed in the other two biological replicates. EB – embryoid bodies, ES – embryonic stem cells, NTC – no template control.

The morphology of the embryoid bodies

The difference in GFP fluorescence between EBs cultured in IMDM and DMEM medium was shown above. Moreover, EBs cultured in DMEM medium showed different, to EB cultured in IMDM medium, morphology (Fig. 3.7). The DMEM EBs developed visible basement membrane (Reichert's membrane, Fig. 3.7 arrow) and plenty of primitive endodermal cells surrounding it, whereas EB cultured in IMDM medium did not develop basement membrane and primitive endodermal cells (Fig. 3.7).

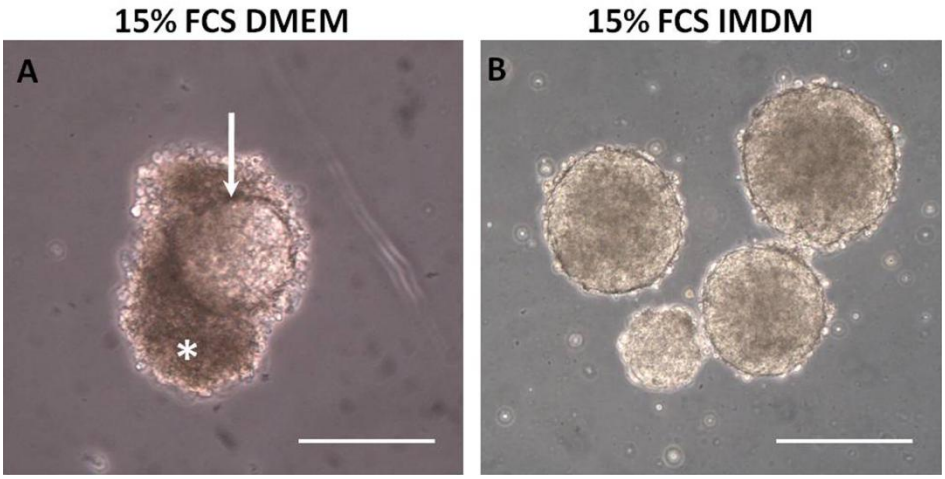

Figure 3.7 Differences in morphology of EBs cultured in DMEM and IMDM. Bright field photographs presenting A) high number of primitive endodermal cells (*) surrounding EB basement membrane (arrow) in EBs cultured in DMEM medium and B) lack of basement membrane and primitive endodermal cells in EBs cultured in IMDM medium. Scale bar – 100μm.

Frozen sections of day 7 EBs cultured in 15% FCS IMDM were analysed morphologically and immunostained for laminin to detect the presence of basement membranes. The results showed that only ~10% of EBs cultured

in 15% FCS IMDM developed a defined layer of peripheral extra-embryonic endoderm with underlying basement membrane, primitive ectodermal epithelium and central cavity by day 7 of culture, whereas the majority of EBs appeared to be simple aggregates with no obvious structural features (Fig. 3.8). To investigate if the cells within the simple EBs were still undifferentiated, immunostaining was performed for the pluripotency marker, Oct4. The results showed that in day 7 simple EBs, although some Oct4+ cells were present in the centre of EB, the majority of outer cells had down-regulated Oct4, indicating that they had differentiated (Fig. 3.8B).

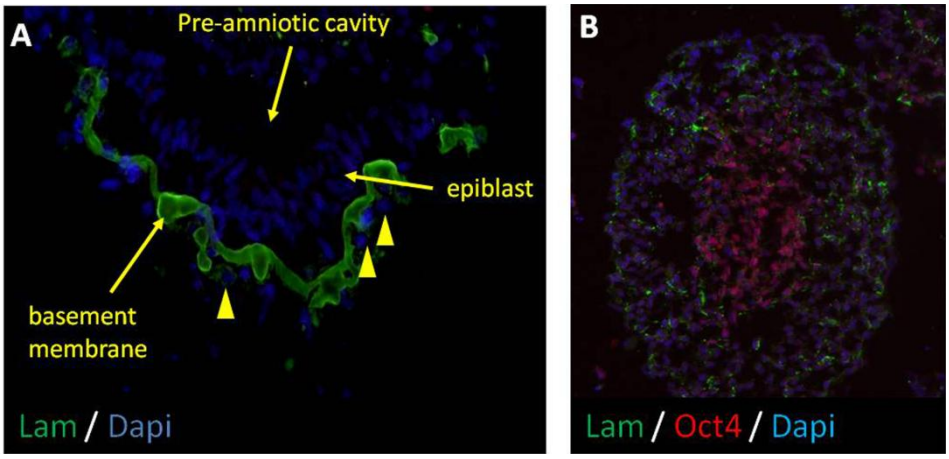

Figure 3.8 Development of EBs in conditions optimized for mesoderm differentiation. A) By day 7, 10% of EBs developed laminin layer (green) between extraembryonic endoderm cells (yellow arrowheads) and primitive ectoderm epithelium. Cells that do not have contact with basement membrane undergo programmed cell death leading to cavity formation (Coucouvanis E., 1995). B) Majority of EBs stayed underdeveloped as no signs of basement membrane and/or polarised epithelium formation were seen.

These results may suggest that DMEM medium is optimal for endodermal cells differentiation, whereas IMDM is optimal for mesodermal differentiation as was shown by GFP expression (Fig.3.4). Therefore, the 15% FCS IMDM medium was used in further part of this study as conditions optimal for mesodermal differentiation.

3.2.3 The proportion of mesodermal cells in embryoid bodies cultured under optimal conditions

To determine the proportion of GFP positive (Bry+) cells present in EB populations cultured in conditions optimal for mesodermal differentiation (15% FCS IMDM) and to establish the optimal seeding cell density, Bry-GFP cells were used to generate EBs at seeding densities of $25x10^3$ cells ml^{-1} and $75x10^3$ cells ml^{-1}. At day 4 and 6 of development EBs were dissociated into a single cell suspension and the proportion of GFP+ cells was analysed using Fluorescent Activated Cell Sorting (FACS). FACS results demonstrated that at both seeding densities, about 60% of the population was GFP+ at day 4 of development, but this dropped to around 10% at day 6 (Fig. 3.9). The density of $75x10^3$ cells ml^{-1} was selected for future experiments to improve yield. Therefore, the established conditions to efficiently direct mesoderm differentiation of mESC were as follows: 15% FCS IMDM medium and density of $75x10^3$ cells ml^{-1} in suspension culture for 4 days.

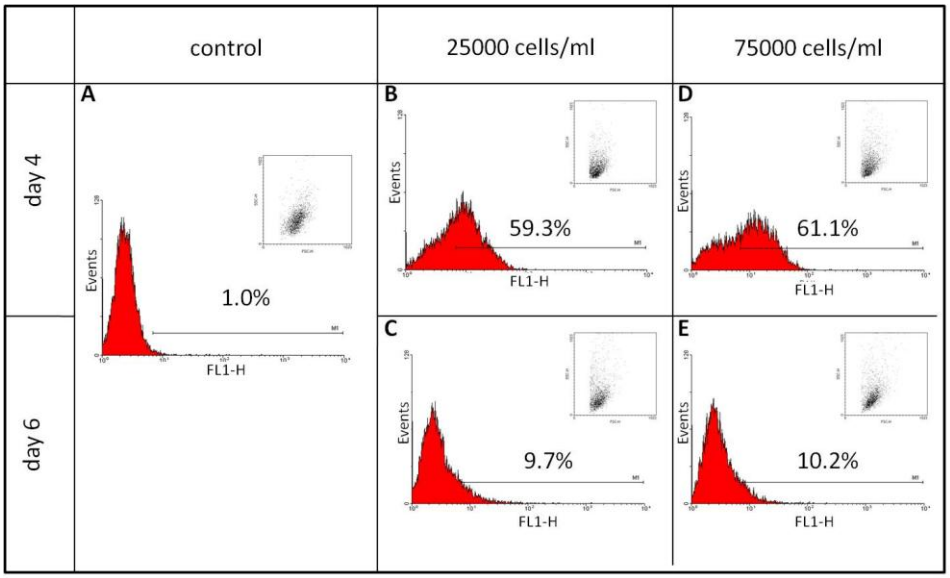

Figure 3.9 Percentage of GFP+ cells. A) E14.1 cells without GFP insertion cultured in the same conditions as BRY-GFP samples at random density; B) BRY-GFP cells cultured in 15%FCS IMDM at density of $25x10^3$ cells ml^{-1} showed ~60% GFP+ cells at day 4 of differentiation; C) GFP+ cells number dropped till 10% by day 6 of differentiation at density of $25x10^3$ cells ml^{-1}; D) BRY-GFP cells cultured in 15%FCS IMDM at density of $75x10^3$ cells ml^{-1} showed ~60% of GFP+ cells at day 4 of differentiation; E) GFP+ cells number dropped till ~10% by day 6 of differentiation at density of $75x10^3$ cells ml^{-1}. Experiment was performed two times, the results shown being representative of those observed in the other biological replicate.

3.2.4 Gene expression profiles of GFP+ and GFP- cells

The previous experiments established the optimal culture conditions for directing mesoderm differentiation, and showed that under these conditions, 60% of cells in day 4 EBs expressed the mesodermal marker *T*. For future work, it was necessary to isolate GFP+ cells from GFP- cells and establish their gene expression profiles. Cells cultured under optimal conditions formed embryoid bodies which were collected at day 4 of

development and sorted using FACS in order to obtain two populations: GFP+ (Bry+) cells (mesodermal cells) and GFP- (Bry-) cells (non-mesodermal cells). In order to characterise these cell populations sqRT-PCR (semi-quantitative reverse transcriptase PCR) was performed to investigate the expression of various mesoderm, endoderm, ectoderm, kidney specific and pluripotency genes. Results showed that FACS sorting purity was about 80% (Fig. 3.10A).

Therefore some GFP+ (Bry+) cells could be still found in GFP- (Bry-) fraction of cells and vice versa. Hence, it is necessary to analyse gene expression profile bearing in mind that there is a low level of contamination.

The RT-PCR results showed that GFP+ cells expressed high levels of *T*, *Foxc1* and *Tbx6*, and low level of *Osr1* and *Foxf1*. *T*, *Foxc1* and *Tbx6* expression was also detected in GFP- cells, but given that the expression levels of these genes was markedly lower than in GFP+ population, it is likely due to the presence of GFP+ cells in the GFP- cell fraction (Fig. 3.10 B, green stars). GFP+ cells showed expression of most of the endodermal markers tested: strong expression of *BMP4*, *Gata4* and *Sox17*, weak expression of *AFP* and lack of expression of *Gata5*. GFP- cells showed expression of *BMP4*, *Gata4* and *Sox17* but *Gata4* and *Sox17* expression could be due to presence of GFP+ cells within GFP- cells fraction (Fig. 3.10 B, green stars), whereas *BMP4* expression was at the same level as in

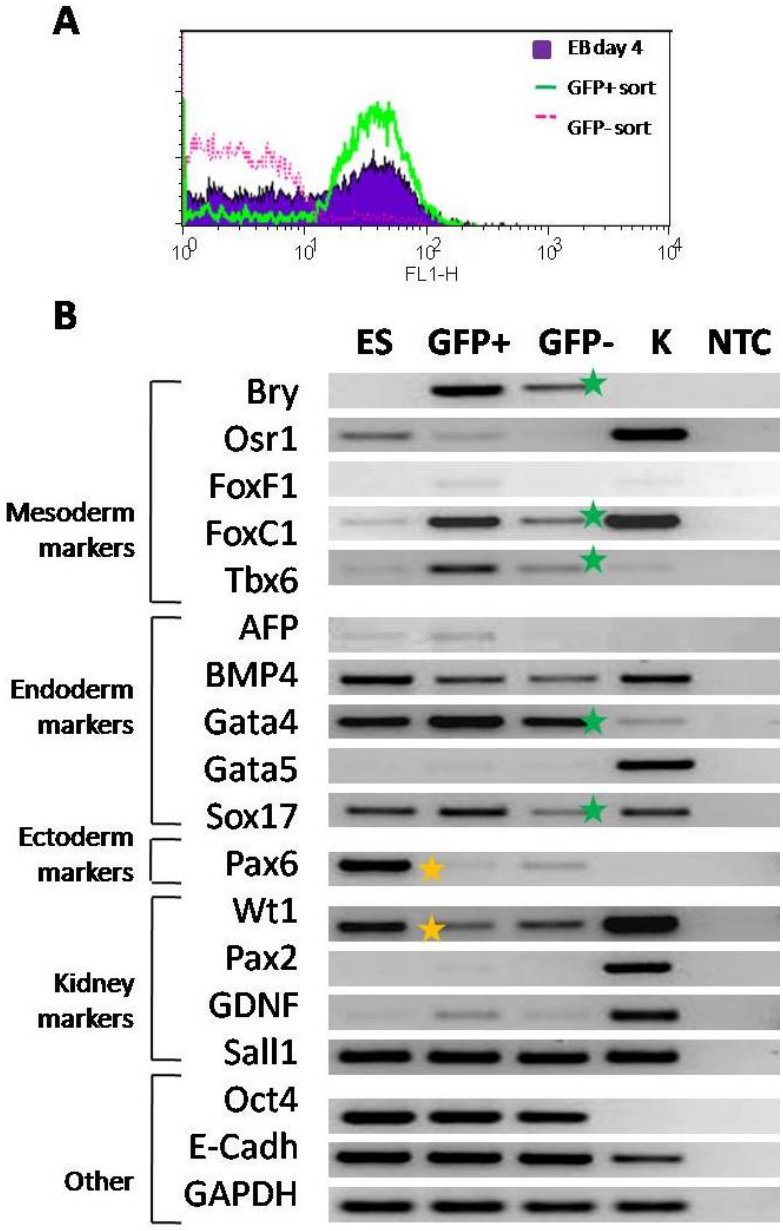

Figure 3.10 Gene expression profiles of GFP+ and GFP- cells. A) Histogram showing ~60% of the cells are GFP+ at day 4 EBs (blue), and purity (~80%) of sorted populations of cells; GFP+ (green line) and GFP- (red line); B) gene expression profile of FACS sorted cells. Green stars indicate gene expression likely to be affected by GFP+ cells within GFP- cells fraction; orange stars indicate gene expression likely to be affected by GFP- cells within GFP+ cells fraction. ES – undifferentiated mESC, GFP+ – GFP positive cells, GFP- – GFP negative cells, K – kidney at E13.5, NTC – no template control. GAPDH – reference gene. Experiment performed two times with similar results.

GFP+ cells. Therefore both populations (GFP+ and GFP-) showed similar expression of *BMP4*. The ectodermal marker *Pax6* was expressed in GFP- cells at higher levels than in GFP+ cells; therefore, expression of *Pax6* in GFP+ cells could be due to the presence of GFP- cells within the GFP+ population. A similar situation was observed with the kidney specific markers *Wt1*, where GFP- cells showed stronger expression than GFP+ cells (Fig. 3.10 B, orange stars). Of the other kidney specific genes tested, *GDNF* and *Pax2* showed stronger expression by GFP+ cells, but levels of *Pax2* were almost undetectable. *Sall1* on the other hand, was expressed by both GFP+ and GFP- at the same level. Other investigated genes included the pluripotency marker, *Oct4* and the epithelial marker, *E-cadherin* (E-cadh), both of which showed similar levels of expression in the GFP+ and GFP- populations.

3.2.5 Timing of expression of key mesodermal and kidney specific genes in embryoid bodies

Gene expression profiling in the developing mouse embryo is usually investigated by using the very sensitive but difficult and time consuming method of in situ hybridisation (ISH). ISH allows the identification of regions of specific gene expression in very early mouse embryos, starting from E5.5. Table 3.1 (see page 80) summarises the results of various ISH studies of mesodermal marker genes, giving the timing of expression in the normal mouse embryo. These studies showed that the mesodermal marker,

Brachyury, is expressed in the early mouse embryo prior to gastrulation (Rivera-Perez, 2005). Mesoderm, identified by *T* expression, gives rise to three subpopulations: PM, IM and LM. Therefore, in the developing embryo, *T* expression is followed by PM marker expression – *Foxc1* and *Tbx6*, which is in turn followed by expression of the IM marker – *Osr1*, and finally, the LM marker *Foxf1*.(Chapman, 1996; Kume, 2000a; Mahlapuu, 2001; Sasaki, 1993; Wang, 2005a).To investigate if the timing of expression of the aforementioned mesodermal markers in developing EBs resembled that observed in the mouse embryo, sqRT-PCR was used to determine the expression levels of these key genes from day 2 to day 14 of EB development. EBs were cultured under the previously defined optimal culture conditions (15% FCS IMDM, 75K cells ml^{-1}). The results showed that the expression pattern of mesodermal genes in the developing EBs was similar to that of the normal mouse embryo.

The RT-PCR showed expression of *T* at day 4 of culture, which was followed by expression of the PM markers, *Tbx6* and *Foxc1*. *Tbx6* expression peaked at day 4 and then decreased and peaked again at day 12 of culture, whereas *Foxc1* expression was observed at day 4 and gradually increased to reach maximum expression at day 12 of culture. PM marker expression was followed by the IM marker, *Osr1*, which was first detected at day 8 of culture and gradually increased till the end of the experiment (day 14). The LM marker, *Foxf1*, is the only exception to the similarity of

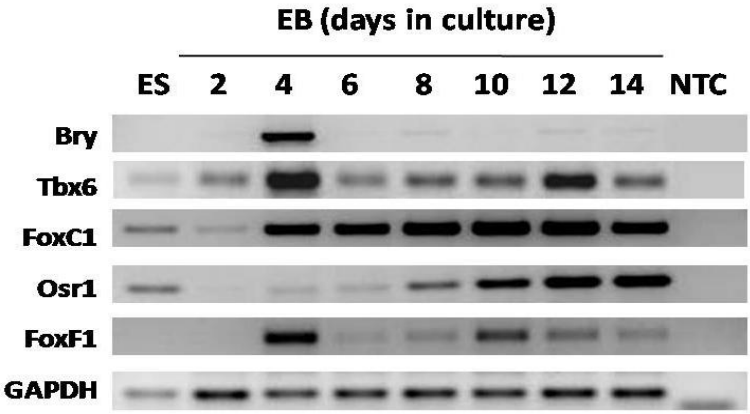

Figure 3.11 Semi quantitative RT-PCR of mesodermal markers expression profile. Electrophoresis gels presenting dynamics of expression of mesodermal markers: pan-mesoderm – Bry, PM – Tbx6 and FoxC1, IM – Osr1, LM – FoxF1 and housekeeping gene GAPDH. EB – embryoid bodies, ES – embryonic stem cells, NTC – no template control. Experiment was performed two times with similar results.

EB development in culture to the normal mouse. *Foxf1* expression was detected at day 4 of culture, the same day as *T* and PM markers, but its expression decreased and peaked again at day 10 of culture (Fig. 3.11).

Next, the expression of key kidney marker genes was detected in EBs cultured under optimal conditions. Low level of *Pax2* expression was observed at day 6 but high level of expression was not observed until day 14 of suspension culture (Fig.3.12), which followed the expression of *Osr1* (Fig. 3.11) and *Wt1* expression was detected at all time points, including the undifferentiated mESC. There was an obvious decrease in *Wt1* expression at day 4 of culture (reproducible) which increased at day 6 and stayed high until the end of the experiment. Both genes were found to be expressed at high levels at day 14 of EB differentiation (Fig. 3.12).

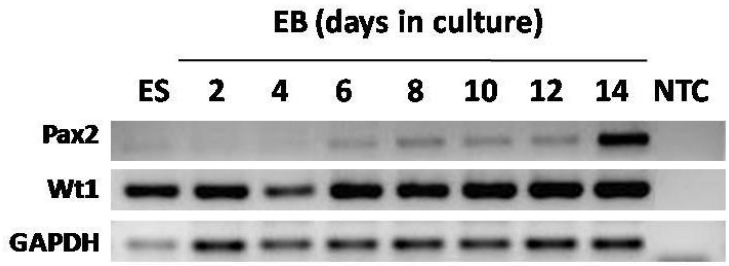

Figure 3.12 Semi-quantitative RT-PCR showing the expression profile of key kidney genes in developing EBs. Pax2 and Wt1 are the first markers to be co-expressed during kidney development by condensed metanephric mesenchyme (MM) and this electrophoresis gel showed strong Pax2 and Wt1 expression at day 14 of differentiation. Experiment performed two times with similar results.

Both genes *Pax2* and *Wt1* are known to be co-expressed in condensed metanephric mesenchyme (MM) during kidney development (Moore, 1999). Therefore, to investigate if any MM-like cells were present in developing EBs, dual immunostaining for Wt1 and Pax2 was performed on cytospinned cells of day 14 EBs to investigate if *Pax2* and *Wt1* were co-expressed in any of the EB cells (fig. 3.13).

The results showed that some of the EBs cells at day 14 of culture showed presence of both proteins, Pax2 and Wt1 (Fig 3.13 G, H), but with different locations within the cell. In other words, Pax2 was expressed in the nucleus of the cells whereas Wt1 was in the cytoplasm. Control staining, where primary antibody was omitted did not show any background staining (data not shown).

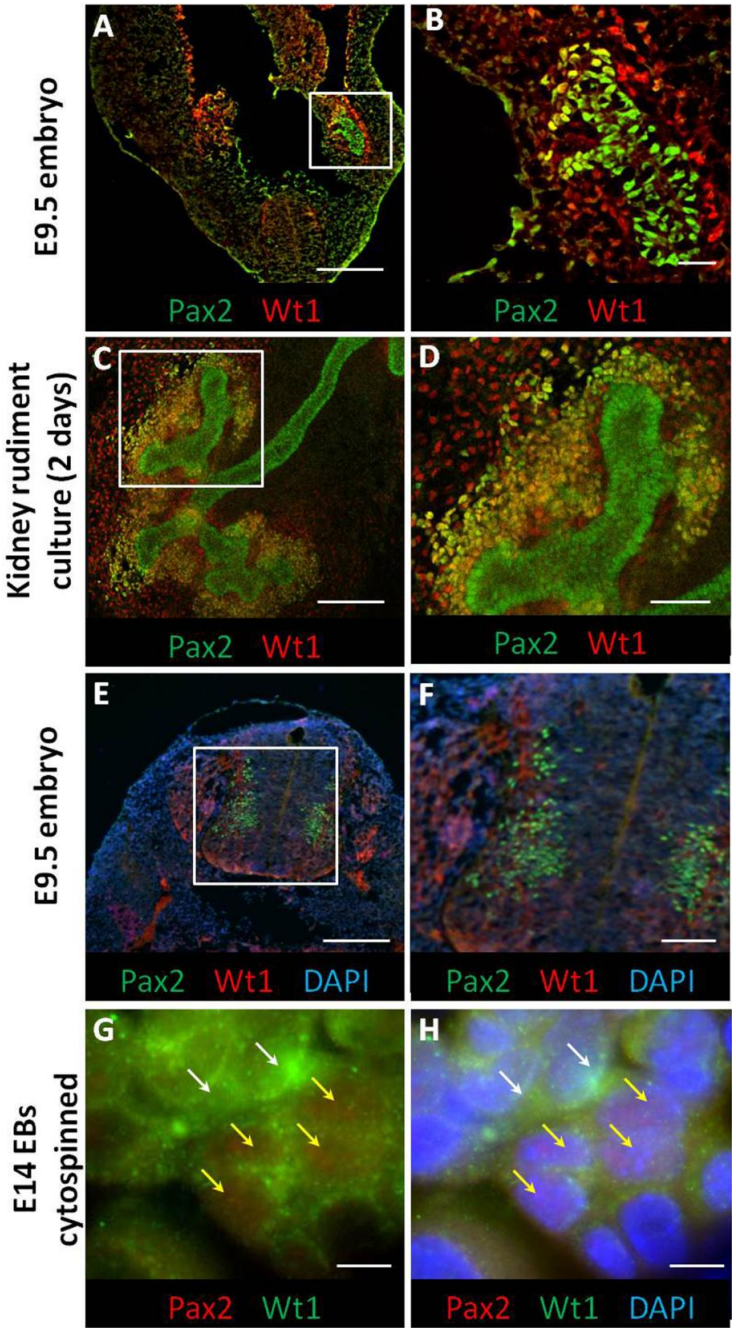

Figure 3.13 Immunofluorescent staining of Pax2 and Wt1. A-F) Pax2 (green) and Wt1 (red) staining presenting: co-expression in developing mesonephros *in vivo* at E9.5 embryo (A, B); co-expression in metanephric mesenchyme in cultured kidney rudiments (C, D); expression in mouse brain *in vivo* at E9.5 embryos (E, F) counter stained with DAPI; G-H) Pax2 (red; yellow arrows) and Wt1 (green; white arrows) expression in some cytospinned cells of EBs at day 14 of differentiation. Experiment was performed two times with similar results. Scale bars: A, C, E – 150µm, B, D, F – 50µm, G, F – 10µm.

Although many mesodermal (Fig.3.11) and kidney specific (Fig. 3.12) genes were up-regulated in EBs cultured in optimal conditions, the pluripotency marker Oct4, has not been down-regulated and stayed expressed until the end of the experiment (day 22) (Fig.3.14).

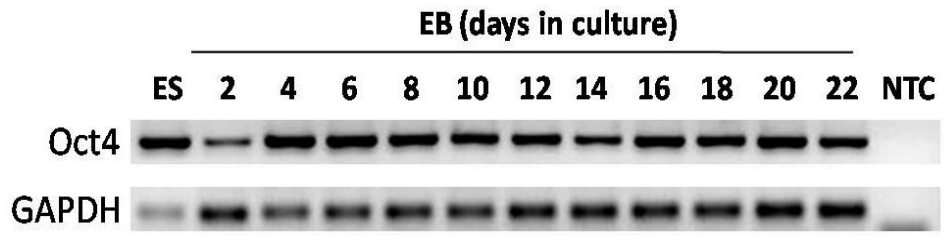

Figure 3.14 Semi-quantitative RT-PCR of pluripotency marker Oct4 expression profile in EBs. Oct4 expression during EBs culture remains high until day 22 of culture. Housekeeping gene GAPDH showed similar levels of expression in all samples. Experiment performed twice.

3.3 Conclusion

In this chapter, it has been shown that the optimal conditions to direct mesoderm differentiation from mESC is suspension cell culture in 15%FCS IMDM medium using a cell density of $75x10^3$ ml^{-1}. Under these conditions, the EB cells not only expressed the nascent mesodermal marker *Bry*, allowing for isolation of Bry+ (GFP+) cells, but also expressed markers of PM, IM and LM at a similar time course as that seen in the normal embryo.

3.3.1 Mesoderm differentiation

Using a Bry-GFP mES cell line, it was demonstrated that mesoderm differentiation occurs more efficiently in EB culture rather than monolayer. Although Johannson and Wiles (1995) optimised amounts of Activin A and BMP4 very precisely (2ng/ml and 0.25ng/ml respectively) to induce mesoderm differentiation in serum free EB culture, in the current study it was found that these growth factors were unable to induce mesoderm differentiation in a monolayer culture system. The failure of mesoderm differentiation in the aforementioned condition is rather surprising because it has recently been shown that short-term BMP4 treatment can efficiently induce mesoderm differentiation in monolayer culture of human ESC (hESC) (Zhang, 2008). However, it is important to bear in mind that there are several differences between mESC and hESC. Firstly, mESC are cultured in the presence of mouse leukaemia inhibitory factor (mLIF) whereas hESC do not respond to LIF and need to be cultured on mouse embryonic fibroblasts (MEF) (Humphrey, 2004; Thomson, 1998) or on special matrices in the presence of either MEF-conditioned medium, or FGF2, NT4 and activin (Baxter, 2009; Koestenbauer, 2006; Stojkovic, 2005). Furthermore, whereas FGF signalling is required to maintain hESC in an undifferentiated state, it promotes the differentiation of mESC (Ying, 2003). Recently it was suggested that hESC might be at slightly later stage developmentally than mESC, and more equivalent to mouse epiblast stem cells than mESC (Nichols, 2009b; Tesar, 2007). In support of this

hypothesis, it was demonstrated that mouse epiblast stem cells have the same culture requirements as hESC; i.e., they do not respond to LIF and require FGF to maintain their self-renewal (Nichols, 2009b; Tesar, 2007). Therefore, given that mESC and hESC are probably not equivalent, it is not surprising that they require different culture conditions for mesoderm induction.

As mesoderm differentiation in mESC monolayer was not successful, the EB culture system was optimised to promote maximal mesoderm differentiation. Although many studies used IMDM medium to induce mesoderm (Fehling, 2003; Johansson, 1995), it was not clearly stated what advantages IMDM had over DMEM. In the current study it was shown that only IMDM medium induced efficient mesoderm differentiation whereas DMEM was only partially successful. This might be due to very small but significant differences in the medium formulation. IMDM medium is supplemented with vitamin B12, which is normally involved in cellular metabolism and regulates synthesis of nucleic acids (Stryer, 1995), and also contain HEPES buffer, which is known to regulate pH in the physiologically important range (pH= 7.0 – 7.4) (Baicu, 2002). Although the difference in pH between DMEM (pH= 8.0 – 8.4) and IMDM (pH= 7.0 – 7.4) was not high, this could be the main factor influencing mESC differentiation. It has been shown previously that pH has an effect on cell differentiation (McAdams, 1996), and lower pH (~7.3) can significantly

increase the ability of mESC to form EBs (Chaudhry, 2009). Therefore, this could explain why IMDM with lower pH induced mesoderm differentiation more efficiently.

Another finding of this study is that 15% FCS was more effective for promoting mesoderm differentiation than 10% FCS. This is probably due to growth factors present in the FCS. FCS is known to contain various growth factors, the concentration of which vary between different batches (Notariani, 2006). In FCS formulations, the presence of Activin A (Sakai, 1992) and BMP4 (Kodaira, 2006) was shown, and it is known that both factors play an important role during fruit fly and vertebrate development (Asashima, 1990; James, 2005a; Kaufmann, 1996; Kingsley, 1994). Therefore, in higher serum concentration, there would be increased levels of growth factors, which were likely to have a positive impact on mesoderm differentiation. Another possibility is that mESC are producing/secreting inhibitors of BMP4, such as noggin (Gratsch, 2002), which is known to play inhibitory role *in vivo* (Tonegawa, 1998). If this were the case, it would explain a delay in *T* expression at higher cell seeding densities in low serum concentration (10% FCS). In other words, in low serum concentration, the level of growth factor inhibitors produced by mESC might be higher than the level of growth factors in the medium, and therefore in high cell seeding densities, this could lead to a the delay in mesoderm differentiation (*T* expression).

Previous work has shown that using optimal conditions, 80% of Bry-GFP cells were positive at day 4 of culture (seeding cell density – unknown) (Fehling, 2003). Although similar culture conditions were used in the current study, Fehling results could not be recapitulated in our lab, and the best GFP positive cell score was ~60%. This could be due to the fact that the batch of FCS and MEFs used in the current study were different from those in the Fehling study. Nevertheless, the Fehling protocol was used in this study as an efficient and simple way to direct mesoderm differentiation.

In normal mouse embryo development, after the basement membrane has been deposited between the extra-embryonic endoderm and primitive ectoderm epithelium (epiblast) and the pro-amniotic cavity has formed, the embryo undergoes gastrulation. At the onset of gastrulation, part of the basement membrane is degraded, allowing for cell migration through the primitive streak and mesoderm differentiation (Tam, 1997). In EBs, a gastrulation-like process also takes place, although it is much more chaotic than the tightly orchestrated process that occurs in the embryo. Interestingly, it has been shown that in EBs, the basement membrane inhibits gastrulation, as demonstrated by the fact that basement membrane-deficient EBs show more extensive mesoderm formation than their wild-type counterparts (Fujiwara, 2007). In the current study, it was found that under optimal conditions for mesoderm differentiation, the majority of EBs

did not form a basement membrane. Taken into account the results of the Fujiwara study, it is possible that the absence of basement membrane in the majority of EBs might have played a role in promoting mesoderm differentiation. It is not clear why basement membrane deposition occurred at such low frequency in the current study, but it is possible that cell density might have played an important role. In the current study the initial seeding density was much lower than used in the Fujiwara work ($75x10^3$ and $25x10^4$, respectively).

3.3.2 Characteristic of FACS sorted cells

EBs cultured in optimised conditions, showed quick and efficient differentiation into mesoderm, recognised by GFP fluorescence and confirmed by RT-PCR. At day 4 of culture, EBs were dissociated and sorted to obtain two populations: GFP+ and GFP-. FACS sort showed ~80% purity and therefore some GFP+ cells could be found in the GFP- cell fraction and vice versa.

Gene profile analysis of both populations showed that GFP+ cells are Bry+ and therefore they are mesodermal cells, and apart from expression of the pan-mesodermal marker *T*, they also expressed other mesodermal genes (*Tbx6, Foxc1, Foxf1, Osr1*). GFP+ cells also expressed various endodermal markers (*AFP, BMP4, Gata4, Sox17*), suggesting that the GFP+ cell population is multipotent and can give rise to mesodermal and endodermal

lineages (Yasunaga, 2005). This gene expression profile is similar to what has been found *in vivo* and can be called a 'salt and pepper' mix of endodermal and mesodermal gene expression, which has been observed in the pan-mesodermal region of the primitive streak (Nagy, 2003; Tam, 1997). GFP+ cells showed expression of some kidney specific markers as *Wt1* and *GDNF*, suggesting differentiation toward the kidney lineage. Therefore, GFP+ cells were shown to be cells with mesodermal/mesendodermal characteristics, with some signs of kidney lineage specification.

The population of GFP- cells showed weak expression of some mesodermal and endodermal markers (*Bry, Foxc1, Tbx6, Gata4* and *Sox17*), but this was probably due to the presence of GFP+ cells within the GFP- cells fraction, as showed by ~80% purity of the sort. GFP- cells showed stronger expression of *Pax6*, an ectodermal marker, than the GFP+ cell population, and therefore expression of *Pax6* in GFP+ cells is probably due to presence of GFP- cells within the GFP+ cell fraction. Therefore, GFP- cells are likely to be of the origin of the third germ layer – ectoderm, which develops in EBs and in the embryo proper during mouse development (Tam, 1997).

Both populations of cells, GFP+ and GFP-, showed high levels of *Oct4* expression, a known ESC pluripotency marker (Ovitt, 1998). Surprisingly, *Oct4* was still present at high levels at day 22 of EB development (Fig.

3.14). One possible explanation is that the expression of *Oct4* is due to the presence of pseudogenes or different splice variants of *Oct4* which are expressed at different stages of development and might be recognised by the primers used, as was shown for hESC (Atlasi, 2008; Liedtke, 2007). Whether it is true for mice remains to be tested, but the observations that Oct4 protein was down-regulated in the majority of EB cells by day 7 (Fig. 3.8), suggests that at least during the later stage of EB development, there appears to be little correlation between levels of Oct4 mRNA and protein. One possible reason for the persistence of Oct4 mRNA transcripts in later stages of EB development could be the high serum concentration (15% FCS) used: a recent study has shown persistence of Oct4 mRNA in EBs cultured in high serum conditions (Mansergh, 2009). However, the presence of real undifferentiated (pluripotent) cells in late EBs (EB day 20) could be investigated in two ways. First, would investigate the ability of dissociated EBs cells to give rise to ES cells (when seeded onto adherent dishes), and the second would investigate the ability of dissociated EBs to give rise to secondary EBs (when seeded onto non-adherent dishes), both confirming presence of pluripotent stem cells.

3.3.3 Timing of expression of mesodermal genes in EBs is similar to that of the mouse embryo

In order to be able to obtain kidney progenitor cells from mESC that would be able to give rise to kidney cells in an *in vitro* model system, it was

important to establish if mESC could differentiate towards the kidney lineage. It is well known that the kidney develops from mesoderm, which gives rise to other mesodermal lineages PM, IM, LM during mouse development and leads to kidney organogenesis (Saxen, 1987). Therefore, the principle was to direct the differentiation of the cells, taking lead from normal mouse development (Keller, 2005), considering all stages of mesoderm induction and commitment to become kidney progenitors as a very important signal that builds cell history and determines their fate. Here, it was shown that conditions optimised for mesoderm differentiation allowed as well for other mesodermal types to differentiate, namely PM, IM and LM showing very high similarity in timing of gene expression between EB culture and mouse embryos. Although minor differences in gene expression profile were noticed (*Tbx6* expression at day 12 of culture, and *Foxf1* expression at day 4 of culture) and remain unclear, they did not disturb EB development, leading to differentiation of beating cells by day 12 of culture (data not shown).

Another observation showed that some genes expressed by undifferentiated ESC, like *Osr1* or *Foxc1* are strongly down-regulated during the first two days of EB culture and become up-regulated at later time points (i.e., *Osr1* is up-regulated at day 8 and *Foxc1* at day 4 of culture; Fig. 3.11). Possible reasons for this are: (i) differences in media used to maintain mESC in a pluripotent state and to promote their differentiation; for instance, the

presence of LIF in medium to promote self-renewal might induce low level expression of various lineage-specific genes, because LIF is known to activate various signalling pathways, including Erk and STAT3 (Nichols, 2009a; Silva, 2008); (ii) different culture conditions: adherent culture dishes to maintain pluripotency of mESC and non-adherent dishes for suspension EB culture to differentiate mESC. The transition from attached to suspension culture conditions can have a dramatic effect on cell-cell contact, cell cycle and finally, cell signalling (Burdon, 2002), which can have an impact on gene expression.

As mesodermal genes were expressed in EBs in the same sequence as they are in embryos, it was interesting to see if optimised conditions led to differentiation of kidney progenitors. Suitable markers for identifying metanephric mesenchyme (MM) cells were *Pax2* and *Wt1*, as these transcription factors are co-expressed in condensed MM, which is known to give rise to functional nephrons (Saxen, 1987). RT-PCR results showed expression of *Pax2* and *Wt1* at day 14 of EBs culture. Although both genes are expressed in organs other than the kidney; e.g., *Pax2* is expressed in the developing central nervous system, eye (Bouchard, 2000; Pfeffer, 2002) and urogenital system (Dressler, 1990) and *Wt1* is expressed by mesenchymal cells in the brain, heart, gonads and spleen (Hohenstein, 2006; Niksic, 2004), they are only co-expressed in the metanephric mesenchyme of the developing kidney (Moore, 1999), which was

confirmed by performing a whole embryo immunostaining for Pax2 and Wt1. Therefore, expression of both genes would be a good identification of cells differentiating into MM cells. However, immunostaining of day 14 EBs showed expression of both genes but they did not overlap. In other words, Pax2 expression was found in nucleus of some EB cells whereas Wt1 was expressed by the majority of the cells but was located in the cytoplasm (Niksic, 2004). Thus, it may be necessary to treat EBs at a certain point of culture (after day 10 when expression of IM marker *Osr1* occurs) with a nephrogenic cocktail of factors to induce renal progenitor differentiation (Kim, 2005).

The described conditions of mesoderm differentiation (15%FCS IMDM , $75x10^3$ ml^{-1}) were used in this study to efficiently differentiate mesoderm from mESC and sort these cells to obtain populations of GFP+ and GFP- cells using FACS. However, before investigating the nephrogenic potential of the sorted cells by incorporating those in developing mouse kidney rudiments *ex vivo*, it was first necessary to establish a method for labelling the mESC derivatives so that they could be distinguish from the host rudiment cells. Therefore, the next chapter describes a series of experiments that were undertaken to identify the most suitable cells labelling system.

Chapter 4: Cell tracking system

4.1 Introduction

It has been shown that mouse ESC can be efficiently differentiated into mesoderm-like cells via embryoid bodies. A key aim of this study is to compare the nephrogenic potential of both undifferentiated ESC and ESC-derived mesoderm cells to that of embryonic kidney progenitor cells by incorporating the different cell types into mouse kidney rudiments *ex vivo*. However, in order to monitor the fate of the aforementioned cells following transplantation into the host tissue it is necessary to establish an appropriate method of cell labelling that does not adversely affect cell behaviour.

There are several methods of cell labelling (see chapter 1.5), however, for the current study it was important that the following criteria were met:

- Labelling should be a vital stain – it should be possible to label living cells without the need for fixation to visualise the stain, due to performance of the vital functionality assay on the kidney chimaera (chapter 6)
- Short incubation time – it should be possible to introduce the label to living cells after a short incubation period, because the ESC-derived mesodermal cells that will be used in later studies, will be isolated from day 4 EBs by FACS, and will need to be introduced into the kidney rudiment within a few hours of isolation.

- High efficiency of labelling – it should be possible to label the vast majority of cells in order for their future integration potential to be accurately quantified.
- Low toxicity – the stain should not be toxic and should have no adverse effect on cell viability, in order to minimize cell death.
- Long signal preservation – it should be possible to localize labelled cells after 7 days of culture, as this is the latest time point of the analysis.

One of the most common methods of cell tracking; namely, labelling with green fluorescent protein (GFP), (either by knock-in or lentiviral transfection), is usually a permanent labelling method, where GFP can be ubiquitously expressed by precisely selected stable cells lines (Nagy, 2003). However, GFP labelling requires cells to be cultured for prolonged periods following transfection with plasmid or lentiviral vectors, in order to allow sufficient time for the GFP to be expressed (Blomer, 1997; Nagy, 2003; Zhou, 2009). For example, about 72h should be allowed for GFP expression to appear in cells transfected with lentiviral vector (personal consultation with S. Theocharatos, University of Liverpool). Therefore, the GFP labels do not fulfil the criteria of short incubation time and rapid signal appearance.

The vital stains, DiI and Vybrant Dye (VD) bind to cell membranes. DiI is an extracellular lipid dye, whereas VD localises to intracellular

proteins (Wang, 1989). However, in previous studies, DiI was shown to flip-flop between the lipid monolayer of contacting cells (Razinkov, 1999), and therefore was excluded from further analysis as there was concern it would cause difficulties in quantifying results, due to the possibility of the dye being transferred to host cells. Although VD fulfilled the criteria of short incubation, high efficiency of labelling and low toxicity, it was not clear how long the label would be retained in mES cells. It was also not clear how long cells retain Quantum Dots (QDs) – small fluorescent nanocrystals, which are up-taken by the cells and located in the vesicles in the cell cytoplasm (Rosen, 2007).

Taking into account the selection criteria, GFP and DiI labelling were discounted for the reasons outlined above. The purpose of this chapter was therefore to establish if VD or QDs were suitable for labelling the mESC and their derivatives. Therefore this chapter will compare the efficiency, toxicity and signal preservation in cells labelled with VD and QDs. Furthermore, the optimal labelling method will be tested to determine the degree of transfer of label to the host cells.

4.2 Results

In order to investigate the nephrogenic potential of ESC and ESC-derived mesoderm (Bry+) cells, it was necessary to establish the most suitable labelling method. Due to the specific criteria for cell labelling required for the successful localisation of cells integrated with kidney rudiments *ex*

vivo; the most promising vital stains appeared to be quantum dots (QDs) and vybrant dye (VD). Therefore, these two labels were tested to establish their intracellular retention time.

4.2.1 Optimisation of labelling method

In order to determine how long the signal was retained by the cells, undifferentiated mouse ESC were labelled according to the manufacturer's recommendations: either with 10nM QDs or 10nM VD concentration and seeded at low cell density (500 cells cm^{-2}) (see chapter 2.9 – 2.10). Cells were fixed after 1, 3 and 7 days in culture and counter-stained with DAPI to visualise cell nuclei.

The results showed that at day 1, both methods were highly efficient in cell labelling, as all cells in both cases were labelled with QDs or VD (Fig. 4.1 and 4.2). However, at day 3 differences in label retention became apparent. QDs were observed in the majority of cells whereas VD labelling had become highly diluted and only very weak stain could be observed in a few cells. By day 7 of culture, although the population had undergone noticeable expansion, QDs were still visible in many cells whereas the VD stain was no longer detected in any of the cells (Fig. 4.1).

Furthermore, apart for having poor retention, VD appeared to be more toxic than QDs: for instance, after the first 24h in culture, more cells labelled with QDs survived and formed colonies, whereas, many VD

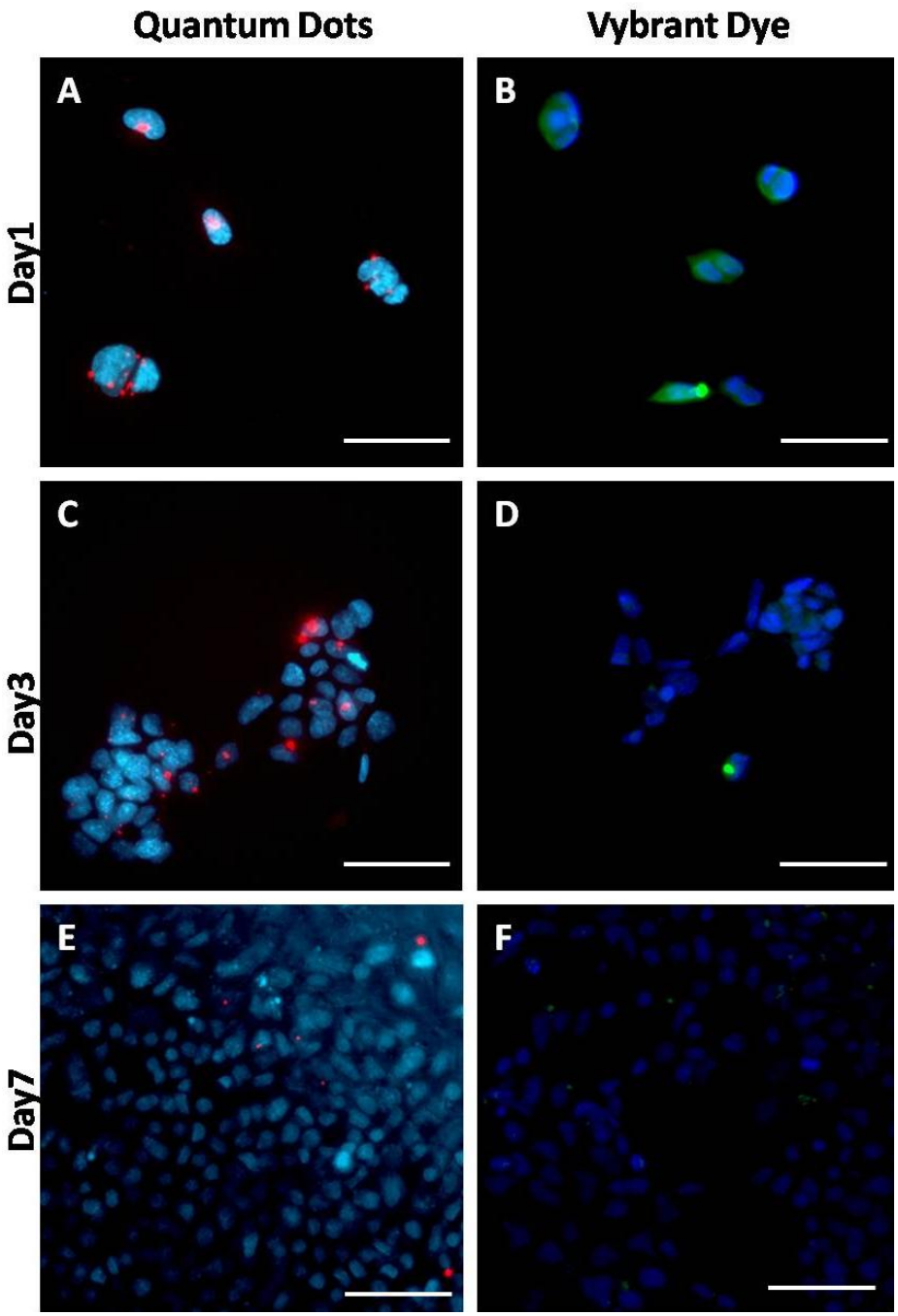

Figure 4.1 Comparison of two cell labelling methods: quantum dots (QDs) and vital stain of vybrant dye (VD). A, C, E - mES cells labelled with 10μM concentration of QDs showed high efficiency of labelling at day 1 (A), day 3 (C) and dilution at day 7 (E); B, D, F – mES cells labelled with 10μM concentration of VD showed high efficiency of labelling at day 1 (B) and very high dilution of labelling at day 3 (D) and lack of labelling at day 7 (F). Scale bar: 50μm.

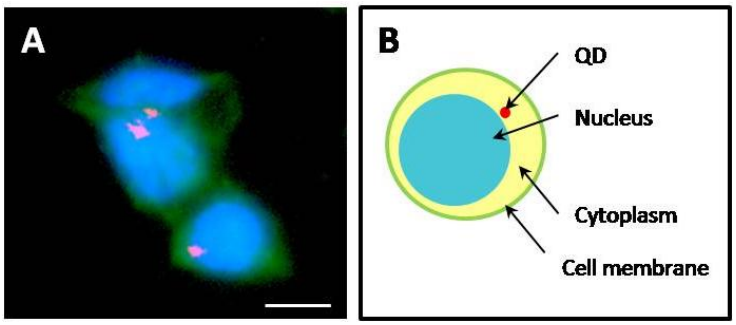

Figure 4.2 Localisation of Quantum Dots (QDs) in the cells. A) Photomicrograph of cells labelled with QDs (red), cell membrane stained with vybrant dye (green) and nuclear stain – DAPI (blue) presenting QDs aggregation; Scale bar – 10µm; B) Schematic localisation of QDs in the cell cytoplasm, very close to the cell nucleus.

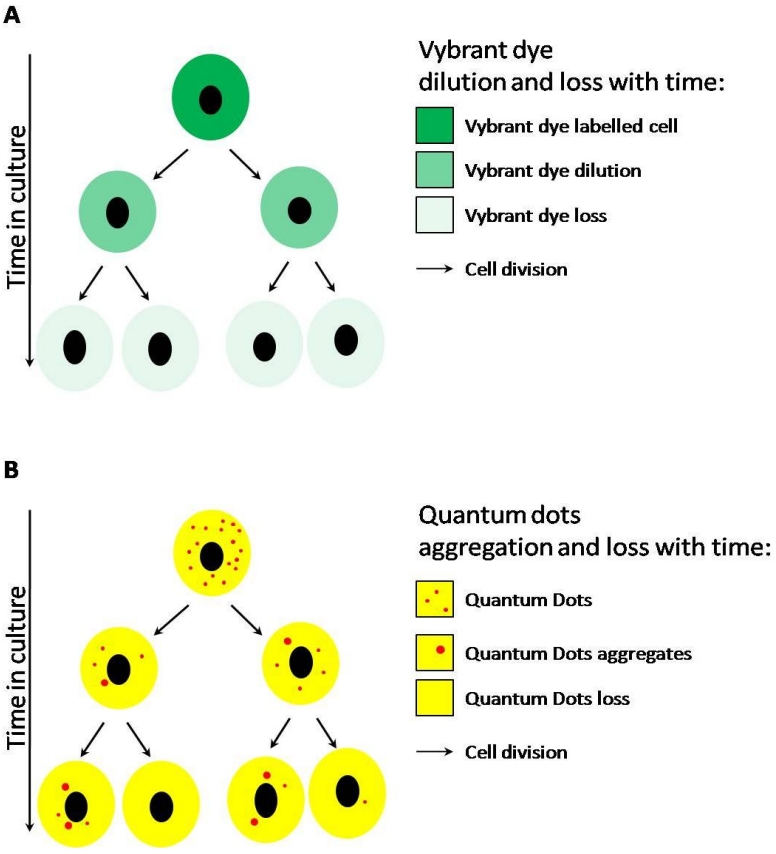

Figure 4.3 Schematic presentation of labelling dilution with cell divisions. A – Dilution and loss of Vybrant dye labelling during cells culture; B – Aggregation of Quantum Dots in cells and their loss during cell culture.

labelled cells detached during the first 24h of culture (Fig. 4.1). Another drawback of VD labelling was photobleaching: although cells labelled with VD were easily visible down the fluorescent microscope, the fluorescence rapidly bleached out during the imaging process, making it impossible to image the same area multiple times.

Table 4.1 Comparison of cell labelling methods with QDs and VD

CRITERIA	QD	d1	d3	d7	VD	d1	d3	d7
Incubation time	1h	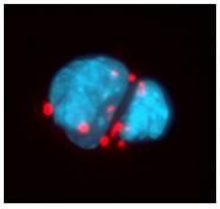			15 min	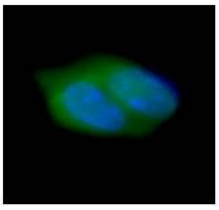		
Efficiency of labelling	high				high			
toxicity	no				weak			
Signal maintenance	QD	+++	++	+	VD	+++	+	-

+++ – all cells labelled; ++ – more labelled cells; + – more unlabelled cells; - – lack of labelled cells;

Dual labelling of cells with QDs and VD showed that after 1 day in culture, QDs are located in the cell cytoplasm of mESC, in the aggregates in the perinuclear space (Fig.4.2). A schematic comparison of VD and QDs behaviour in cultured cells is presented in Fig. 4.3; the VD label is lost during cell divisions and labelled cells can no longer be distinguish from unlabelled cells (day 7), whereas QDs are retained in some cells, and although many cells do not receive QDs during cell divisions, the primarily labelled cells, still maintained QDs (day 7).

To summarise, both investigated methods of vital labelling of cells, QDs and VD fulfilled the criteria of short incubation time: 1h for QDs and 15min for VD; and high efficiency of labelling. However, VD showed slight cytotoxicity and weak signal retention (Tab. 4.1). Therefore, although the QDs labelling method was not perfect due to many cells lacking QDs after 7 days in culture, this was the optimal method as many cells retained QDs after 3 days in culture and some labelled cells could even be detected after a week. Furthermore, there was no obvious toxicity.

4.2.2 Quantum dots do not transfer between cells

Given that the QDs appeared to be the optimal labelling method, it was important to investigate if the QDs could transfer between cells; i.e., from labelled exogenous cells to unlabelled host cells, as a high rate of transfer would make it difficult to investigate the behaviour of exogenous cells in the chimaeric rudiments. Thus, to answer the question if QDs are located only in the labelled cells, and do not transfer between the cells during culture, a cloned cell line of kidney stem cells (KSC-H6) (C. Fuente Mora, University of Liverpool) transfected with GFP lentivirus (see chapter 2.9.3) (E. Ranghini, University of Liverpool) was used. These cells, KSC-H6/GFP, present stable expression of GFP, with minor changes in GFP intensity and were labelled with QDs according to the protocol and introduced into kidney rudiment cells. Following 3h (day 0), 1, 2 and 3

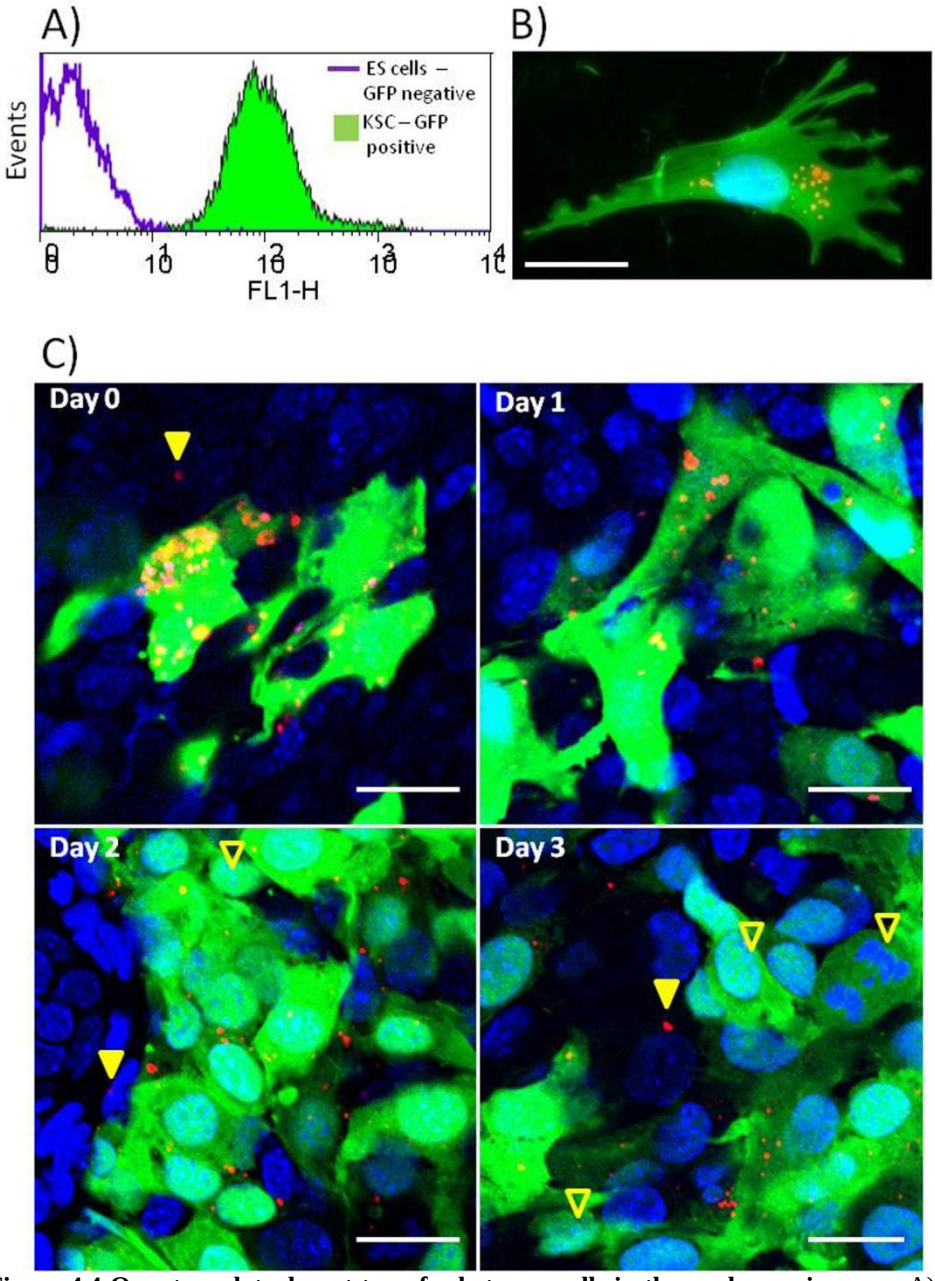

Figure 4.4 Quantum dots do not transfer between cells in the nephrogenic assay. A) FACS graph presenting KSC-H6/GFP being 100% GFP positive (green area), which is opposite to the nontransfected mES cells (violet line); B) Quantum dots inside a KSC-H6/GFP cell after 1 days in culture; scale bar – 10μm C) KSC introduced into E13.5 kidney cells show preservation of QDs in the cells up to day 3 in culture. Full arrowhead pointing onto GFP- cells that gained QDs, empty arrowheads pointing onto GFP+ cells that lost QDs; scale bars - 10μm.

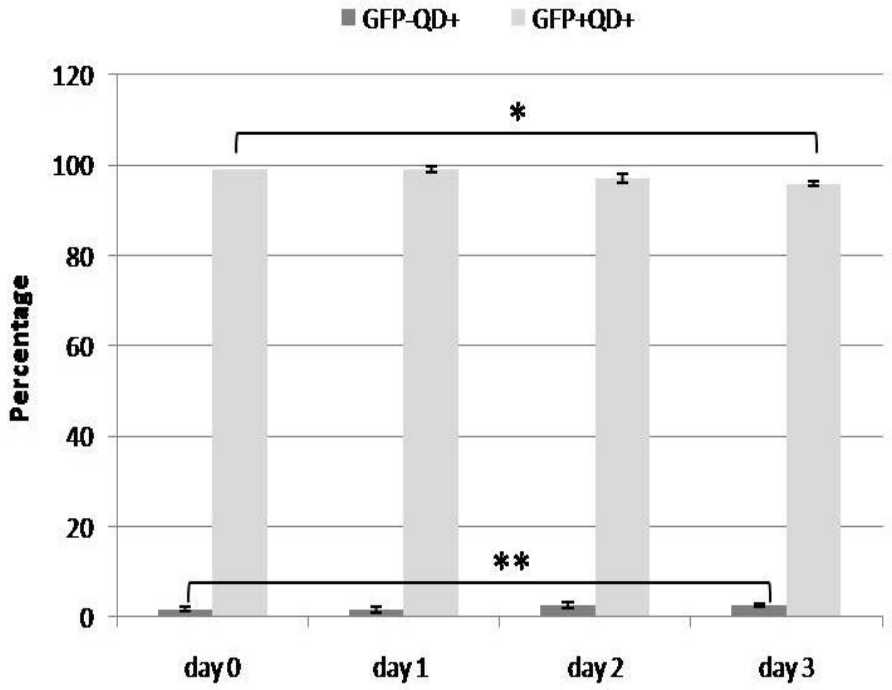

Figure 4.5 Quantum dots do not transfer between the cells. Light grey columns are presenting high preservation of QDs in GFP positive cells (about 95% at day3) (*- $p<0.004$) and dark grey columns are presenting lack of QDs transfer from GFP positive to GFP negative cells as there is no significant difference between the beginning and the end of the experiment (**- $p>0.1$); N=3 for each sample and error bar represents standard error.

days in culture, samples were fixed, counter-stained with DAPI to visualise cell nuclei and analysed.

The results showed that QDs were found in the cell cytoplasm of labelled cells (Fig. 4.4). QD labelled cells could be easily identified until day 3 of culture, although at this time point, some GFP positive cells (GFP+) had lost QDs (empty arrowhead) and some GFP negative cells (GFP-) had gained QDs (full arrowhead) (Fig. 4.4). Statistical analysis of QD loss by GFP+ cells and QD gain by GFP- host cells, showed that at day 0 of

culture, 99.1% of GFP+ cells were labelled with QDs, and only 1.8% of GFP- cells contained QDs. By day 3 of culture, 96% of GFP+ cells were still labelled with QDs, and only 2.5% of GFP- cells contained QDs (Fig. 4.5). Although these numbers are small, QD loss by GFP+ cells showed a significant difference between the beginning and the end of the culture, whereas the percentage of GFP- cells labelled with QDs was not significantly different between the two time points. These results show that the extent of QD transfer to host cells is negligible and does not increase during the time course of the experiment. In fact, it is likely that the small increase in the number of GFP-QD+ cells is due to cell division of the kidney cells within the rudiment.

4.3 Conclusion

In this chapter it has been shown that the optimal method of labelling cells, best fulfilling the requirements of the current study, is QD labelling. This method showed high efficiency, lack of toxicity and long signal preservation as well as low transferability from labelled cells of interest to unlabelled cells.

4.3.1 Quantum dots showed long signal maintenance and lack of photobleaching

Signal maintenance by labelled cells was a very important issue for the current study. Although there are studies using signal/label disappearance

such as fluorescence recovery after photobleaching (FRAP), fluorescence loss in photobleaching (FLIP) or selective photobleaching to investigate protein dynamics (Goodwin, 2005), in the current study, it was important to preserve the signal for a minimum of 1 week without signs of photobleaching during imaging. The cells labelled with VD showed rapid signal loss and strong photobleaching during the cell imaging process, whereas in cells labelled with QDs, photobleaching was not observed, which allowed for extensive imaging of cells following the labelling (Rosen, 2007; Solanki, 2008) (see section 1.5). This photostability of QDs would be very useful in time lapse studies. QDs also showed longer signal preservation than VD. QDs in mESC presented signal preservation for up to 7 days but the number of labelled cells decreased dramatically, which is consistent with a previous report (Lin, 2007). A longer signal maintenance (by up to 6 weeks) could be obtained by labelling cells with large cytoplasm volume and low proliferation rate, such as MSC (Rosen, 2007). The QDs used in the current study have already been shown to be mainly incorporated into cytoplasmic vesicles (endosomes) in the perinuclear space (Koshman, 2008; Rosen, 2007). This could be a potential problem, as endosomes during cell life can develop into exocytotic vesicles and remove QDs outside the cell, although it is worth noting that Rosen and co-workers (2007) did not observe the release of QDs in their studies.

4.3.2 Quantum dots showed lack of toxicity to the labelled cells

Previous studies have shown that the cytotoxicity of quantum dots was strongly dependent on the surface modifications (Hoshino, 2004), and while some modifications, such as silica coatings, have been found to be highly toxic (Derfus, 2004; Kirchner, 2005), other coatings, such as Zn/S, effectively reduced toxicity of QDs with CdSe cores (Kirchner, 2005). QDs used in the current study were shown on MSC to have no effect on cell viability, proliferation and differentiation abilities (Rosen, 2007). In the current study, the viability of QD-labelled cells was compared to VD-labelled cells. Although there are no reports about VD cytotoxicity in the literature, in this study, higher cell death (high levels of cell debris, not shown) was observed during the first 24h of culture among mESC labelled with VD. The factor that may play a role in the decrease of cell viability is dimethyl sulphoxide (DMSO). It is used to deliver the dye into the cells (Invitrogen) by increasing the cell membrane permeability (Yu, 1994). This feature of DMSO may lead to cell membrane breakage and therefore cell death (Yu, 1994). As the incubation of VD took place at 37°C, an increased cell death could be observed as at high temperatures, the DMSO was shown to have a harmful effect on protein stability (Yu, 1994).

4.3.3 Quantum dots show low transferability

Another finding of the current study was negligible levels of transfer of QDs between cells. The number of adjacent cells labelled with QDs was

very low during the time of the nephrogenic assay: 1.8% and 2.6% at day 0 and day 3 of culture, respectively, and did not show significance in increase. The initial number of adjacent GFP- cells labelled with QDs (1.8%) could be an effect of an insufficient number of washes in order to clean up the media from any free QDs. However, the number of washes performed in the current study was already greater than recommended by the supplier, and it was not advisable to increase this number, as it would decrease the yield of labelled cells. It is unlikely that QDs, released from labelled cells, either as a result of exocytosis or cell death, could be taken up by neighbouring host cells, because following initial up-take, QDs form large aggregates which would probably be too big for non-phagocytotic cells to take up by pinocytosis. Furthermore, it is worth noting that the initial up-take of QDs is likely due to the presence of cell penetrating peptides (CPP) on their surface. In the acidic environment of the endosomes/lysosomes, it is envisaged that the CPPs would be removed by lysosomal enzymes (Kim, 2008; Thakur, 2005); making it unlikely that these particles could be taken up by adjacent cells.

Despite a few disadvantages related to QD labelling; e.g., up-take and maintenance in cells may strongly depend on the cell type (Lin, 2007; Rosen, 2007), they have many advantages; e.g., photobleaching resistance, high fluorescent signal, non-toxicity and ability to be modified to target specific cells and cell organelles (Gao, 2004; Gao, 2005; Lidke, 2004).

Therefore, for their advantages QDs were chosen as the tracking method in the current study. The described conditions of cell labelling, which are as follows; ~1h incubation of ~1M cells in 10nM QD solution in suspension, were optimised to allow for medium-term cell tracking (~7 days) in the complex environment of the kidney rudiments. The aforementioned conditions were used to investigate the nephrogenic potential of mES cells and their derivatives in the subsequent part of this study.

Chapter 5: Nephrogenic potential of mouse ES cells and their derivatives

5.1 Introduction

Mouse embryonic stem cells (mESC) are derived from the inner cell mass (ICM) of the blastocyst at E3.5 to E4.5 (E – embryonic day). Mouse ESC were first isolated in 1981 independently by Evans and Martin (Evans, 1981; Martin, 1981), and they were shown to be pluripotent, meaning that they are able to give rise to cells of all three germ layers of the embryo: mesoderm, endoderm and ectoderm, as well as the gametes following transplantation into mouse blastocyst (Nagy, 1993). They are also able to generate cells of the three germ layers *in vitro* when cultured as embryoid bodies. Furthermore, ESC in culture are immortal and do not become senescent or lose their potential (Evans, 1981). It was also reported, that ESC form teratomas containing: gut epithelium, cartilage, bone, smooth muscle, neural epithelium and nephron-like structures following subcutaneous injection of adult mice (Stojkovic, 2005; Thomson, 1998; Yamamoto, 2006). Although ESC have the potential to form tumours, they are a suitable tool to investigate the potency of ESC *in vitro*.

The first study investigating the potential of mESC to generate kidney structures and integrate with host tissue involved injecting undifferentiated ESC into mouse E12.5 kidney rudiments *ex vivo* (Steenhard, 2005). Injected cells appeared to show integration into developing tubules of the

host; however the tubules that ESC formed within the rudiment were derived solely from ESC and there was no contribution from host rudiment cells. This raised the question of whether the ES-derived tubules were in fact non-renal tubular structures (Steenhard, 2005). This is an important issue because it has been well documented that that mESC/hESC readily form a range of non-renal cell types following subcutaneous injection (Thomson, 1998; Yamamoto, 2006), and transplantation under the kidney capsule of adult mice (Stojkovic, 2005). Following the Steenhard 2005 study, various groups have investigated the ability of mESC to generate renal cell types using the embryoid body system (Kim, 2005; Kramer, 2006; Yamamoto, 2006) (see summary in Table 5.1). Kramer and co-workers showed that following differentiation in embryoid bodies, ESC formed ring-like structures positive for podocin, nephrin, podocalyxin and cytokeratin suggesting that the cells had differentiated into podocyte-like cells and some cells were THP (tamm-horsfall glycoprotein) positive suggesting their differentiation into distal tubule cells of the nephrons (Kramer, 2006). Using a nephrogenic cocktail of retinoic acid, activin A and BMP7, Dressler's group achieved nearly 100% integration of ESC into the tubular epithelium, of developing mouse kidney rudiments *ex vivo*, but it was not clear from this study if the tubules were metanephric mesenchyme or ureteric bud origin. Furthermore, the cells were unable to integrate into the glomerular tufts (Kim, 2005). The potential of mESC to form renal cells was also investigated by injecting subcutaneously into

adult mice to generate tumours (Yamamoto, 2006). Following 14 to 28 days of *in vivo* development, some of the mESC had differentiated tubular epithelium and avascular glomeruli. Moreover, the tubules and nephrons were shown to be positive for Pax2, cytokeratin and Ksp-cadherin confirming their renal fate (Yamamoto, 2006). However, teratomas are known to consist of developing structures of different origins, such as meso-, endo- and ectodermal (Stojkovic, 2005; Thomson, 1998), and therefore many non-renal cell types are present. Wilson's group (Vigneau, 2007) have shown that mESC can integrate into proximal tubules following transplantation into kidney rudiments *ex vivo* and neonatal mice *in vivo*. In this study, prior to transplantation, mESC were pre-differentiated using the EB culture system and were found to express renal markers such as Pax2, Wt1, Wnt4 and cadh-11. In addition to integrating successfully with proximal tubules, the pre-differentiated mESC did not form tumours following *in vivo* transplantation (Vigneau, 2007).

Taken together, the aforementioned studies show that mESC can integrate into developing renal structures, but it is not yet clear how this ability to integrate compares with that of the renal progenitor cells themselves; nor is it clear if the mESC or their derivatives have any detrimental effect on the developing kidneys, and the persistence of undifferentiated mESC following transplantation has not been thoroughly investigated. Furthermore, although mESC – derived mesodermal cells have potential to generate some renal cell types following transplantation into embryonic or

neonatal kidneys (Kim, 2005; Vigneau, 2007); it appears that they are unable to generate podocytes. However, the lack of podocyte differentiation could be due to the experimental protocols used. For instance, in all studies performed to date, the mESC were transplanted into the intact host tissue as a bolus injection, which could make it difficult for the cells to integrate into structures that had already differentiated.

Table 5.1 Summary of experiments investigating nephrogenic potential of mESC.

Author	Year	Stem cell type	Differentiation method	Experimental design	Cell integration/ differentiation	Markers
Steenhard et al.	2005	Undifferentiated mESC	None	Injection into E12.5 kidney rudiment *ex vivo*	Proximal tubules	Morphology, LTA+
Kim & Dressler	2005	Undifferentiated mESC	EB assay supported with nephrogenic cocktail of factors	Injection into E11.5 kidney rudiment *ex vivo*	Tubules	E-cadherin+/ Pax+
Kramer et al.	2006	Undifferentiated mESC	EB assay	EBs plated on adherent dishes (*in vitro*)	Podocyte-like cells and distal tubules	Podocin+, nephrin+, podocalyxin, cytokeratin, THP
Yamamoto et al.	2006	Undifferentiated mESC	Tumour formation assay	Subcutaneous injection	Tubular epithelium, avascular glomeruli	Pax2+, cytokeratin+, ksp-cadherin+
Vigneau et al.	2007	Undifferentiated mESC	EB assay (Pax2, Wt1, Wnt4+ cells)	Injection into E11.5 kidney *ex vivo*; Injection into neonatal mice *in vivo*	Proximal tubules	Morphology, Alkaline phosphatase+

Therefore, the aims of this chapter were to:

- Compare the integrative potential of mESC, mESC-derived mesoderm, mESC-derived ectoderm and kidney progenitors into mouse kidney rudiments.

- Ascertain if these cells types had any detrimental effect on kidney development.
- Determine if the mESC and their derivatives can generate renal-specific cell types such as podocytes, proximal tubules and ureteric bud cells.
- Determine if any undifferentiated mESC are present at various time points following transplantation into rudiments and *ex vivo* culture.

5.2 Results

In order to achieve all aforementioned goals, it was important to select an appropriate cell incorporation method. Therefore, in the current study, use was made of a novel rudiment culture method recently established in the Davies laboratory (Unbekandt, 2010), which has been shown to facilitate the integration of exogenous cells into the kidney rudiments. This method involves disaggregating the rudiment; incorporating the stem cells and allowing the chimaeric rudiment to re-aggregate and undergo morphogenesis.

5.2.1 Optimisation of conditions of cell integration with kidney rudiments

The method of creating kidney chimaeras required the kidney rudiments to be disaggregated into single cell suspension, mixed with labelled cells of interest, pelleted and plated onto a filter membrane. In the original method (Unbekandt, 2010), E11.5 kidney rudiments were used; however, the number of cells present in the E11.5 rudiment is quite low, necessitating the use of large number of embryos. Therefore, to improve yield, older kidney rudiments, from E13.5 mouse embryos were used. Therefore, the ability of E13.5 kidney rudiments to re-aggregate and reform kidney structures was investigated, and the optimal ratio of disaggregated rudiment cells to exogenous cells was established.

The results demonstrated that E13.5 kidney rudiments that were disaggregated to a single cell suspension could re-aggregate and undergo normal development, reforming kidney structures by day 3 of culture (Fig. 5.1). To establish the optimal ratio of labelled to unlabelled cells in the kidney chimaeras, E13.5 disaggregated kidney rudiments were labelled with quantum dots (QDs) and mixed with unlabelled disaggregated kidney rudiments in the following ratios: 1:8, 1:20 and 1:50. Results showed that the ratios of 1:20 and 1:50 were too low; as few labelled cells could be observed following the 3 day culture period (data not shown). However, using the ratio 1:8, many labelled cells could be observed both at the initial

time point, where they were found to be evenly distributed within the chimaera, following a 3 day culture period (Fig.5.2).

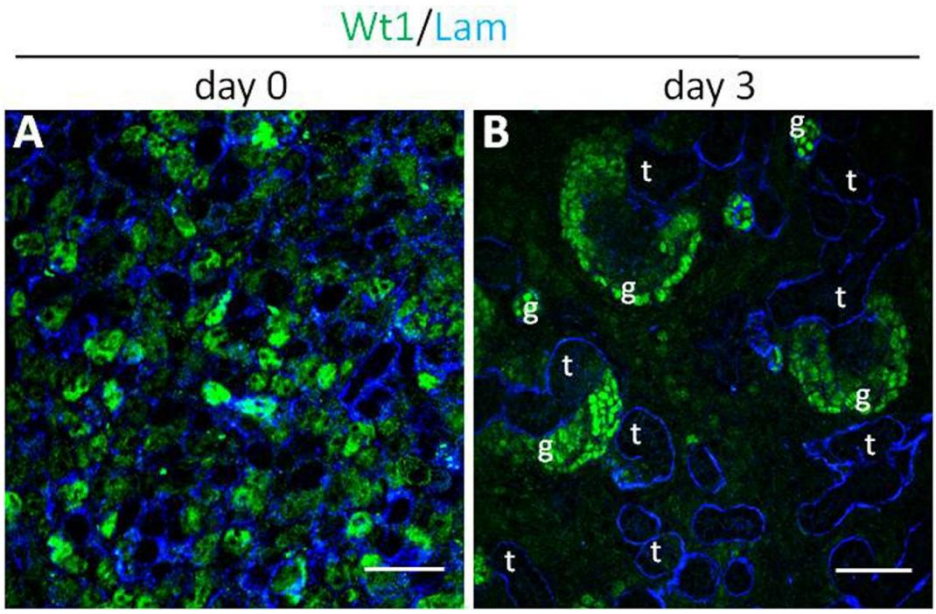

Figure 5.1 Kidney chimaera formation. Wt1 (green), Laminin (blue), staining of kidney chimera pellet at day 0, presenting random distribution of cells within the pellet without any structures (A); and after 3 days in culture, presenting tubule-like (t) and glomeruli-like structures (g) formation (B). Scale bars: A) 30μm, B) 60μm.

Therefore, in subsequent experiments, chimaeras were always made as follows: 20000 QD-labelled cells per 160000 unlabelled kidney cells, so that the total number of cells per chimera at day 0 was ~180000.

These results showed that older embryonic kidneys derived from E13.5 mouse embryos, can efficiently re-aggregate and re-differentiate to form kidney structures, and established that the optimal ratio of unlabelled to labelled cells is 1:8.

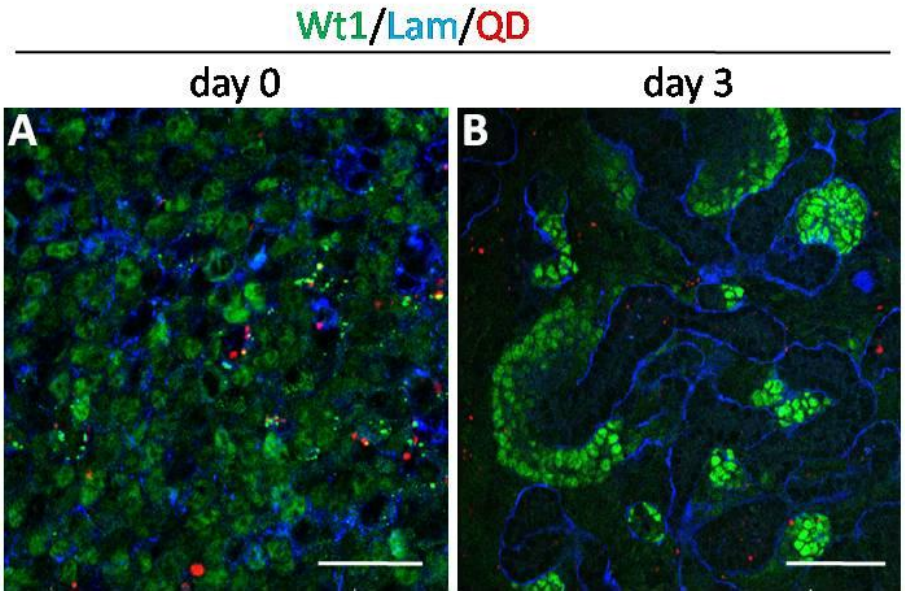

Figure 5.2 Ratio 1:8 of QDs labelled cells to unlabelled kidney rudiment cells. Wt1 (green) and laminin (blue) staining of chimaeras at day 0 of culture presenting lack of any structures and even distribution of QDs (red) labelled cells (A); and at day 3 of culture where kidney structures can be observe with QDs labelled cells incorporated into kidney structures (B); Scale bars: A – 30μm, B – 60μm.

5.2.2 Growth and development of rudiment chimaeras

To investigate the ability of mESC and their derivatives to generate renal cell types, the following chimaeras were formed:

- Undifferentiated mESC mixed with the kidney rudiment cells that will be called 'ES chimaera' in further parts of this work.
- mESC - derived Bry+ cells (i.e., mesoderm cells) mixed with kidney rudiment cells that will be called 'Bry+ chimaera'.
- mESC - derived Bry- cells (i.e., non-mesodermal cells) mixed with kidney rudiment cells that will be called 'Bry- chimaera'.

- Kidney rudiment cells mixed with kidney rudiment cells used as a positive control of development and integration that will be called 'kidney chimaera'.

These chimaeras were stained for markers of kidney-specific cell types, where Wt1 positive cells represented early glomeruli, synaptopodin positive cells represented mature podocytes, Six2 positive cells represented condensing MM, calbindin positive cells represented UB, LTA (*Lotus tetragonolobus lectin*) represented proximal tubules, and laminin positive regions presented basement membrane.

The results showed that following 3 days of culture, there were noticeable differences in sizes of the different types of chimaeras. The surface area of each chimaera was either round or ellipse in shape and therefore either the formula for the surface area of a disc or an ellipse was used. For each chimaera type three samples were measured, the mean was calculated and the *t test* was performed to investigate the size difference significance.

The biggest chimaeras were formed by the positive control kidney chimaeras (4.4 +/- 0.1 mm^2), followed by the ES chimaeras (3.5 +/- 0.08 mm^2), Bry+ chimaeras (2.5 +/- 0.2 mm^2) and finally, the Bry- chimaeras (1.4 +/- 0.4 mm^2) (Fig. 5.3). The kidney chimaera was shown to be significantly ($p<0.003$) bigger than the other three chimaera types of ES, Bry+ and Bry-, whereas no significant ($p<0.07$) difference between Bry+

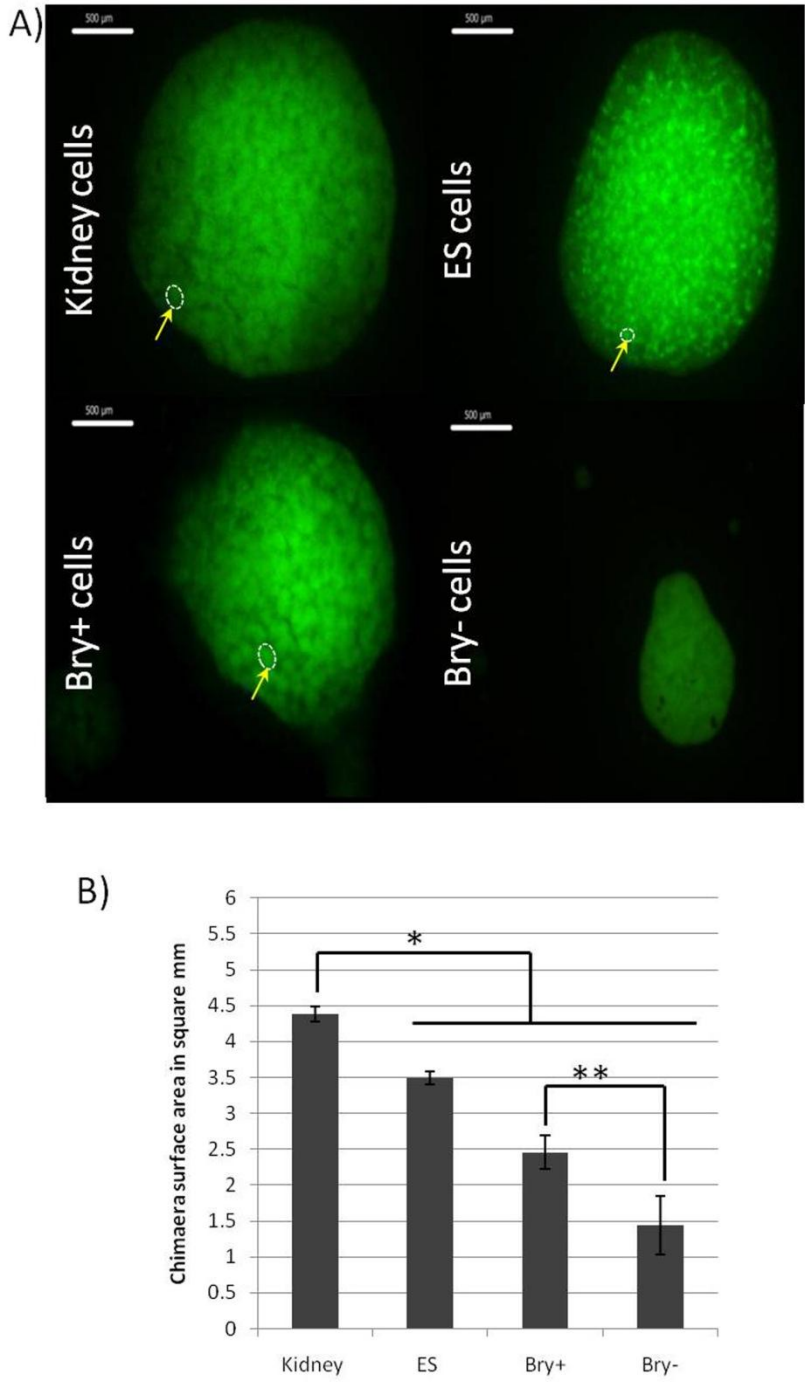

Figure 5.3 Chimaera surface areas. A) Chimaera surface area visualised by Wt1 immunostaining, demonstrating formation of glomeruli-like structures (white dashed line and yellow arrows). Scale bar – 500µm; B) Graph presenting chimaera size ratios; N=3 for each sample and error bar represents standard error; * - $p<0.003$, ** - $p<0.07$.

and Bry- chimaeras was observed. Immunostaining of the chimaeras for Wt1 showed that in three of the chimaera types: kidney, ES and Bry+, developing kidney structures were observed (glomerular-like structures indicated by the intense Wt1 staining), whereas no staining was observed in Bry- chimaeras indicating that no structures had formed (Fig. 5.3). Considering the fact that Bry- chimaeras did not develop normally, they were excluded from further analyses.

As the cells introduced into the kidney environment seemed to have an impact on chimaera growth, further analysis was undertaken to compare the number developing nephrons in the different types of chimaeras. Results showed that the average number of glomerular-like structures per mm^2 in kidney, ES and Bry+ chimaeras was 25, 50 and 30 respectively (Fig.5.4). Therefore, kidney and Bry+ chimaeras developed a similar number of glomeruli while ESC formed twice the number of glomeruli. Moreover, ES chimaeras formed very small glomeruli, which were about one fourth of the size of the glomeruli that developed in the kidney and Bry+ chimaeras. Immunostaining showed that cells expressing high levels of Wt1, characteristic of maturing podocytes, had differentiated in the kidney and Bry+ chimaeras, whereas these cells were not observed in the ES chimaeras (Fig.5.4).

In order to investigate if the glomeruli in ES chimaeras were able to increase in size and mature with time, the culture period was extended to 7 days, following which, the chimaeras were fixed and co-stained with

synaptopodin and laminin. The comparison of sizes and maturity of nephrons between kidney, ES and Bry+ chimaeras at day 7 of culture, showed that glomeruli of the ES chimaeras were still smaller (similar to day 3 results) in comparison to kidney and Bry+ glomeruli, but showed expression of synaptopodin (Fig. 5.6), which is a sign of their maturity. However, synaptopodin expression in ES chimaeras was noticeably less than in kidney and Bry+ chimaeras, indicating that ESC had a negative impact on nephron maturation.

All types of chimaera showed development similar to the one observed in intact kidneys, with minor differences. Firstly, the Wt1 and laminin immunostaining showed that ES chimaeras had smaller glomeruli-like structures, in comparison to kidney and Bry+ chimaeras (Fig. 5.4 and 5.5). Secondly, the Six2 and calbindin immunostaining revealed that in all chimaera types the condensing MM was present. However, in the ES chimaera, the Six2 positive cells were present along the entire ureteric bud structure, and not only at the UB tip (Fig. 5.7). Thirdly, all chimaera types presented proximal tubule development (LTA staining); however, the number of proximal tubules appeared to be reduced in the ES chimaeras (Fig. 5.8).

Therefore, exogenous cell types have an effect on rudiment chimaera growth and development. The most obvious effect on chimaera growth

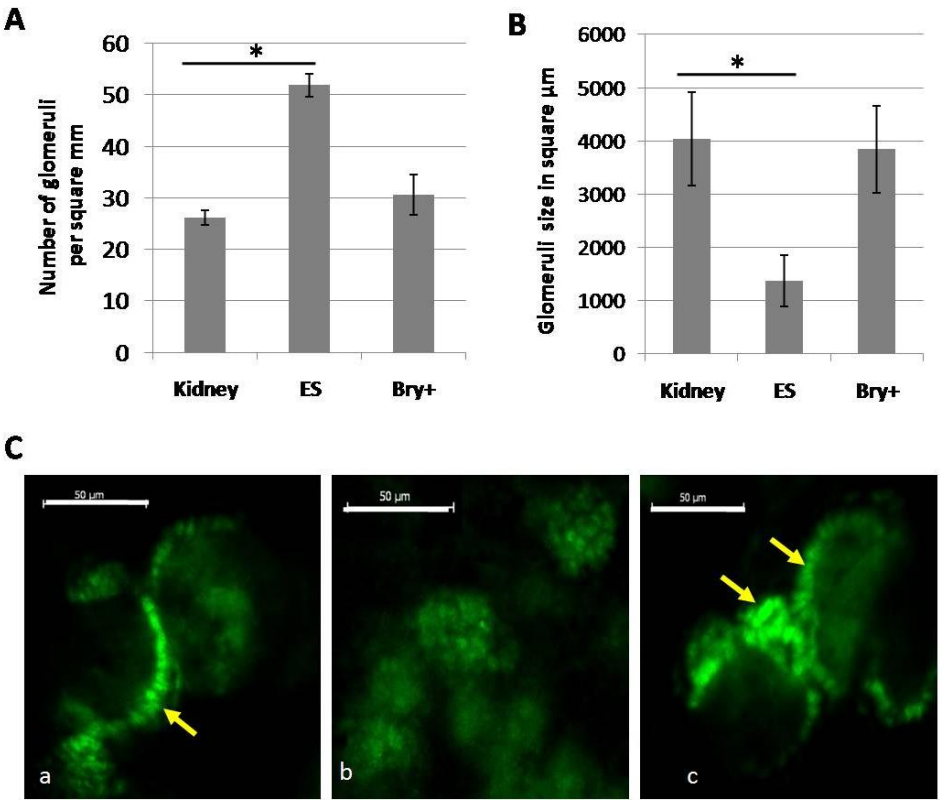

Figure 5.4 Glomerular size and number differ between chimaeras. A) Number of glomerular-like structures formed during three-day culture by kidney, ES and Bry+ cells in respect of area; B) Size of glomerular-like structures formed by kidney, ES and Bry+ chimearas; C) Comparison of glomerular-like structures formed in the kidney chimaeras (a), ES chimaeras (b) and Bry+ chimaeras (c), identified by Wt1 (green) immunostaining; Note that kidney and Bry+ chimaeras showed development of podocyte-like cells (yellow arrow in a and c), whereas glomerular-like structures in ES chimaeras are very numerous but immature, with no evidence of podocyte differentiation ; * - $p<0.001$, N=3, error bar represents standard error; Scale bar – 50µm.

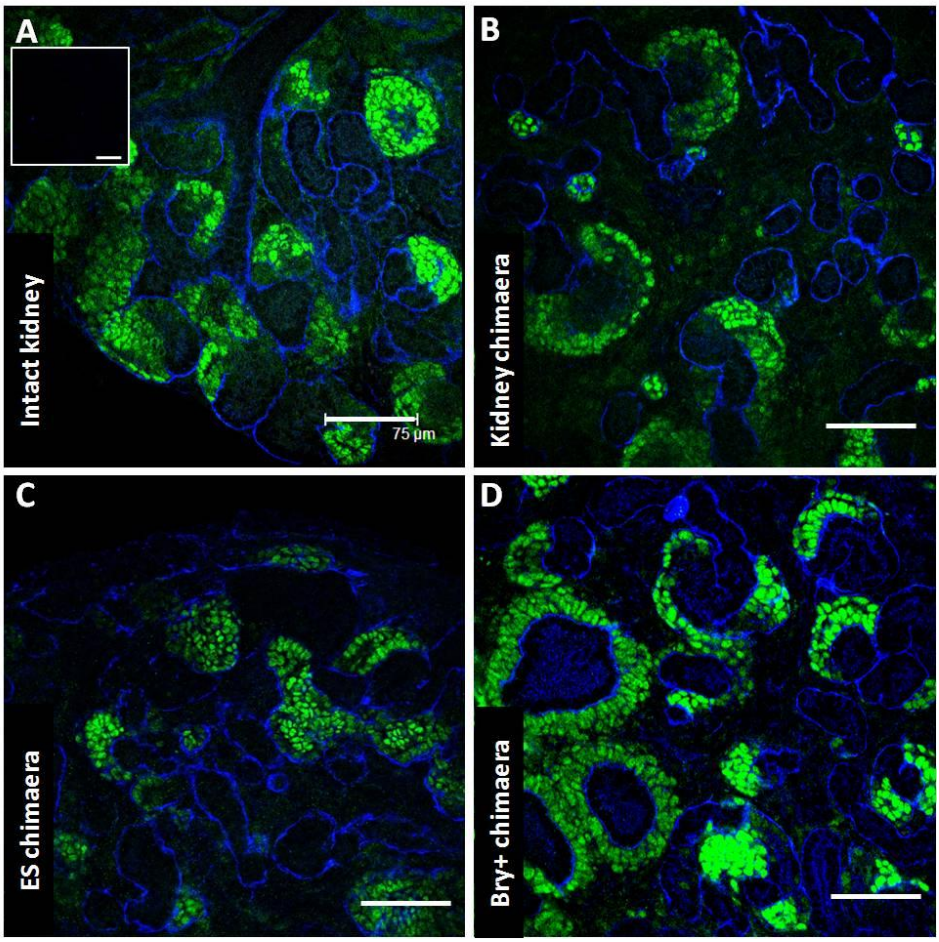

Figure 5.5 Confocal photomicrograph of MM condensation and nephron development in kidney, ES and Bry+ chimaeras by day 3 of culture. Wt1 (green) and laminin (blue) immunostaining of intact kidney (A), kidney chimaera (B), ES chimaera (C), and Bry+ chimaera (D), presenting abilities of all chimaera types to condense MM and develop nephrons. Photograph in left upper corner of A presents secondary antibody (Goat α Mouse IgG1 (488) and Goat α Rabbit (350)) control staining (where the primary antibody was omitted), and applies to all stainings presented in this chapter. Scale bar – 75µm.

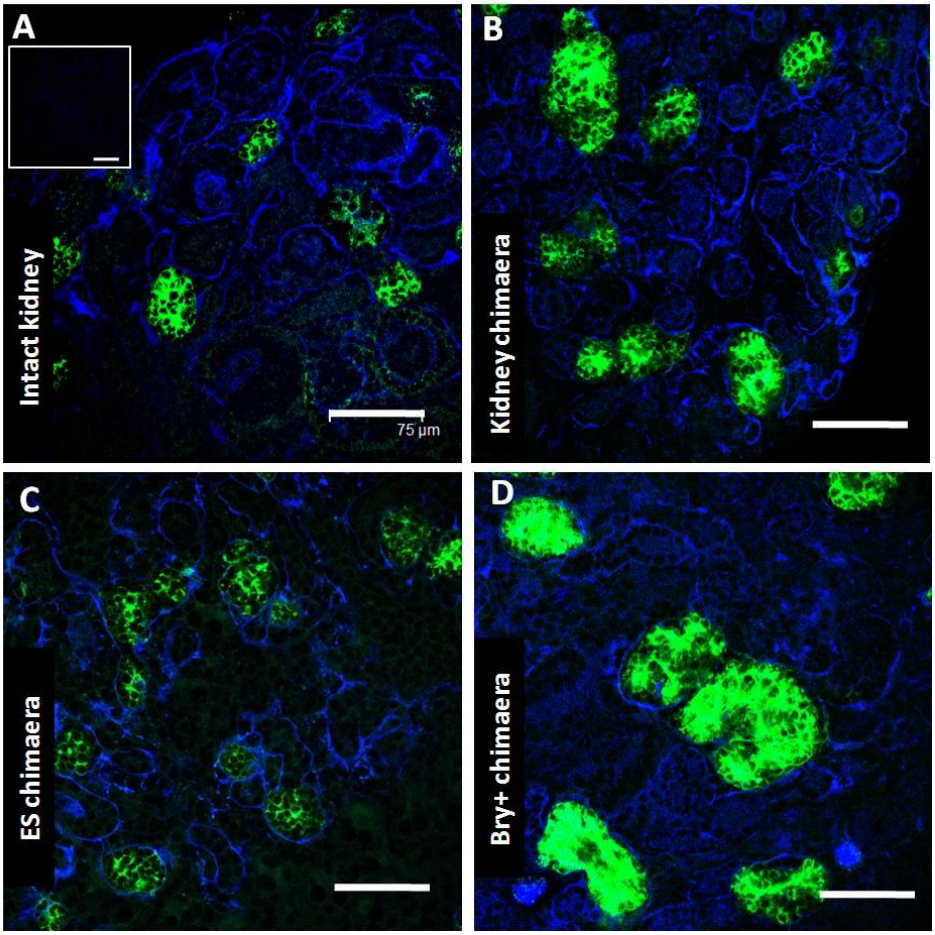

Figure 5.6 Presence of mature podocytes in glomeruli in kidney, ES and Bry+ chimaeras by day 7 of culture. Synaptopodin (green) and laminin (blue) immunostaining of intact kidney (A), kidney chimaera (B), ES chimaera (C) and Bry+ chimaera (D). ES chimera developed mature glomeruli (synaptopodin positive) but were much smaller in comparison to kidney and Bry+ chimaeras. Photograph in left upper corner of A presents secondary antibody (Goat α Mouse IgG1 (488) and Goat α Rabbit (350)) control staining (where the primary antibody was omitted), and applies to all stainings presented in this chapter. Scale bar – 75µm.

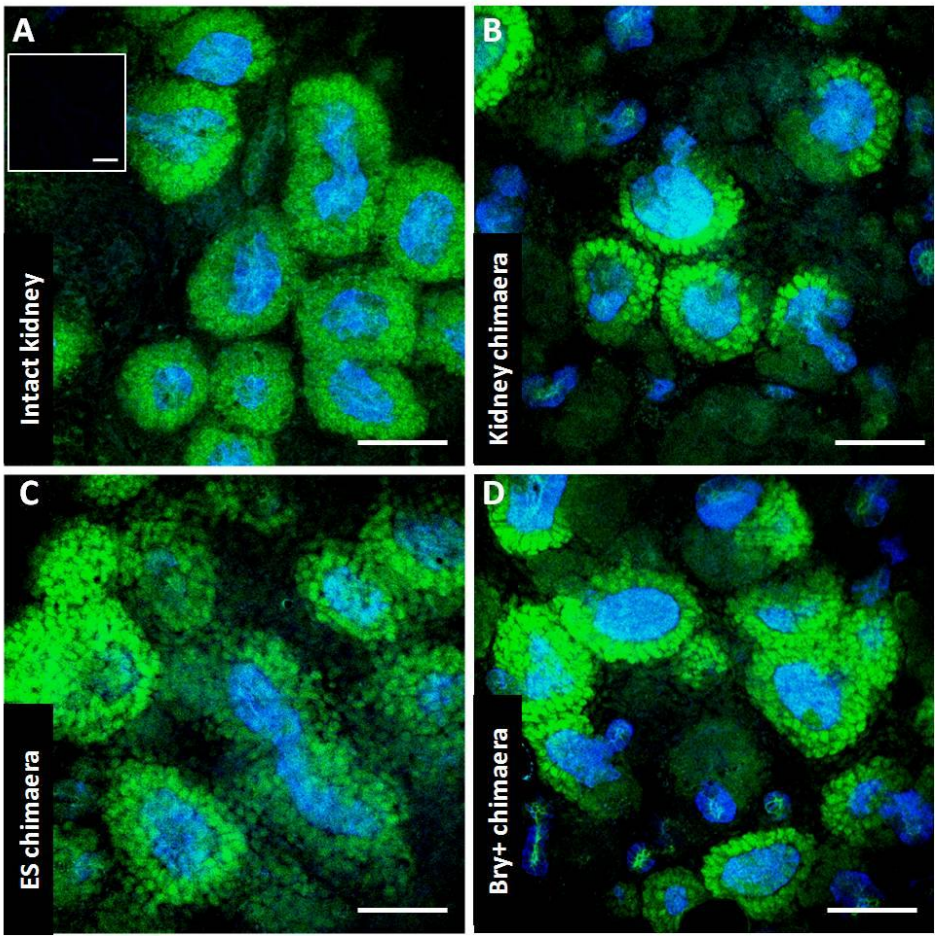

Figure 5.7 Confocal photomicrograph of condensing MM in kidney, ES and Bry+ chimaeras by day 3 of culture. Six2 (green) and calbindin (blue) immunostaining of intact kidney (A), kidney chimaera (B), ES chimaera (C) and Bry+ chimaera (D) presenting abilities of all chimaera types to develop ureteric bud structures (calbindin positive) and condensed MM (Six2 positive). Photograph in left upper corner of A presents secondary antibody (Chicken α Rabbit IgG (488) and Goat α Mouse IgG1 (350)) control staining (where the primary antibody was omitted), and applies to all stainings presented in this chapter. Scale bar – 75μm.

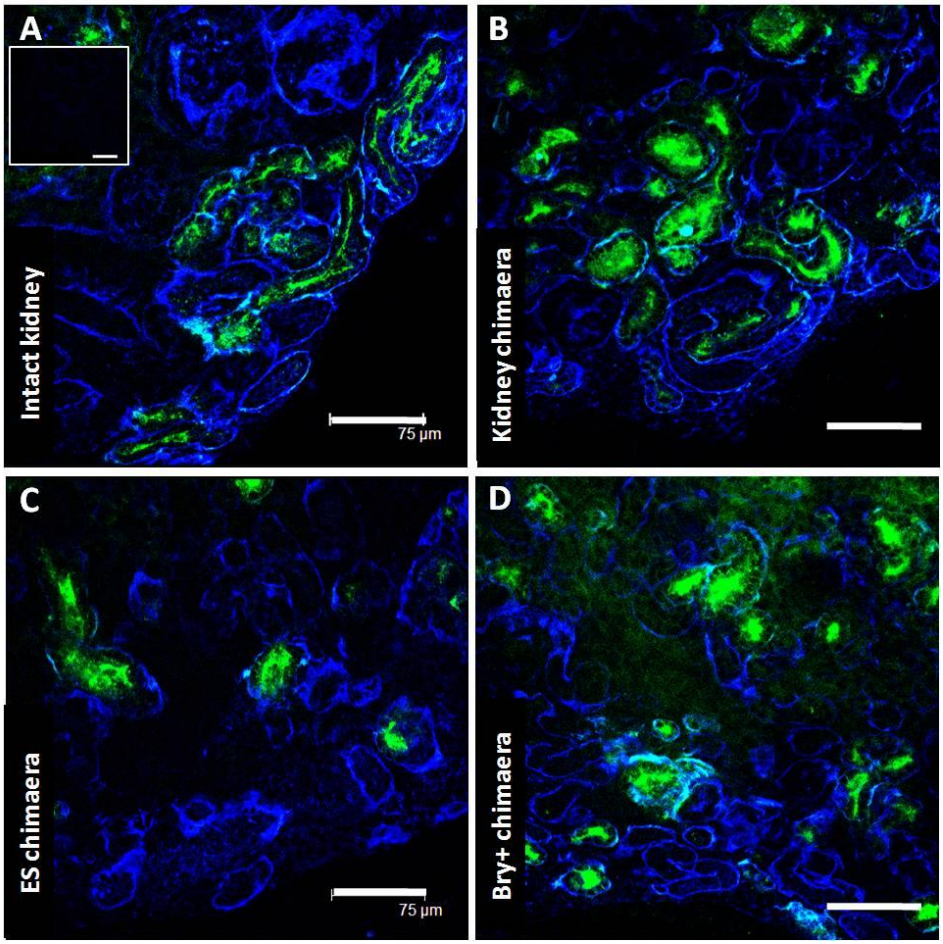

Figure 5.8 Confocal photomicrograph of proximal tubules development in kidney ES and Bry+ chimaeras by day 5 of culture. LTA (green) and laminin (blue) immunostaining of intact kidney (A), kidney chimaera (B), ES chimaera (C) and Bry+ chimaera (D) presenting abilities of all chimaera types to develop proximal tubules. Photograph in left upper corner of A presents LTA lectin and secondary antibody (Goat α Rabbit IgG (350)) control staining (where the LTA and primary antibody was omitted), and applies to all stainings presented in this chapter. Scale bar – 75µm.

had the non-mesodermal (Bry-) cells, which prevented the kidney structures from re-aggregating and re-formatting. Another cell type that induced abnormal rudiment chimaeras development was ESC. The ES chimaeras developed numerous but small glomerular-like structures and formed noticeably fewer proximal tubules. Importantly, ESC – derived mesoderm (Bry+), showed lack of negative impact on rudiment chimaera development. Although, the Bry+ chimaeras were significantly smaller than kidney chimaeras (positive control) they showed most normal development in regard of proximal tubule development and glomeruli number and size, although the later were slightly bigger than observed in the intact kidney.

5.2.3 Integration abilities of mESC and their derivatives

To establish the regions of the developing kidneys into which the exogenous cells integrated, the cells were labelled with QDs prior to chimaera formation. The different regions of the developing kidney were identified, in chimaeras cultured for 3 days, as follows (Fig.5.9):

- Developing glomeruli were identified as aggregates of cells with intense staining for Wt1 surrounded by basement membrane.
- Developing tubules (of both UB and MM origin) were identified as regions not expressing Wt1 surrounded by basement membrane.
- The stroma was identified as a region not expressing Wt1 that were not surrounded by basement membrane.

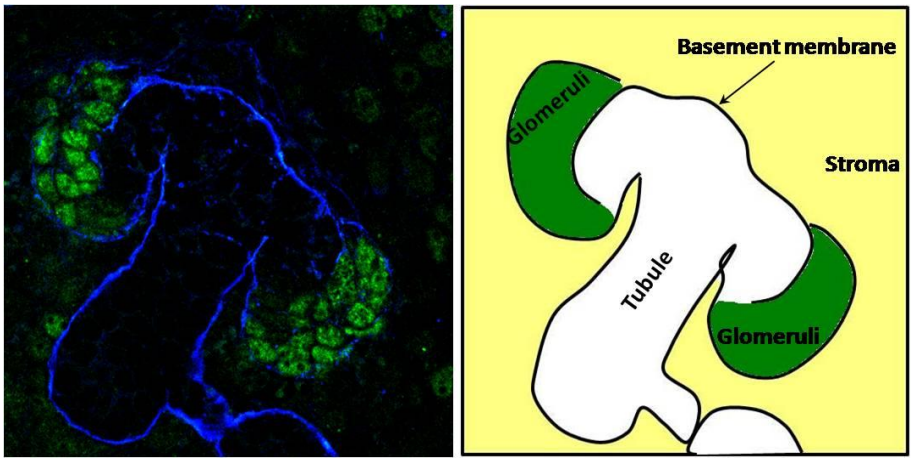

Figure 5.9 Kidney structures developed during three-day culture. Wt1 (green) and laminin (blue) immunostaining presenting tubules of both MM and UB origin, developing glomeruli, surrounded by basement membrane and stroma cells.

The cells of interest, i.e. kidney, ESC and Bry+ cells were easy to identify due to red QD labelling (see chapter 4). Counting of labelled cells in each of the three regions was performed on confocal images taken under a 40X oil objective. For each type of chimaera, three separate experiments were performed and analysed.

The labelled cells showed the following integration pattern:

- kidney cells: stroma (68.6% +/- 10), tubules (26.0% +/- 8.7), glomeruli (5.3% +/- 1.4).
- ESC: stroma (32.2% +/- 2.0), tubules (66.5% +/- 2.2), glomeruli (1.2% +/- 0.5).
- Bry+ cells: stroma (75.5% +/- 1.8), tubules (20.6% +/- 1.8), glomeruli (4.1% +/- 0.5).

The results showed that kidney cells (positive control) and Bry+ cells showed a very similar integration pattern, whereas ESC presented a significantly different integration potential. In other words, kidney cells and Bry+ cells integrated mainly into stroma, whereas ESC integrated mainly into tubules. Figures 5.10 and 5.11 present the integration of labelled cells within the kidney structures of chimaeras at day 3 of culture and the percentage of cells integrated within described structures, respectively.

To establish if the exogenous cells integrated into MM- or UB – derived tubules, staining was performed for the proximal tubule marker, *Lotus tetragonolobus*, a lectin that stains the brush border of proximal tubule cells (Kim, 2005; Steenhard, 2005), and for the UB marker, calbindin.

Statistical analysis of cell integration into proximal tubules versus ureteric bud was performed on confocal images taken under the magnification of 100X. For each sample six images were analysed, from two independent experiments.

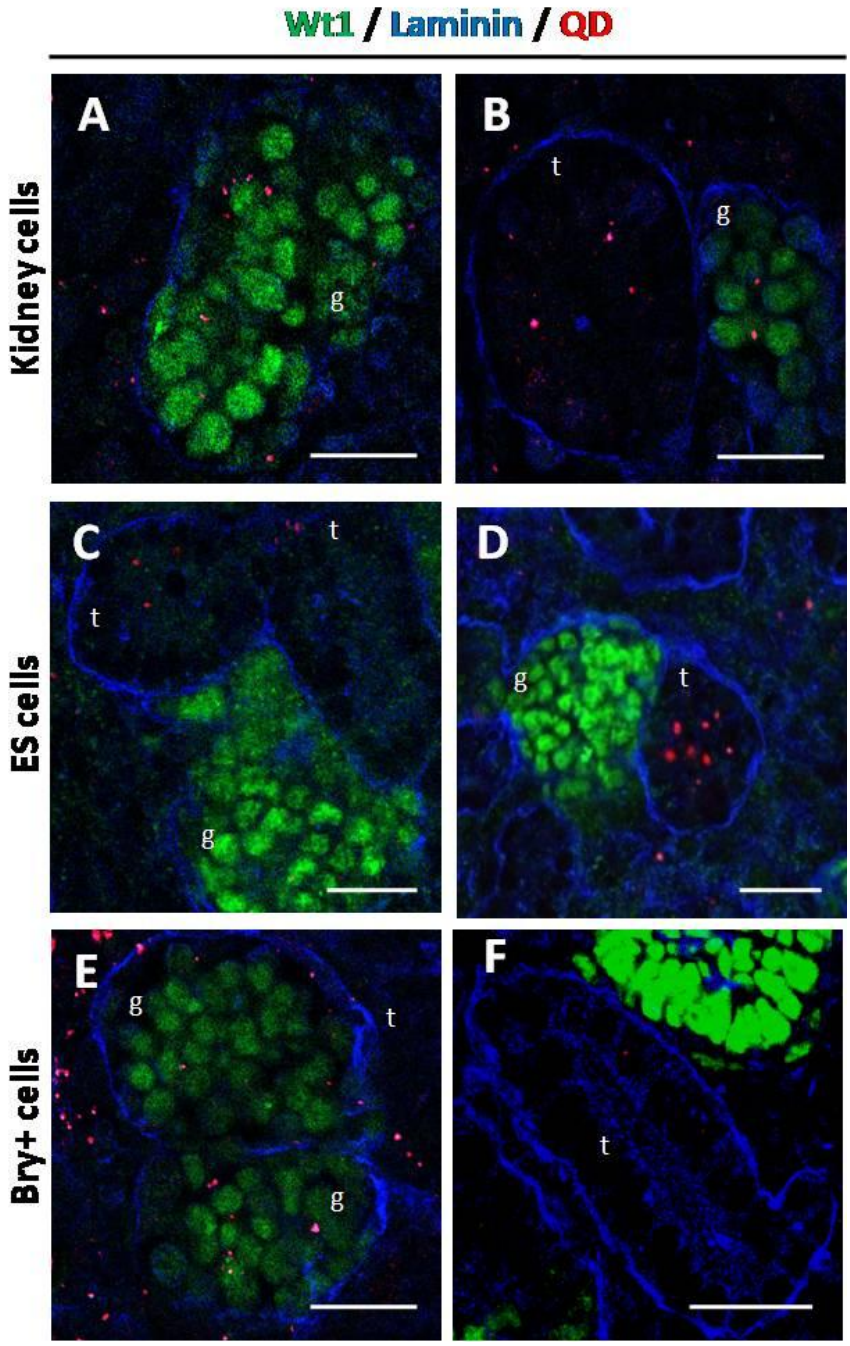

Figure 5.10 Confocal photomicrographs of integration of labelled cells within chimaera structures following 3 days in culture. A & B) labelled kidney cells integrated into glomerular-like structure (A) and tubules (B) in kidney chimaeras; C & D) labelled ESC integrated into glomerular-like structures (C) and tubules (D) in ES chimaeras; E & F) labelled Bry+ cells integrated into glomerular-like structures (E) and tubules (F) in Bry+ chimaeras; g – glomerular-like structure, t – tubule-like structure. Scale bar – 20μm.

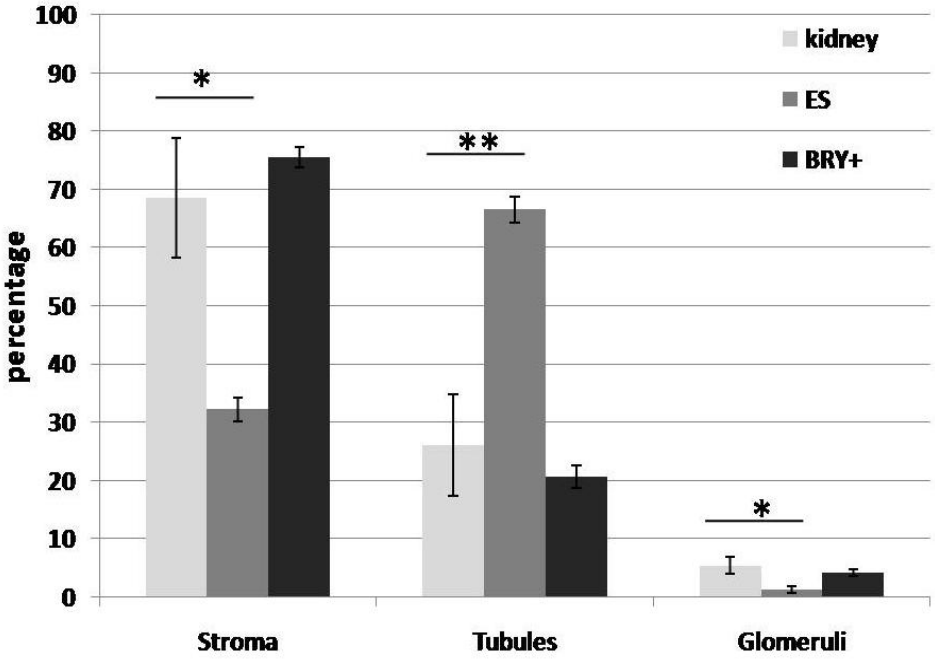

Figure 5.11 Integration potential of kidney cells, embryonic stem (ES) cells and mesoderm-like cells (Bry+) into different regions of the developing kidney. Kidney cells and Bry+ cells showed similar integration pattern whereas ES cells showed significantly different integration potential. ES – embryonic stem cells; N=3 for each sample and error bar represents standard error; * - $p < 0.05$, ** < 0.01.

The results showed that all investigated cell types; kidney, ESC and Bry+ cells, integrated into both MM- and UB-derived tubules (Fig.5.12). However, statistical analysis revealed that in all investigated cells types, more cells integrated into the collecting duct tubules than into proximal tubules. Moreover, significantly ($p<0.05$) lower numbers of ESC

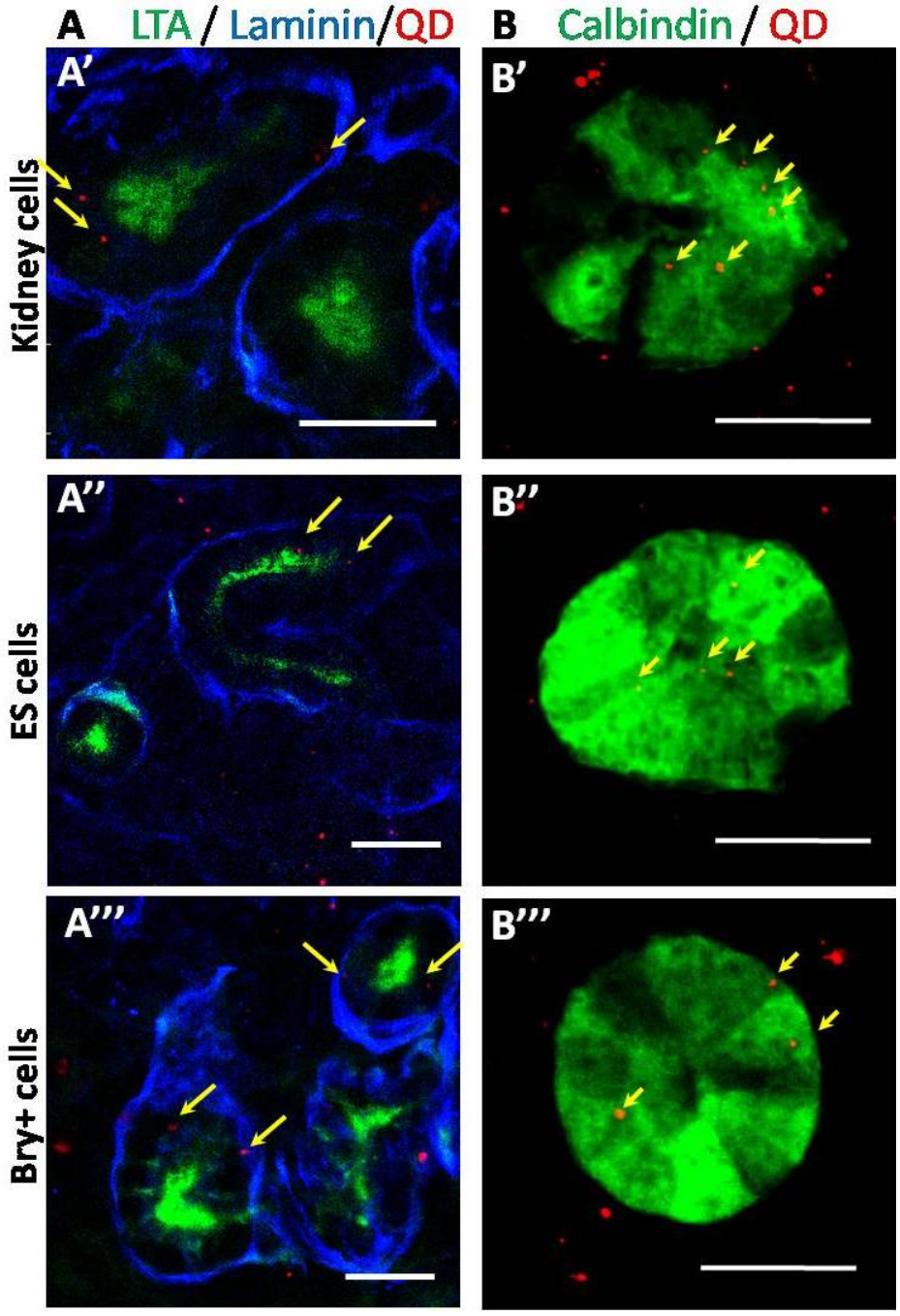

Figure 5.12 Confocal photomicrograph showing differentiation of exogenous cell to proximal tubules cells (A) following 5 days in culture and ureteric bud cells (B) following 3 day in culture, within rudiment chimaeras. Labelled kidney cells (A'), ESC (A'') and Bry+ cells (A''') integrated into proximal tubule of the nephron and into ureteric bud, B' – kidney cells, B'' – ESC, B''' – Bry+ cells; Yellow arrows indicate QD- labelled cells; Scale bar – 20μm.

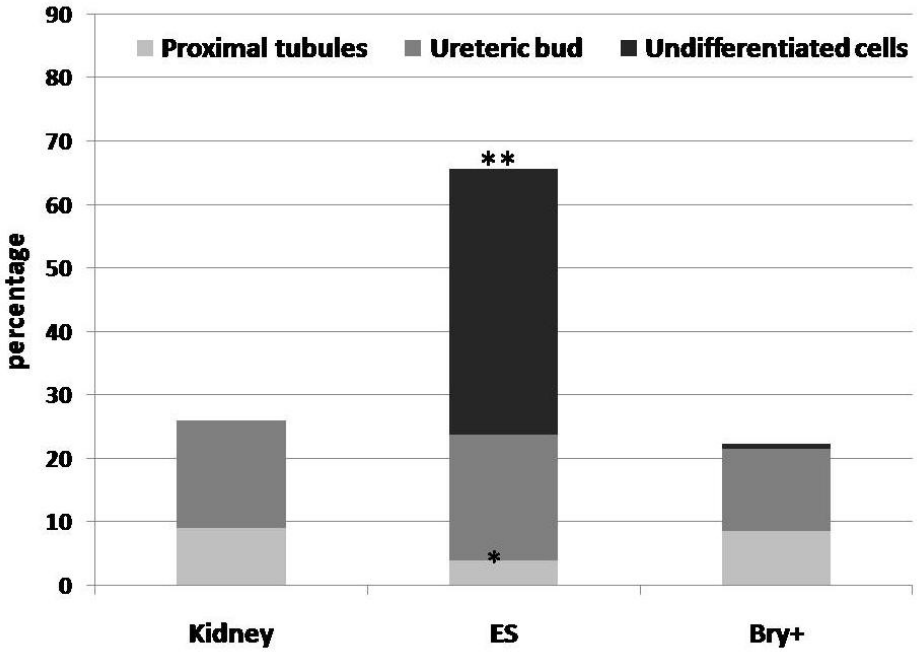

Figure 5.13 Relative integration of cells into tubules of both: MM and UB origins. Percentage of cells integrated into proximal tubules (bottom column); ureteric bud (middle column) and not integrated – undifferentiated cells (upper column). ESC showed significantly lower integration into proximal tubules than kidney and Bry+ cells and showed significantly more undifferentiated cells not integrated into any structures. N=6 for each sample, * - $p<0.05$, ** - $p<0.001$.

integrated into the proximal tubules in comparison to the kidney and Bry+ cells, and more importantly the ESC showed a significant ($p<0.001$) number of cells (>40%) not integrated into proximal tubules neither UB structures, which were later identified as still undifferentiated cells clusters surrounded by basement membrane (see chapter 5.2.4), whereas in Bry+ chimaeras, Bry+ cells presented only 1% of these undifferentiated cells (Fig. 5.13).

The results demonstrated that mES-derived mesoderm (Bry+) cells integrated into the kidney structures in a similar manner as kidney progenitor cells (positive control) into stroma, tubules of MM and UB origin, and glomerular-like structures, whereas undifferentiated mESC showed integration mainly into tubule-like structures. mESC integrated into proximal tubules and collecting duct, but a large number of ESC (>40%) were not integrated into tubular structures but remain in undifferentiated state.

5.2.4 Differentiation potential of mES cells and their derivatives

To investigate the differentiation / nephrogenic potential of mESC and their derivatives (Bry+ cells), exogenous cell types were labelled with QD (see chapter 4) and used to generate ES and Bry+ chimaeras. These chimaeras were stained for markers of kidney-specific cell types, where Wt1 positive cells and synaptopodin positive cells represented mature podocytes, Six2 positive cells represented condensing MM, and calbindin positive cells represented UB tubules. The expression of the aforementioned markers was investigated in exogenous cells before they were used to generate chimaeras.

The results showed that neither ESC nor Bry+ cells showed expression of any of the aforementioned renal markers, Wt1, synaptopodin, Six2 or

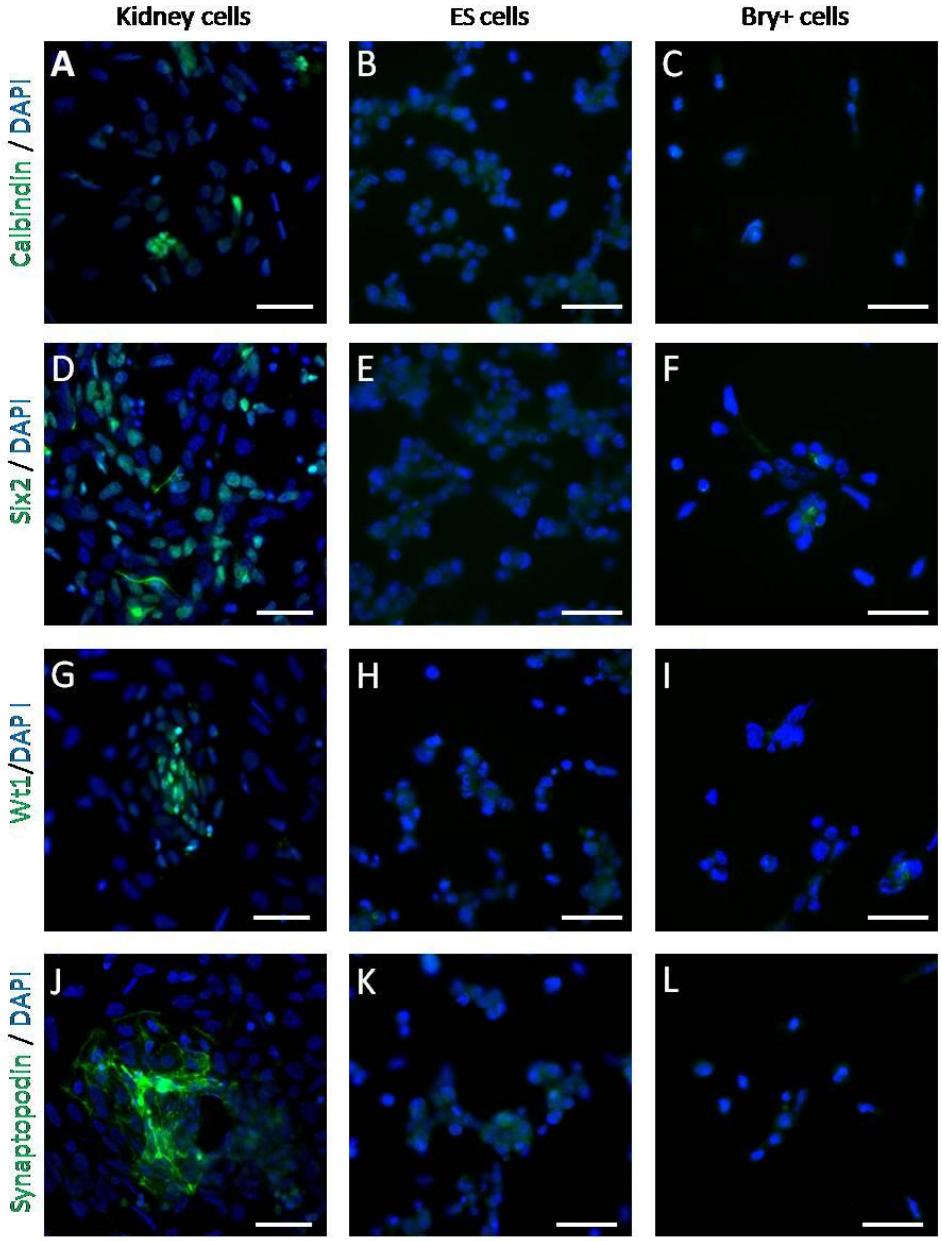

Fig. 5.14 Expression of kidney specific genes: calbindin, Six2, Wt1 and Synaptopodin by kidney, ESC and Bry+ cells (cultured for 24h after dissociation/FACs sort) prior to chimaeras formation. A, D, G, J) Kidney (E13.5) cells presented expression of Calbindin (A) ,Six2 (D), Wt1 (G) and Synaptopodin (J); B, E, H, K) ES cells showed lack of expression of calbindin (B), Six2 (E), Wt1 (H) and Synaptopodin (K); C, F, I, L) Bry+ cells showed lack of expression of Calbindin (C), Six2 (F), Wt1 (I) and Synaptopodin (L); Scale bar 50μm; Experiment performed twice.

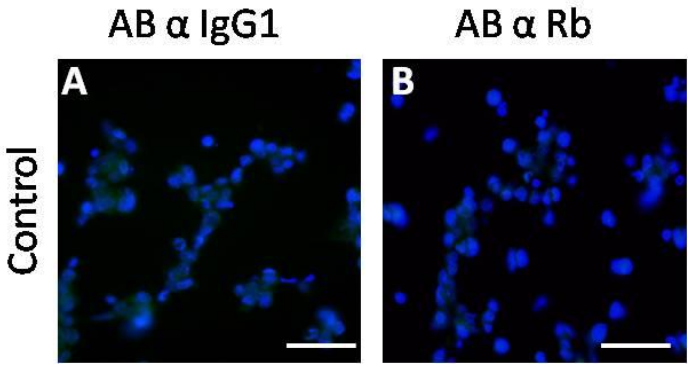

Figure 5.15 Control staining where primary antibody was omitted, on kidney cells cultured for 24h after dissociation, showed light background. A) Goat anti mouse IgG1 antibody; B) Goat anti rabbit IgG antibody. Scale bar – 50m; Experiment performed twice.

calbindin prior to generating chimaeras in comparison to kidney cells (positive control) (Fig. 5.14). The negative control of the experiment, where primary antibody was omitted, showed light background staining (Fig. 5.15). However, after integration, QD-labelled Bry+ cells showed expression of Wt1, synaptopodin, Six2 and calbindin (Fig. 5.16), when integrated into appropriate renal structures. This was very similar to the positive control of kidney chimaeras. Undifferentiated ESC showed up-regulation of calbindin, but very few were found to up-regulate Wt1, and all failed to show up-regulation of synaptopodin and Six2 (Fig. 5.16). The negative controls for all previously mentioned staining on chimaeras, where primary antibody was omitted, showed lack of unspecific staining (Fig.5.5-5.8).

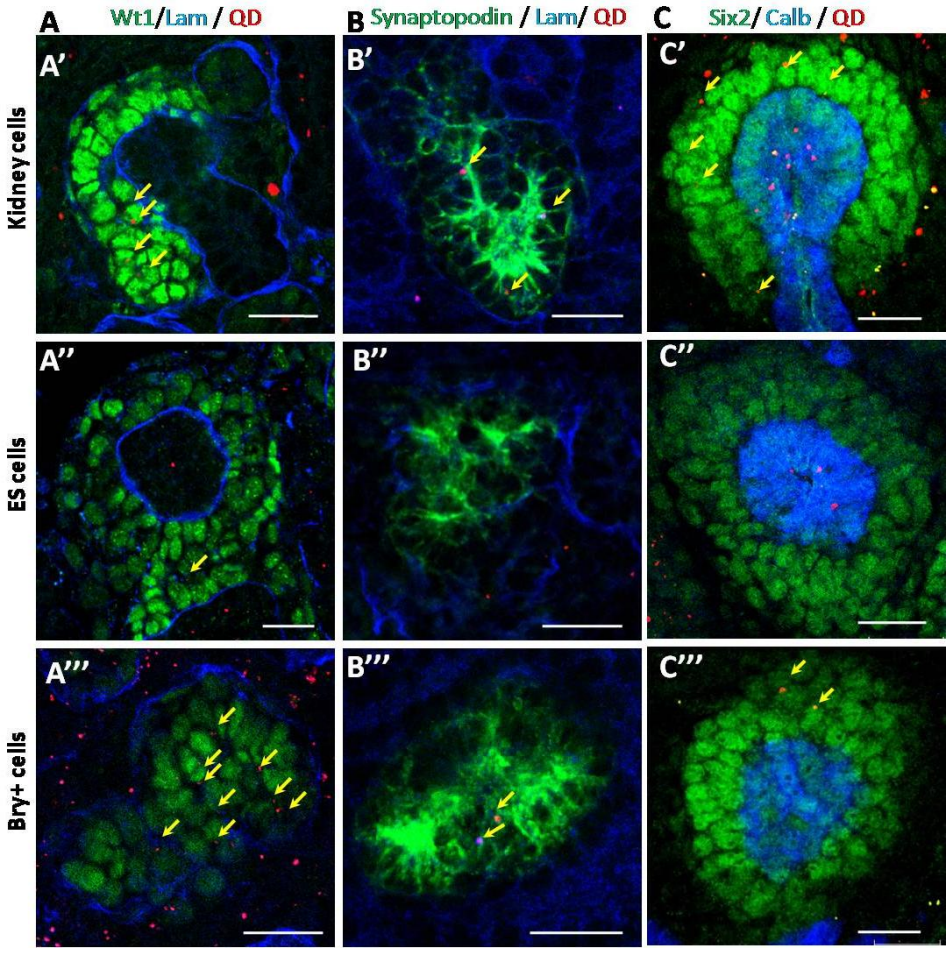

Figure 5.16 Confocal photomicrographs presenting up-regulation of kidney specific markers by integrated exogenous cells. A) Wt1 (green) and laminin (blue) staining present QD-labelled cells of kidney (A') and Bry+ (A''') that integrated into glomeruli-like structures and up-regulated Wt1, while ES cells (A'') did not up-regulate Wt1; B) Synaptopodin (green) and laminin (blue) staining present QD labelled cells of kidney (B') and Bry+ (B''') that integrated into glomeruli-like structures and formed podocyte-like cells, whereas ES cells (B'') did not up-regulate synaptopodin and were not found in the podocyte-like cells; C) calbindin (blue) staining present QD-labelled cells of kidney (C'), ES (C''), Bry+ (C''') cells that integrated into ureteric bud structures up-regulated calbindin (blue); Six2 (green) staining show QD-labelled cells of kidney (C') and Bry+ (C''') that were present in condensed MM and up-regulated Six2 (green), while only ES (C'') cells did not show up-regulation of Six2 as none of labelled cell was found in the condensed MM region. Scale bar – 20μm. Yellow arrows pointing onto integrated cell that have up-regulated Wt1 (A), synaptopodin (B), and Six2 (C).

The results demonstrated that Bry+ cells after integration into kidney structures, showed up-regulation of all important kidney markers of podocytes (Wt1 and synaptopodin), condensing MM (Six2), and UB tubules (calbindin), whereas undifferentiated ES cells showed convincing up-regulation of calbindin only.

5.2.5 Investigating the presence of undifferentiated (Oct4 positive) ESC in rudiment chimaeras

Although expression of organ specific markers is an important process after cell integration, the opposite important process that will demonstrate cell profile changes is down-regulation of expression of markers specific for pluripotency, for example the marker gene Oct4.

Therefore, Oct4 expression was investigated in cells before generating chimaeras and in the chimaeras after 3, 5 and 8 days in culture. Results showed that ESC and Bry+ cells presented Oct4 expression prior to chimaera formation as well as at day 0 of culture.

ESC showed a tendency to continue Oct4 expression as long as day 8 of chimera culture. During the first 3 days of culture, cells seemed to clump together, and formed laminin surrounded colonies within the chimera. By day 5 of culture, ESC colonies enlarged in size and were found mainly in the outer area of the chimera. At day 8 of culture, ESC colonies decreased in size, but still remained in the outer area of the chimera forming big clusters.

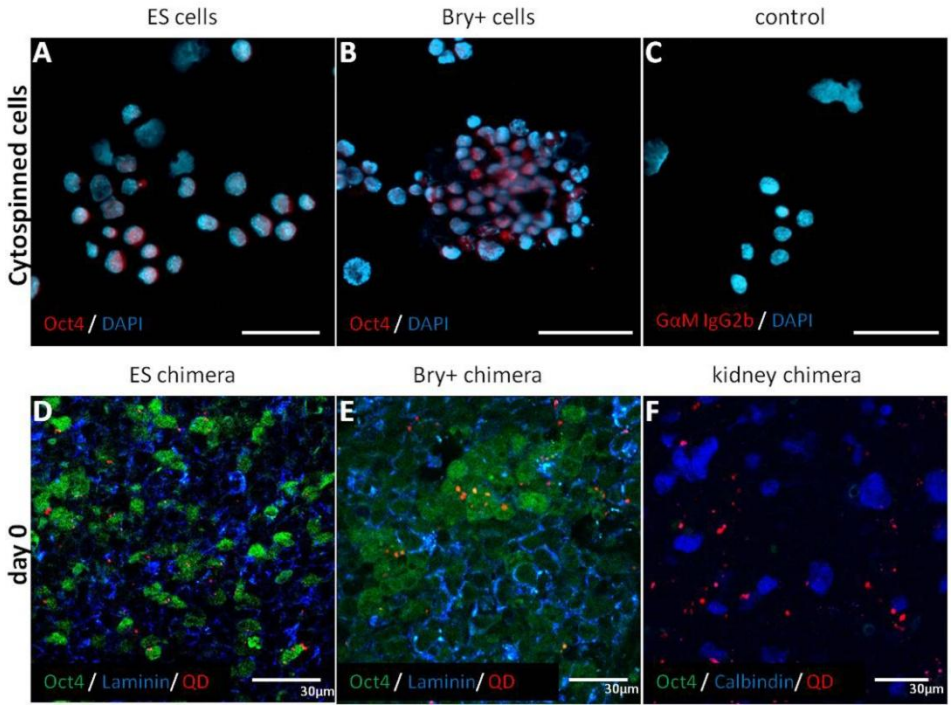

Figure 5.17 Oct4 expression in the ES cells and Bry+ cells before making chimaeras and after 3 hours in culture (day0). A-C) Oct4 (red) and DAPI (blue) staining of cytospinned cells; ES cells (A), Bry+ cells after FACS sort (B) and control of Oct4 staining where the primary antibody was omitted (C); D-E) Oct4 (green) and laminin (blue) staining of chimeras; expression of Oct4 in chimaeras of ESC (D), and Bry+ cells (E); F) Oct4 (green) and calbindin (blue) staining of kidney chimera; control of Oct4 staining in the kidney chimera (F). Scale bar: A-C – 50µm, and D-F – 30µm.

Bry+ cells expressed Oct4 straight after FACS sort and at day 0 of chimera culture, although not in all cells (Fig. 5.17). However, the number of Oct4 positive cells became highly reduced by day 8 of chimera culture. Bry+ chimaeras showed only a few Oct4 positive cells at day 3 and 5 of culture (couple of small colonies composed of 4-12 cells) which decreased even

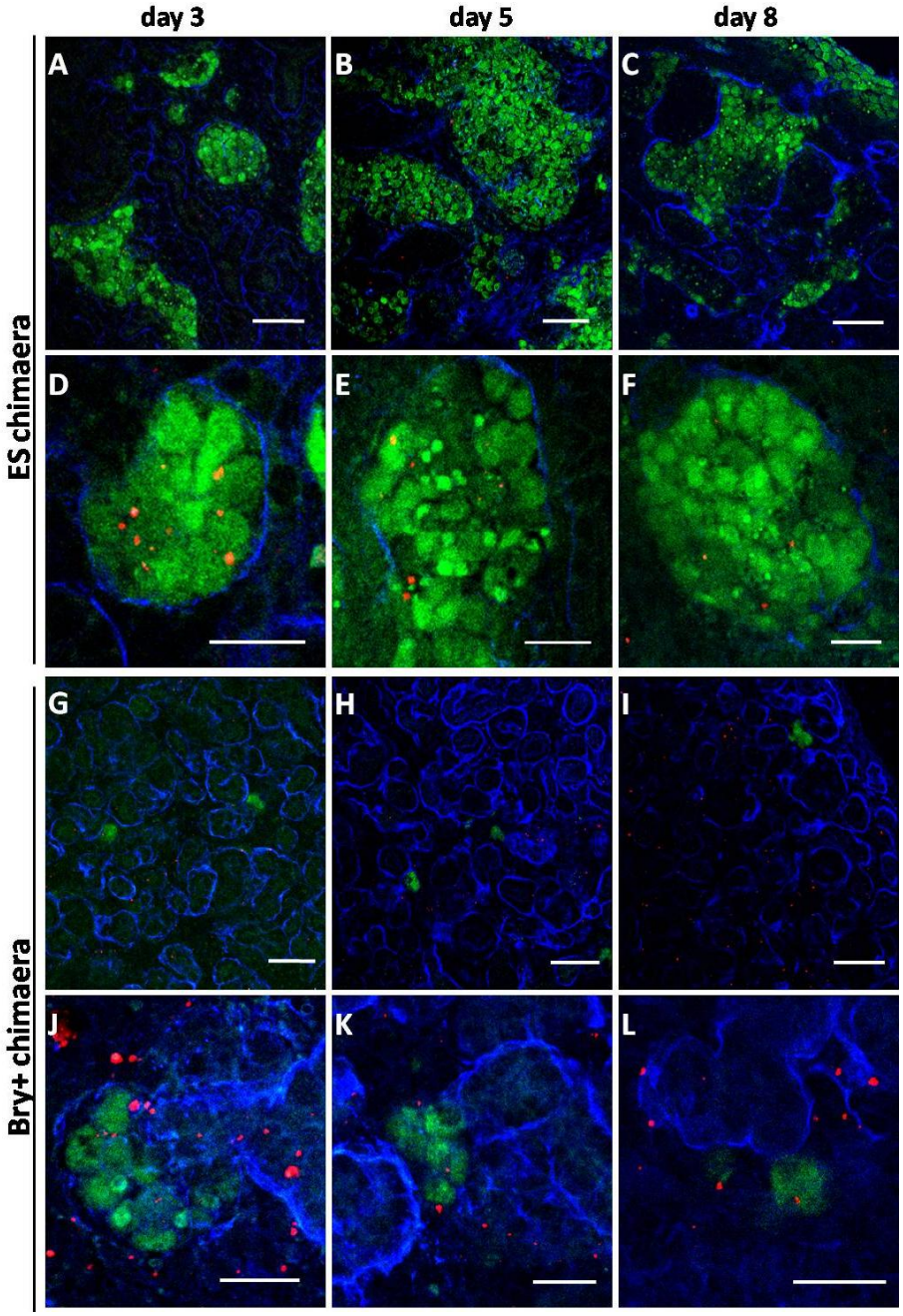

Figure 5.18 Confocal photomicrograph demonstrating the Oct4 positive cells presence in ES and Bry+ chimaeras. Oct4 (green) and laminin (blue) immunostaining of ES and Bry+ chimaeras at day 3, 5 and 8 of culture. A-F) presence of Oct4 positive cells in ES chimaeras at day 3 (A, D), day 5 (B, E), and day 8 (C, F) of culture. G-L) presence of Oct4 positive cells in Bry+ chimaeras at day 3 (G, J), day 5 (H, K) and day 8 (I, L) of culture. Scale bars: A-C and G-I – 60μm; D-F and J-L – 20μm. Experiment was performed twice.

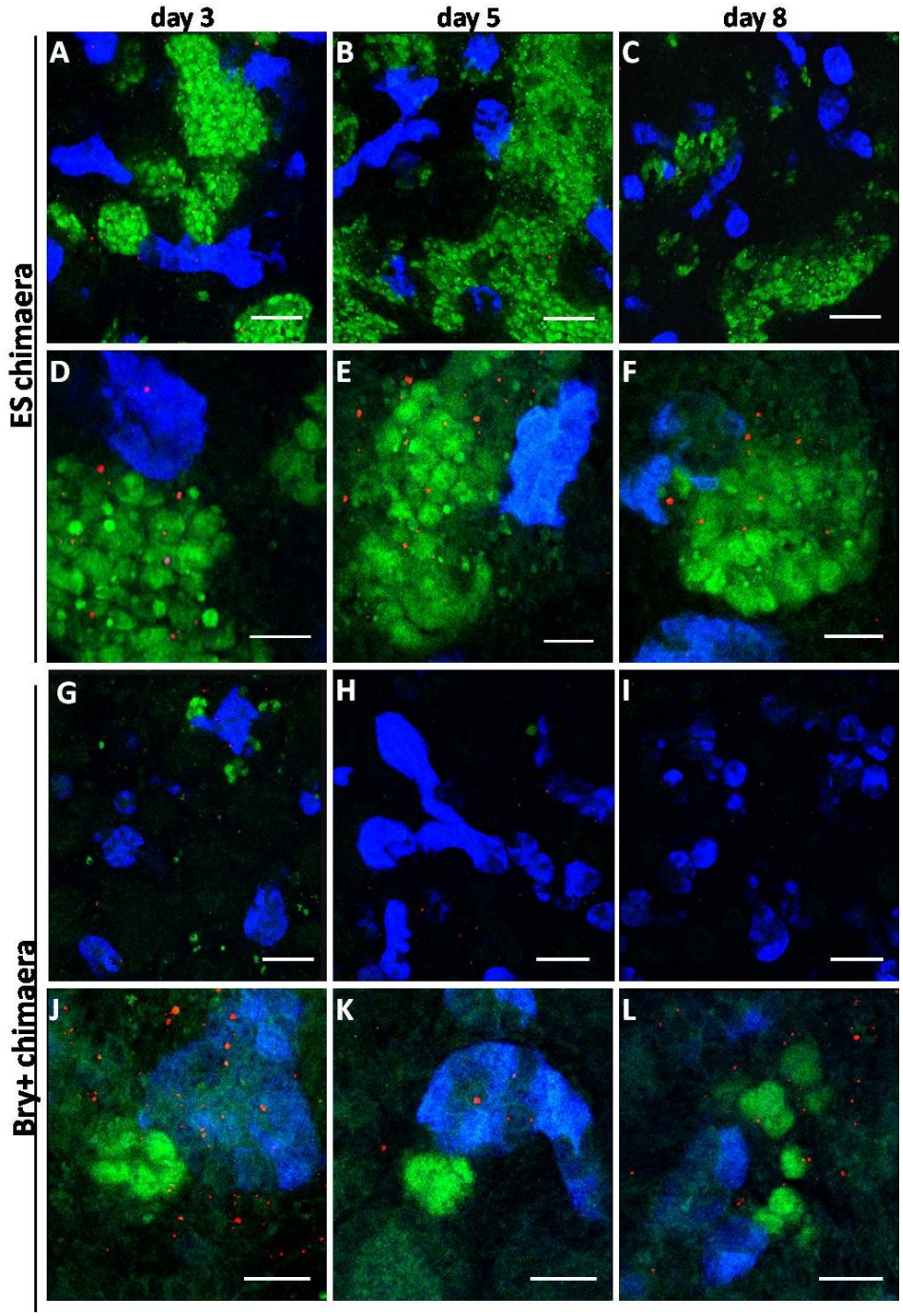

Figure 5.19 Confocal photomicrograph demonstrating presence of Oct4 positive cells in ES and Bry+ chimaeras. Oct4 (green) and calbindin (blue) staining of ES and Bry+ chimaeras at day 3, 5, and 8 of culture. A-F) presence of Oct4 positive cells in ES chimera at day 3 (A, D), day 5 (B, E), and day 8 (C, F) of culture; G-L) presence of Oct4 positive cells in Bry+ chimera at day 3 (G, J), day 5 (H, K) and day 8 (I, L) of culture. Scale bars: A-C and G-I – 60μm; D-F and J-L – 20μm. Experiment was performed twice.

more in size and number by day 8 of chimera culture (Fig. 5.18 and Fig. 5.19).

Therefore, the elaborated results demonstrated, that mESC – derived mesoderm cells (Bry+) have successfully and rapidly down-regulated the pluripotency marker Oct4, in Bry+ chimaeras by day 8 of culture, although a few small colonies still could be observed. However, in ES chimaeras Oct4 positive cells increased in number during the 8 days of culture demonstrating failure of ESC in rapid down-regulation of this pluripotency marker.

5.3 Conclusion

In this chapter, it has been demonstrated that exogenous cell types have an effect on kidney growth and development. On the one hand, the non-mesodermal cells were shown to have a strong detrimental effect on kidney growth, whereas ESC had an effect on normal kidney development. On the other hand, Bry+ cells were shown to have an impact on kidney growth but not on the development. Mesoderm-like cells (Bry+) were shown to have a very similar integration profile to positive control (kidney progenitor cells) as well as the ability to up-regulate kidney specific markers (Wt1, Six2, calbindin, synaptopodin) and down-regulate the pluripotency marker Oct4.

5.3.1 Embryonic kidney rudiments are able to re-form kidney structures after disaggregation at embryonic day 13.5

Saxen's well established method of intact mouse kidney rudiment *ex vivo* culture (Saxen, 1987) is suitable to investigate kidney developmental processes such as ureteric bud branching morphogenesis, metanephric mesenchyme condensation and nephron formation, whereas on the other hand, it is not suitable to investigate the behaviour of exogenous cells introduced to the organ culture system. The majority of cells injected into intact kidneys, remain at the injection site, as the kidney is very compact and organized organ and therefore it is difficult for injected cells to migrate away from the injection site (Steenhard, 2005). It is also possible that cells find it difficult to integrate into structures already delineated by the basement membrane and therefore form their own tubular structures not mixed with the host (Steenhard, 2005), which due to their morphology are characterized as a proximal tubules. This could be due to BMP7 produced by the podocytes of the host that induces proximal tubule growth and development (Kazama, 2008). Therefore, to solve the aforementioned limitations of metanephric organ culture, a novel method was employed, which used dissociated kidney cells to form kidney chimaeras (Unbekandt, 2010). This method was used in the current study to introduce exogenous cells into the embryonic kidney environment and investigate their nephrogenic potential. Although culture conditions were optimised for E11.5 kidneys in Unbekandt's method, in the current study it was shown

that E13.5 kidneys are also able to re-aggregate after dissociation into single cell suspension, and re-form appropriate kidney structures. In this system, no nephron to nephron or bud to bud connections were observed, which is consistent with Unbekandt's study (Unbekandt, 2010).

In the current study, the kidney chimaera formed about 25 glomeruli-like structures per mm^2 by day 3 of culture, and a previous report demonstrated the same number of glomerular-like structures by day 7 of culture (Unbekandt, 2010). This could be an effect of using older embryonic kidneys, E13.5 in the current study and not E11.5, which possibly develop more rapidly than younger kidneys; as well as more cells used at the beginning of the experiment, i.e. 180K and not 80K cells.

5.3.2 The effect of exogenous cells on development of rudiment chimaeras

Embryonic kidneys were shown to be able to re-form kidney structures *in vitro* following dissociation into single cell suspension. However, introduction of different exogenous cell types had an impact on the chimaera growth, development and structure formation. As expected, chimaeras made only from kidney cells developed normally and served as a positive control for all experiments investigating the effect of exogenous cells on kidney development, and the nephrogenic potential of mESC and their derivatives.

mES-derived mesoderm cells (Bry+) chimaeras showed a similar number of glomerular-like structures of similar morphology to kidney chimaeras: large glomeruli with a visible podocyte-like cell layer. In contrast, ES chimaeras formed numerous small underdeveloped glomerular-like structures. This is probably due to the comparable gene expression profile between Bry+ cells and E13.5 kidney cells, especially the mesodermal genes (*Foxc1* and *Osr1*) and kidney marker (GDNF) (see chapter 3); whereas mESC did not show expression of the aforementioned genes. Despite the lack of integration of mESC into glomerular-like structures, they influenced their development. It is known, that elevated levels of FGF7 can increase the number of nephrons in intact kidney cultures by about 50%, and moreover, prolonged exposure to exogenous FGF7 can partially inhibit nephron maturation (Qiao, 1999). Although there is minimal information concerning FGF7 expression by mESC in the literature, it must not be excluded that mESC express FGF7 and therefore elicit a similar phenotype of the many immature nephrons in culture conditions used in the current study.

In contrast to the results of Vigneau and co-workers (Vigneau, 2007), Bry- cells not only did not incorporate into collecting duct structures but had a negative impact on the total kidney development, so that no structures could be observed. The discrepancy between Vigneau and the current study could be due to a different cell differentiation method used. Vigneau added activin A into the embryoid body culture medium, whereas in the

current study only high FCS concentration was used. Therefore, the Bry- cells obtained in the current study could differ from those obtained by Vigneau, in their potential.

The negative effect of Bry- cells on chimaera development could possibly be due to:

- Sequestration of signalling molecules.
- Inhibition of signalling pathways important for kidney development.
- Overexpression of growth factors.

GDNF is a signalling molecule that is crucial for kidney development. Numerous transcription factors, for example: *Pax2*, *Pax8*, *Six1*, *Six2*, *Sall1*, *Eya1* and the *Hox11* paralogous are playing important roles in inducing MM cells to secrete GDNF (Boyle, 2006; Sajithlal, 2005; Takasato, 2004; Wellik, 2002; Xu, 2003). Once secreted, GDNF binds to its receptor c-Ret, localized on the surface of the UB, where it induces UB branching morphogenesis by activating the Wnt pathway (Vize, 2003). Apart from many transcription factors (for example, *Slit2*, *Robo2*) that can inhibit GDNF secretion (Grieshammer, 2004), there are molecules that have a high affinity for GDNF and would be able to sequestrate it (Parkash, 2008). Therefore, a possible explanation for the negative impact of Bry- cells on chimaera development could be due to either direct sequestration of GDNF by Bry- cells or by secretion of heparin sulphates, which could

bind to GDNF and/or c-Ret and block them and therefore prevent their interactions and nephrogenesis induction. However, it is also possible that the negative action of Bry- cells can take place in the later stages of kidney development. For instance, after binding to c-Ret, GDNF activates the Wnt/β-catenin pathway during kidney development (Park, 2007; Vize, 2003). This pathway can be inhibited by Wnt antagonists: e.g., the sFRP class which bind to Wnt ligands or by the Dkk class that bind to a component of the Wnt receptor (Kawano, 2003). Therefore, if Bry- cells are expressing any of the Wnt antagonists they could prevent nephrogenesis in the chimaera rudiment.

Another possibility is high expression of factors such as BMP4 (a member of the transforming growth factor-β (TGF-β) family), which *in vivo* is known as a ureteric bud inhibitor that prevents multiple ureters from forming (Ichikawa, 2002). However, the similar levels of BMP4 expression in Bry- cells to Bry+ cells and mESC (see chapter 3) suggests that this factor is not responsible for inhibiting nephrogenesis in Bry- chimaeras. Nevertheless, another member of the TGF-β family, BMP7, could be involved in inhibiting Bry- chimaera growth. BMP7 was demonstrated as an important survival factor for metanephric mesenchyme in culture, which can efficiently inhibit nephrogenesis and promote expansion of stromal progenitor cells *in vitro* (Dudley, 1999). Moreover, the stromal cells were shown to inhibit nephrogenesis (Yang, 2002). Thus, if Bry- cells express high levels of BMP7, they could induce stromal fate in

the kidney metanephric mesenchymal cells and therefore decrease Wt1 expression in the chimaeras as it was observed in the current study.

All three discussed possibilities are feasible explanations of the detrimental effect of Bry- cells in kidney rudiment development, although they may act independently or in combination.

5.3.3 mES-derived mesoderm and kidney progenitors show similar nephrogenic potential

The results presented have showed that in kidney chimaeras, the majority of labelled kidney cells integrated into renal stroma, fewer cells into tubules and even less into the glomerular-like structures. In the current work, the renal stroma is characterized as cells that are Wt1 negative and not surrounded by the laminin positive basement membrane. In this way, the renal stroma contained both: cells being a real stroma precursor (Six2 negative and Wt1 negative) that inhibit glomerulogenesis (Yang, 2002), and cells of condensed metanephric mesenchyme (Six2 positive), which form the condensed MM cup and represent the cells that are committed to develop into nephrons (Kobayashi, 2008). A key goal in stem cell-based renal therapies would be to have a stem cell that was able to integrate into glomerular-like structures as well as being able to undergo tubular integration (Vigneau, 2007). Importantly, the current study suggests that cells integrated into the renal stroma are able to become part of the nephrons, including glomerular-like structures, during development.

mES-derived mesoderm cells (Bry+) integrated in a similar pattern to kidney cells, mainly into stroma, which may be due to similar gene expression profile, especially the expression of paraxial mesodermal gene *Foxc1*. It was recently shown that paraxial mesodermal cells contribute to the renal stroma during kidney development (Guillaume, 2009) and therefore, expression of *Foxc1* may have a significant impact on cell integration. Moreover, many of these cells (Bry+) were calbindin positive indicating their integration and differentiation into ureteric bud cells. Bry+ cells were also Six2, Wt1, and synaptopodin positive, indicating differentiation into condensing MM cells, early and late (mature) glomeruli, respectively. Furthermore, Bry+ cells and also integrated into proximal tubules, as evidenced by LTA binding thereby proving their nephrogenic potential.

In contrast, undifferentiated ESC which lack the expression of *Foxc1*, showed integration mainly into tubules. Immunostaining for calbindin and LTA confirmed integration of ESC with ureteric bud tubules (calbindin positive) and much less into proximal tubules of the nephron (LTA positive). This is in agreement with previously presented data (Steenhard, 2005), although different methods of cell integration with kidney rudiments were used. Moreover, ESC did not integrate into glomerular-like structures. A possible explanation for this finding may be the kidney microenvironment, which provides specific signals to exogenous cells, which can be properly recognised by ESC derived mesoderm (Bry+) but

possibly not by the undifferentiated ESC. This might be due to the fact that kidney develops from mesoderm and therefore, mESC – derived mesoderm cells (Bry+) are already committed to read signals sent by kidney cells, whereas undifferentiated ESC need to first differentiate into mesoderm within the kidney environment to be able to differentiate into kidney specific cells. Therefore, the differentiation of mESC into kidney specific cells occurs at low frequency.

5.3.4 Undifferentiated ES cells failed to down-regulate Oct4 expression

Undifferentiated ESC, unlike Bry+ cells, failed to up-regulate kidney specific markers (Six2, Wt1, synaptopodin) and down-regulate the pluripotency marker (Oct4). Undifferentiated ESC showed expression of Oct4 until day 8 of culture and there was a visible increase of Oct4 positive cell "colonies". This observation is consistent with the previous report by Steenhard (2005), who demonstrated that ESC constituted about 5% of the total kidney area by day 5 of *in vitro* culture. However, this report did not investigate if ESC remained in an undifferentiated state, whereas in the current study, failure of mESC in down-regulating Oct4 was demonstrated. It is known that for mESC to remain in an undifferentiated and pluripotent state, supplementation of the culture medium with leukaemia inhibitory factor (LIF) is required (Williams, 1988). UB cells within kidney rudiments were shown to express LIF (Yoshino, 2003), and therefore, the

signals for mESC to stay undifferentiated after ES chimaera generation can originate from kidney cells and cause delay in ESC differentiation.

The immunostaining of chimaeras showed many Oct4 positive cells within ES chimaeras and only a few within Bry+ chimaeras. These observations are in agreement with statistical analysis performed in the current study, which demonstrated, that about 40% of cells within ES chimaeras are not integrated into any kidney structure in comparison to only 1% in Bry+ chimaeras at day 3 of culture.

The aim of this work was to determine if ESC and their derivatives are able to respond to developmental signals obtained from the microenvironment of the kidney and to investigate their abilities to incorporate into kidney structures. Based on the presented analysis it was concluded that undifferentiated ESC did not incorporate into kidney structures, but rather stayed in an undifferentiated state. Only mES-derived mesoderm cells (Bry+) can efficiently, not only integrate with kidney structures, but as well up-regulate key kidney specific markers. More importantly, Bry+ cells showed down-regulation of the pluripotency marker Oct4, and therefore could be a potential source of cells for cell therapies. Although integration into kidney structures and up-regulation of kidney specific markers is an important attribute of Bry+ cells, it is also essential to investigate if incorporated cells are able to display kidney functions. The latter will be investigated in the following chapter.

Chapter 6: ESC derived mesodermal cells display normal kidney functionality

6.1 Introduction

The main kidney functions are to regulate the level of water and salts in the blood, and to produce hormones that regulate the blood pressure and retain the homeostasis of the organism. Maintenance of homeostasis is via selective reabsorption of important molecules such as glucose, water and amino acids, and active secretion of toxins of endo- and exogenous origin, including clinically important compounds such as antibiotics or other drugs (Brenner, 2000; El-Sheik, 2008). Such actions take place in the proximal tubule of the nephron although the distal tubule is more active in water reabsorption (Brenner, 2000). The basolateral and apical (brush border) membrane of the proximal tubule is filled with organic anion (OA) and organic cation (OC) transporters (Sweet, 2001). The organic anion transporters (OATs) belong to the solute carrier family that play an important role in anionic drug transport throughout the body and have been identified in fish (Sweet, 1999), mouse (Kobayashi, 2005b), rat (Sweet, 2006), rabbit (Makhuli, 1995) and human (Kimura, 2002).

The active up-take of organic anions from the renal plasma (interstitial renal fluid) is mediated by exchange with other intracellular anions, i.e.

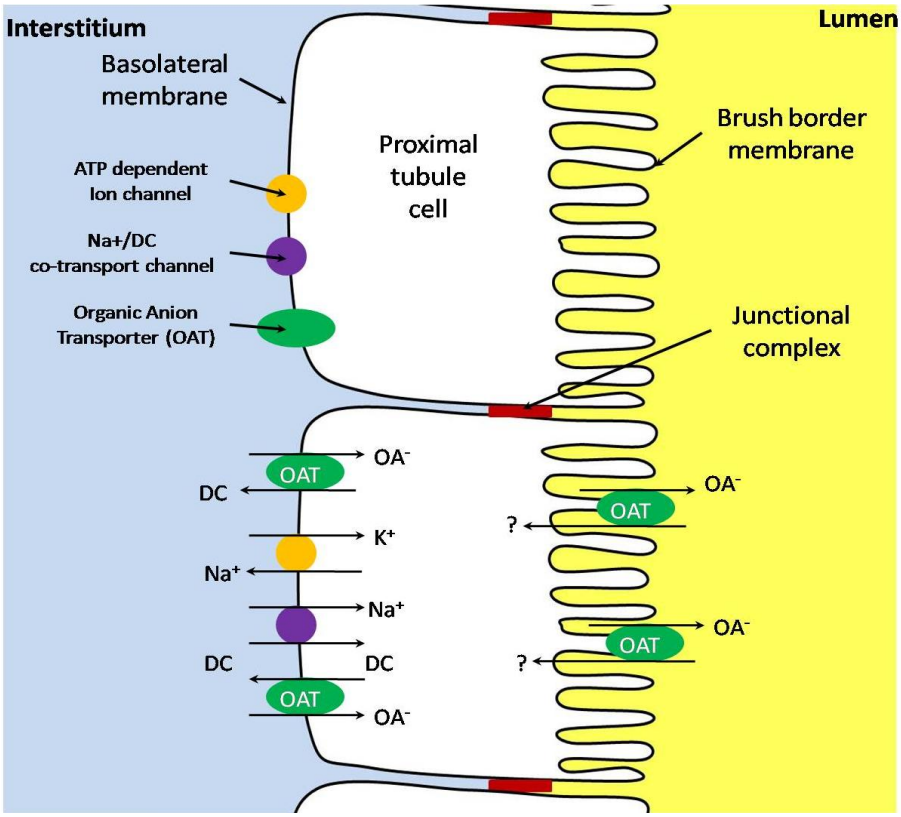

Figure 6.1 Schematic of the organic anion transport mechanism in proximal tubule cells. On the basolateral membrane of the proximal tubule cells, organic anions (OA-) are taken up from the interstitial fluid and transported to the apical membrane (brush border membrane) where OA are secreted into the proximal tubule lumen. On the basal membrane, the OA transport indirectly depends on the Na+ gradient. The ATPase Na+/K+ channel is pumping Na+ outside the cells (interstitium), where it is used as a co-transporter in the Na+/DC (dicarboxylate) co-transport channel. Dicarboxylates (DC) (i.e. α-ketoglutarate), which are pumped into the cell by Na+/DC channels, are used by organic anion transporters (OAT) to carry OA into the cell. On the apical membrane OA are transported outside the cells, but the exact molecules taking part in this exchange process are unknown. Drawing prepared on the basis of: Brenner 2000, Sweet 2001, Sweet 2003 and El-Sheik 2008.

α-ketoglutarate, and depends directly or indirectly on Na^+ gradients (El-Sheik, 2008; Russel, 2002; Sweet, 2003). The transport through the proximal tubule cell from the basolateral to apical membrane is probably mediated by the microtubules (Masereeuw, 2001; Russel, 2002), whereas the transport out, into the proximal tubule lumen is similar to the basolateral membrane mechanisms; however, the anions taking part in that exchange have not yet been identified (Fig. 6.1) (El-Sheik, 2008; Russel, 2002; Sweet, 2001; Sweet, 2003). The basolateral up-take of OA is more efficient than the apical transport, and therefore there is an accumulation of OA in the proximal tubule cell cytoplasm (Masereeuw, 2001).

Knowledge of the mechanism of action of organic anion transporters has led to the identification of OAT inhibitors such as probenecid (4-(dipropylsulfamoyl)benzoic acid) (El-Sheik, 2008; Hsyu, 1988). Probenecid binds to the OA binding site of the transporter and thus inhibits OA transport by preventing the OATs from undergoing the conformational change required for OA transport (Tahara, 2006). Probenecid treatment results in decreased excretion of drugs from the body, and can therefore help to elevate antibiotic concentration in the blood, enabling lower doses to be administered (Butler, 2005).

The functionality of OATs can be investigated in living cells using fluorescent anionic dyes such as lucifer yellow or carboxyfluorescein, (Cole, 1991; Sweet, 2006). Importantly, vital staining with carboxyfluorescein has shown that proximal tubule cells derived from

induced rat metanephric mesenchyme *ex vivo* express functional OATs (Sweet, 2006).

Although previous studies have shown that mESC and mESC – derived mesoderm can generate proximal tubule cells following integration into kidney rudiments *ex vivo* (Steenhard, 2005) and neonatal kidney *in vivo* (Vigneau, 2007), it remains to be established if these cells display normal functionality.

Therefore, the aim of this chapter was to investigate if proximal tubule cells generated from mESC and mESC – derived mesoderm cells displayed normal proximal tubule OAT function. To this end, the vital dye staining method established by Sweet (2006) to investigate function in rat kidney rudiments, was modified and optimised for use in intact mouse kidney rudiments. Following optimisation in intact rudiments, the assay was applied to kidney, ES and Bry+ rudiment chimaeras. In brief, this involved incubating the rudiments in the presence of carboxyfluorescein, and screening the exogenous cells for their ability to transport the anionic dye from the extracellular space into the cytoplasm and finally, into the lumen of the proximal tubule.

6.2 Results

The results will focus on optimising the kidney functionality assay and investigating the OAT function in proximal tubules generated by exogenous cells.

6.2.1 Optimisation of kidney functionality assay

The assay to investigate OAT function in kidney rudiments had been first established using rat kidneys dissected at E13.5, which is equivalent to mouse E11.5. Sweet and co-workers showed that kidneys cultured *ex vivo* begin to function after 7-9 days in culture (Sweet, 2006). In the current study, before investigating the functionality of the ESC and their derivatives in the rudiment chimaeras, it was first necessary to establish the time point when functioning proximal tubule cells differentiated in intact mouse kidney rudiment during *ex vivo* culture.

To enable tubule recognition and help identify the position of the proximal tubules, samples were incubated in the presence of peanut agglutinin lectin (PNA)-rhodamine (red), which labelled tubules of metanephric and ureteric bud origin, and early glomeruli within the kidney and chimaera rudiments (supra-vital staining). Results showed that intact mouse embryonic kidneys, dissected from mouse embryos at E13.5, demonstrated functionality – by active up-take of 6-carboxyfluorescein (6-CF), following 3 days in culture. While, at day 3, only a couple of actively transporting tubules were observed, by day 5 of *ex vivo* culture, many tubules displayed activity. In control samples, accumulation of 6-CF was efficiently inhibited by addition of probenecid into the incubation solution (Fig. 6.2 and Fig. 6.3).

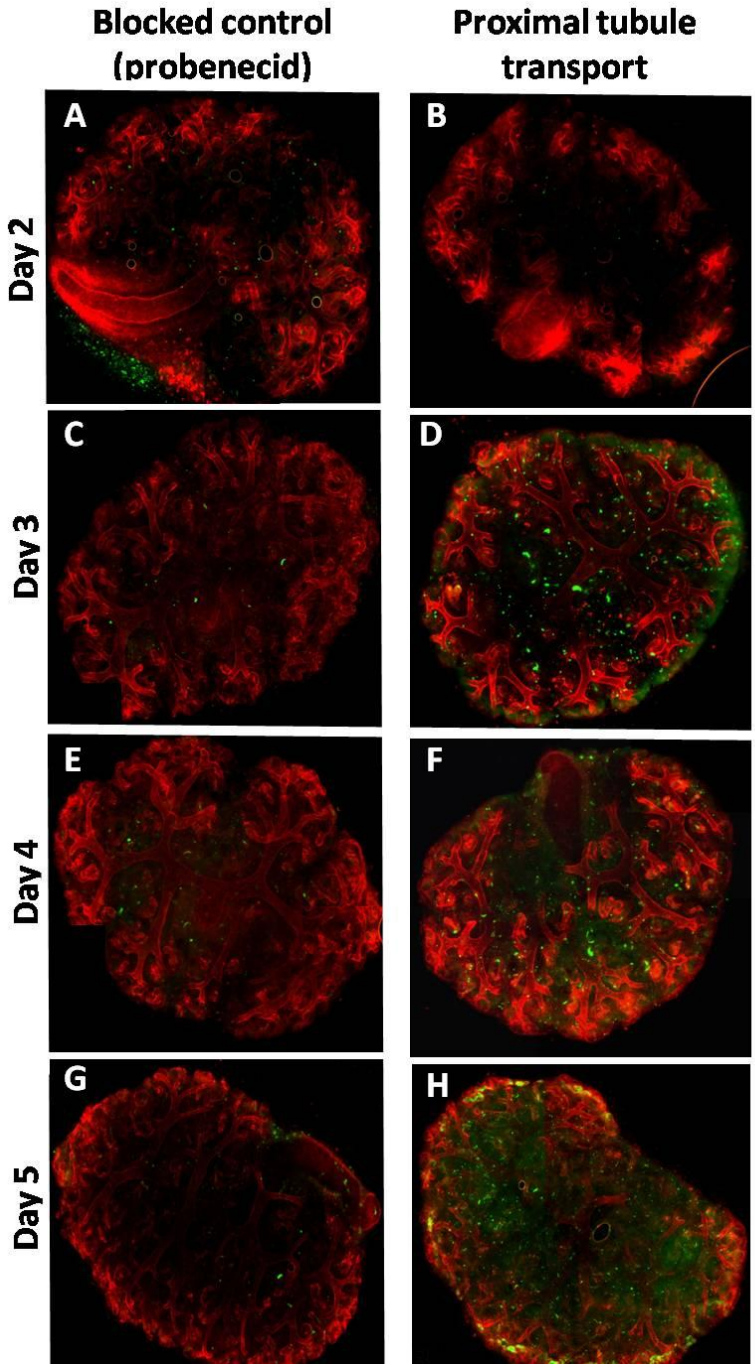

Figure 6.2 Timing of on-set of proximal tubule cell function in kidney rudiments cultured ex vivo. PNA lectin (red) and 6-CF (green) staining presenting OATs function blocked with probenecid (A ,C, E, F) at day 2 (A), day 3 (C), day 4 (E) and day 5 (F) of *ex vivo* culture; and active 6-CF uptake by proximal tubules (B, D, F, H) at day 2 (B), day3 (D) day 4 (F) and day 5 (H). Proximal tubules showed active uptake of 6-CF at day 3 and increased activity by day 5 of culture.

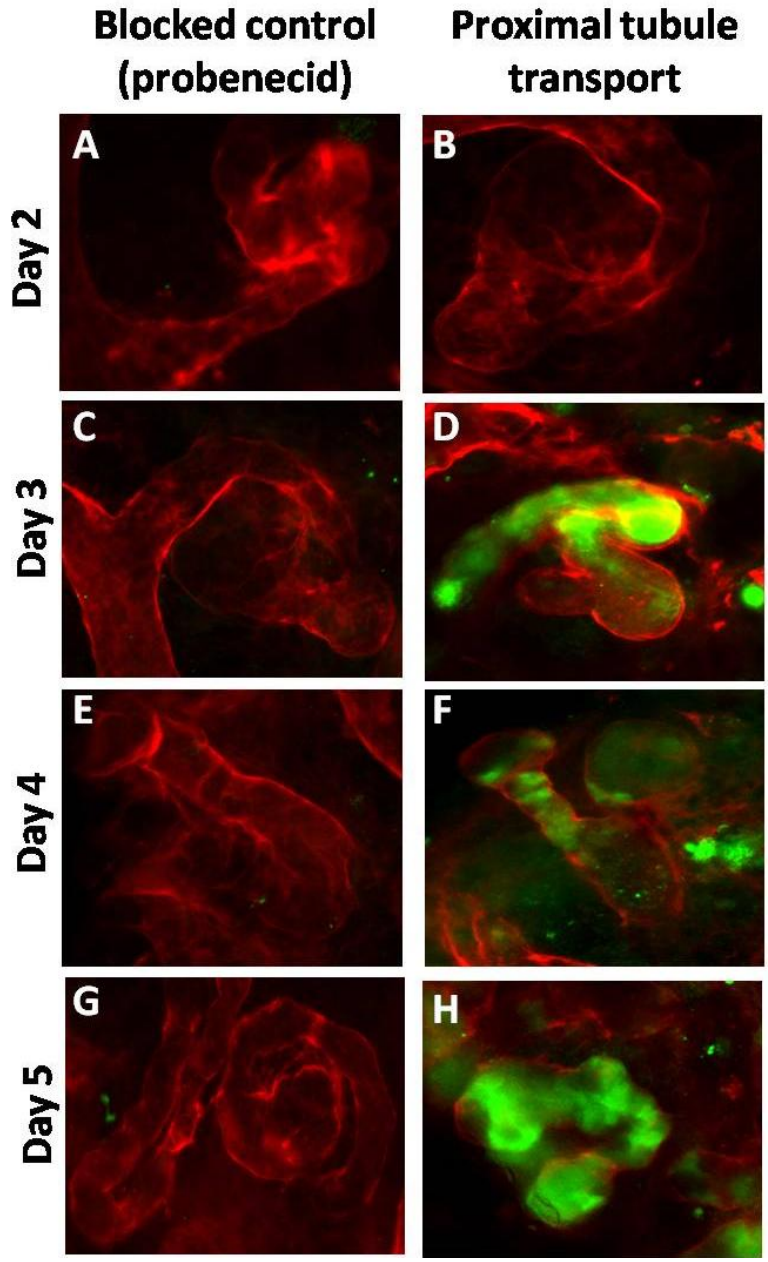

Figure 6.3 Proximal tubule functions. PNA lectin (red) and 6-CF (green) staining presenting effectiveness of probenecid inhibitory functions (A, C, E, G) and 6-CF up-take by proximal tubule cells (B, D, F, H) at day 2 (A ,B), day 3 (C, D), day 4 (E, F) and day 5 (G, H) of *ex vivo* culture.

The results demonstrated that intact mouse E13.5 kidney rudiments began to develop functional proximal tubule cells following 3 day of *ex vivo* culture. By day 5, extensive proximal tubule cell differentiation was observed, as evidenced by the fact that all renal tubules displayed up-take of 6-CF.

6.2.2 Investigating the functionality of proximal tubule cells derived from exogenous cells in mouse rudiment chimaeras

The intact kidney rudiments showed functionality at day 3 of culture and after. The kidney, ES and Bry+ chimaeras, presented very obvious functionality after 4 days in culture (data not shown). Earlier time points (day 2 and day 3) of the samples could not be analysed because of weak adherence and their detachment from the filter membrane. This made the analysis not possible due to sample loss. Therefore, for the reasons mentioned above, day 5 was chosen to investigate the ability of the kidney, ES and Bry+ chimeras to display proximal tubule cells functionality. The active transport of 6-CF in the chimaeras was compared to that in the intact kidney (positive control of the staining), as well as to chimaeras with probenecid (negative controls).

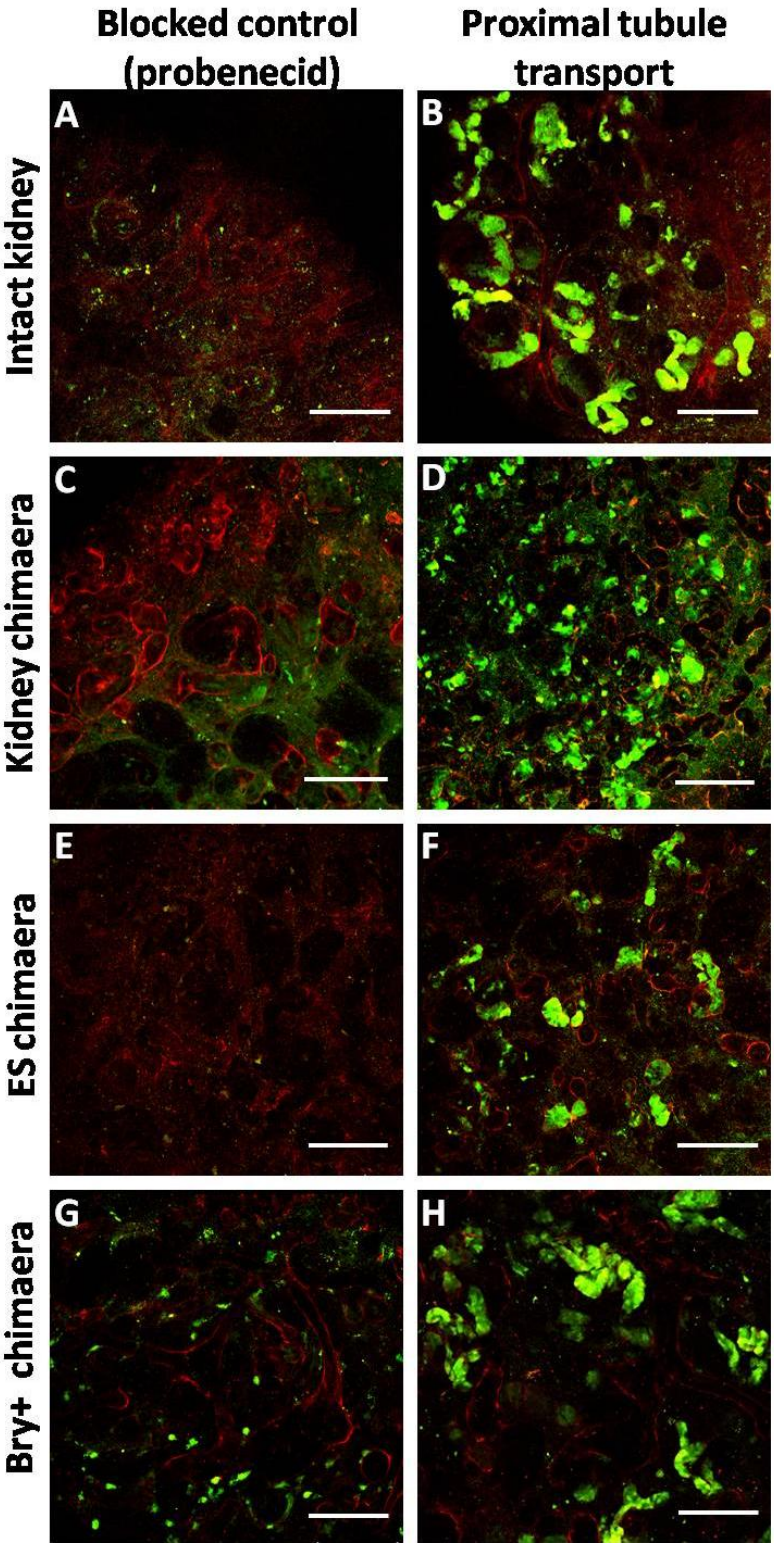

Figure 6.4 Confocal photomicrographs presenting functionality of intact kidney rudiment and the different rudiment chimaeras at day 5 of culture (next page).

Figure 6.4 Confocal photomicrographs presenting functionality of intact kidney rudiment and the different rudiment chimaeras at day 5 of culture. PNA lectin (red) and 6-CF (green) staining presenting effective proximal tubules transport inhibition with probenecid **(**A,C,E,G) in the intact kidney rudiment (A), kidney chimaera (C), ES chimaera (E) and Bry+ chimaera (G); and proximal tubule transport of 6-CF (B,D,F,H) by intact kidney rudiment (B), kidney chimaera (D), ES chimaera (F) and Bry+ chimaera (H). Scale bar – 150μm.

Figure 6.5 Confocal photomicrographs presenting OAT function in integrated exogenous cells in rudiment chimaeras cultured for 5 days. PNA lectin (red) and 6-CF (green) staining presenting effective proximal tubules transport inhibition with probenecid (A,C,F,I) in the intact kidney rudiment (A), kidney chimaera (C), ES chimaera (F) and Bry+ chimaera (I); and proximal tubule transport of 6-CF (B,D,G,J) by intact kidney rudiment (B), kidney chimaera (D), ES chimaera (G) and Bry+ chimaera (J); E, H, K – higher power photomicrographs of functional tubules with QD-labelled cells of kidney (E), ES (H) and Bry+ (K). White arrows are pointing to QD-labelled cells that have integrated with proximal tubule and show active up-take of 6-CF, yellow arrows are pointing to QD-labelled cells that have not integrated into proximal tubules. Scale bar – 20μm.

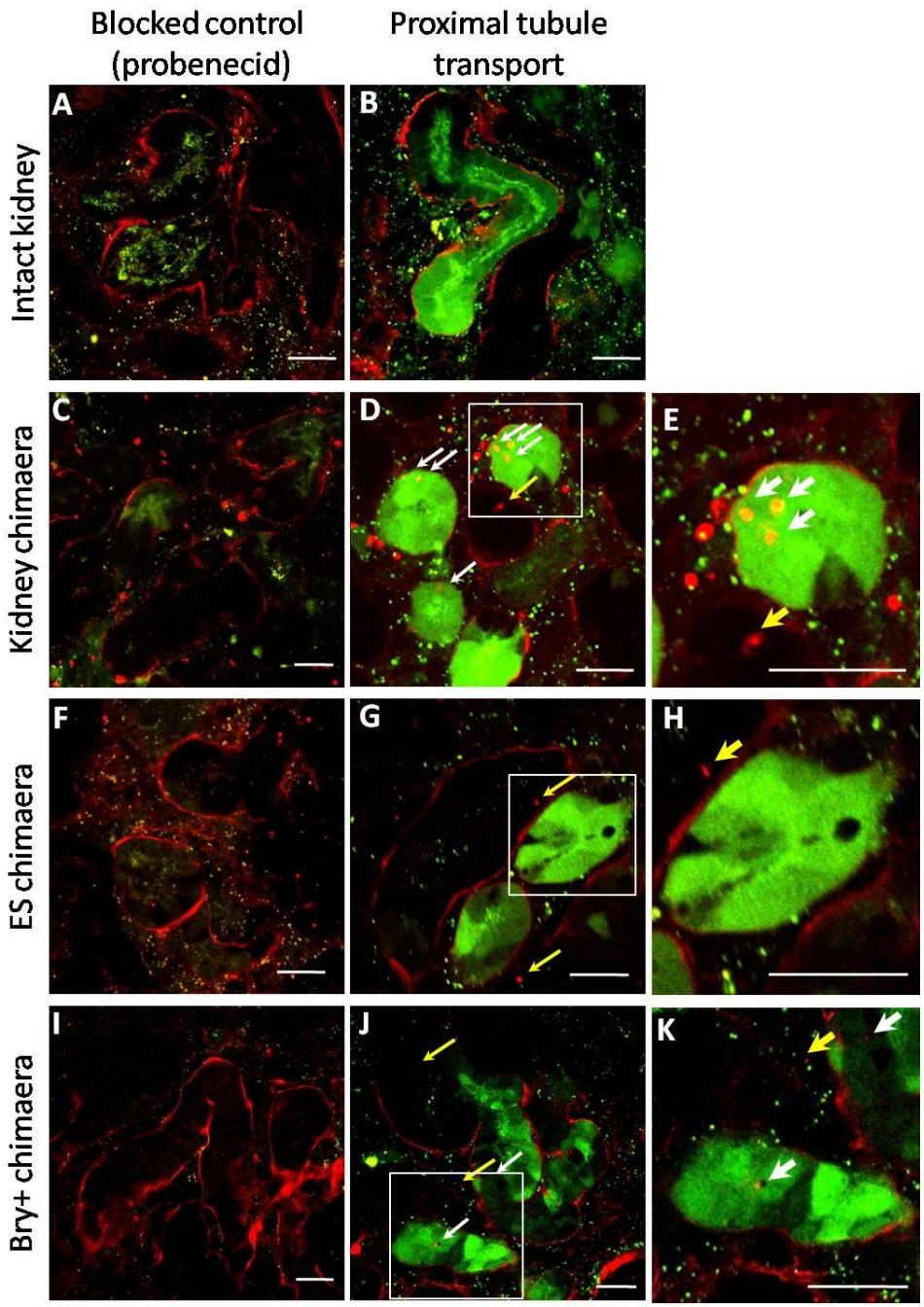

Figure 6.5 Confocal photomicrographs presenting OAT function in integrated exogenous cells in rudiment chimaeras cultured for 5 days (previous page)**.**

The results showed that all chimaera types: kidney, ES and Bry+, were able to transport 6-CF, indicating that functioning proximal tubule cells were present. This active up-take of 6-CF was similar to that observed in the intact kidney although less proximal tubule staining was observed in ES chimaeras, probably due to the fact that fewer proximal tubules develop in these chimaeras (see chapter 5, Fig. 5.8). In all investigated chimaeras, the 6-CF up-take was effectively blocked by probenecid, confirming that 6-CF up-take was OAT dependent (Fig. 6.4). Since all chimaeras showed proximal tubule cell activity, it was important to study if the exogenous cells (i.e., kidney progenitors, ES, Bry+ cells) were able to generate functional proximal tubule cells within the rudiment chimaera. Quantum dot-labelled kidney progenitor and Bry+ cells were found to integrate into the proximal tubules and demonstrated active transport of 6-CF (green label), whereas ESC did not show functionality (Fig. 6.5).

Therefore, the functionality of all types of chimaeras: kidney, ES and Bry+ was presented. Bry+ cells, similarly to kidney cells (positive control), showed transport and accumulation of 6-CF when incorporated into proximal tubules, unlike undifferentiated ESC.

6.3 Conclusion

In this chapter it has been demonstrated that mouse embryonic kidneys show functionality after 3 days in culture, indicated by active up-take of 6-

CF into proximal tubules. Moreover, the chimaeras of kidney, ESC and Bry+ cells presented similar functionality as intact kidney although there were fewer functioning tubules in the ES chimaeras. Detailed analysis showed that mES-derived mesoderm cells (Bry+) display normal OAT function following integration into the proximal tubules of the developing rudiment, indicating that the Bry+ cells are able to generate functioning proximal tubule cells. ESC, on the other hand, did not generate any cells with OAT function.

6.3.1 Mouse embryonic kidney rudiments (E13.5) show functionality after 3 days in culture

Using a well-established method of intact kidney culture (Saxen, 1987), it was shown here that mouse embryonic kidney rudiments dissected at E13.5, showed active 6-CF up-take in proximal tubules, similarly to that observed in rat kidney rudiments *ex vivo* (Sweet, 2006). The accumulation of 6-CF began on the third day of *ex vivo* culture, which is much earlier than was observed in rat kidneys (7 days). This difference in timing is probably due to the fact that the mouse rudiments in the current study were more mature than the rat rudiments used by Sweet and co-workers. It is known that OATs start to be expressed in the developing kidney between day E14 and E16 of normal mouse development and the level of their expression rises as kidney organogenesis proceeds (Sweet, 2001). It was found here that mouse embryonic kidneys dissected at E13.5 showed

functionality after 3 days in culture (E13.5+3), which is comparable to the timing observed *in vivo* (Sweet, 2001).

6.3.2 Kidney dissociation does not affect kidney function

In the current study (see chapter 5), and that of Unbekandt (2010) it has already been shown that dissociated kidney rudiments have the ability to re-aggregate and re-form kidney structures like glomeruli, nephron tubules and collecting duct tubules, and show normal expression of kidney markers. However, in this chapter it is shown for the first time that the proximal tubules that form following re-aggregation, display normal functionality. Furthermore, the onset of the functionality appeared similar in intact and re-aggregated rudiments. The possible support for cells to re-aggregate and re-sort appropriately can be a ROCK inhibitor applied to the culture, which could act via supporting cell survival. It has been shown that ROCK inhibitor can support hESC survival after dissociation (Watanabe, 2007) and following cryopreservation (Li, 2008). It has been also shown to take part in lumen formation in epithelial tubules (Ferrari, 2008). Therefore, the ROCK inhibitor could help epithelial cells to survive in the first 24h following removal from their epithelial sheet and underlying basement membrane, thus enabling them to reform a tubular epithelium.

6.3.3 ESC derived mesodermal cells display proximal tubular cells function

In the previous chapter it was demonstrated using LTA staining, that all investigated cells: kidney, ESC and Bry+, integrated into proximal tubules of the nephron. However, in this chapter, it was presented that only kidney (positive control) and Bry+ cells showed functionality, by active up-take of 6-CF. It is known that the proximal tubule is divided into three segments that differ in their functions. Segment S1 is responsible mainly for selective reabsorption (e.g., glucose and amino acids), S2 for secretion (i.e. metabolites), and S3 for postsecretory reabsorption (mainly water) (Brenner, 2000). The OATs are distributed along the entire proximal tubule, although there are some significant changes between the segments. The highest concentration of OATs is found in the S2 segment (Masereeuw, 2001). Therefore, it is possible that the ESC did not generate proximal tubule cells with secretory function because they only integrated into the S1 and/or S3 segments of the proximal tubules. The other possibility is that ESC which integrated into proximal tubules (see chapter 5, Fig. 5.12) started to differentiate into proximal tubule cells and express OATs, but still on a very low level that was not enough for 6-CF transport at the time point of the experiment.

The proximal tubule cells have secretory functions that have been investigated in the metanephric kidney rudiment culture and rudiment chimaeras as presented in this chapter. They present as well selective

reabsorption functions which are difficult to investigate due to lack of vasculature in the metanephric kidney rudiment culture and therefore lack of ultrafiltrate flow. However, the reabsorption function of the proximal tubule cells generated by exogenous cells could be investigated in an *in vivo* system. For example, following injection of exogenous cells into neonatal mice and their integration (Vigneau, 2007), the fluorescently labelled myoglobin (Gburek, 2003) could be administered. This would induce kidney injury, as myoglobin destroys proximal tubule cells via binding to megalin (Gburek, 2003), and therefore would determine if QD-labelled cells of exogenous origin, become fluorescently labelled and thus represents the same reabsorption functions as kidney cells.

In the previous chapter it was demonstrated that ESC – derived mesoderm (Bry+) cells up-regulated key kidney markes when integrated into appropriate kidney structures, and down-regulated the pluripotency marker Oct4. In this chapter, the ability of Bry+ cells to generate proximal tubule cells with secretory functions was clearly demonstrated by active transport and accumulation of 6-CF within the QD-labelled cells.

Chapter 7: General discussion

In this study the hypothesis that the differentiation of mESCs into mesoderm would significantly improve their ability to integrate into the embryonic kidney was confirmed. Moreover, following successful integration, the mesodermal cells rapidly down-regulated the pluripotency marker Oct4, suggesting that they would be less tumourigenic than undifferentiated precursors. Furthermore, functionality studies indicated that mesodermal cells could generate proximal tubule cells with functioning transporters following incorporation into the kidney rudiment *ex vivo*. Taken together, this study showed that ES-derived mesodermal cells behaved similarly to kidney progenitor cells in regard to integration and functionality *ex vivo*, and could be considered as a serious candidate for future stem cell therapy.

Mesoderm differentiation

The first step in this study was to optimise conditions for directing mesodermal differentiation from mESC. Cells used for this purpose, had GFP knocked into the Brachyury locus and became green if differentiated into mesoderm (Fehling, 2003). Two different conditions for mesodermal differentiation were investigated: the monolayer system and the suspension system. In spite of supplementing the media with growth factors: activin A (2ng/ml) and BMP4 (0.25ng/ml) (Johansson, 1995), mesoderm

differentiation was not induced in the monolayer system. It was reported for hESC that high, short-term BMP4 dose (25ng/ml) can induce mesoderm differentiation in 2-dimension culture (Zhang, 2008). Therefore, one of the reasons, why mESC did not become induced to differentiate into mesoderm in monolayer, could be due to the difference in dose and time of treatment with BMP4. In the current study the BMP4 dose was 100x lower and time of treatment 5x longer than suggested for hESC. On the other hand, the fact that hESC are more similar in their properties and growth requirements to mouse epiblast stem cells rather than mESC (Nichols, 2009b; Tesar, 2007), might explain why the mesoderm induction in these two populations is different; for instance in hESC, mesoderm differentiation is maximal at the 2nd day of induction, whereas in mouse EBs, mesoderm differentiation is maximal at day 4.

High serum concentrations in the media for suspension differentiation of mESC (3-dimension model) (Fehling, 2003) was sufficient for mesoderm differentiation and high numbers of GFP/Bry positive cells (>60%) could be identified and sorted by FACS. However, while only 10% of EBs deposited basement membrane and developed a polarised primitive ectoderm layer, most of EBs showed high mesoderm differentiation. Previous studies on laminin deficient (LamC1^{-}/-) mESC-derived EBs showed that while the basement membrane was required for polarisation of the epiblast to form the primitive ectoderm epithelium, it was not required for undifferentiated mESC in the centre of the EB to differentiate to form

epiblast, as evidenced by expression of FGF5 (Murray, 2000). Moreover, a more recent study has shown that there is an increased level of Bry expression in LamC1^{-}/- EBs (Fujiwara, 2007), indicating that basement membrane deposition inhibits mesoderm differentiation. Therefore, it is not surprising that high numbers of EBs lacking basement membrane gave rise to high numbers of Bry+ cells; however, it is not clear which compound of the media (IMDM) or serum (FCS) could have such a significant effect on laminin deposition in those EBs. Furthermore, the effect of cell density could also play an important role.

Nephrogenic potential of ESC and their derivatives

The next step was to investigate the nephrogenic potential of GFP+, GFP-, and undifferentiated ESC and compare it to that of the kidney progenitor cells. However, to be able to recognize the cells of interest from the kidney rudiment cells following their integration, it was necessary to label the exogenous cells. The label fulfilling the criteria of this study, such as short incubation time, rapid signal appearance, low toxicity, long signal preservation, photobleaching resistance and lack of label transfer between the contacting cells was QDs labelling (Lin, 2007; Rosen, 2007). For cell integration, a method of kidney rudiment disaggregation, incorporation of exogenous cell types and re-aggregation of the chimaeric rudiment was used (Unbekandt, 2010).

The integration experiments investigated the behaviour of four cell types; namely ESC, ES-derived mesoderm (GFP/Bry+), ES-derived ectoderm (GFP/Bry-) and kidney progenitor cells (positive control of the experiments). The ES-derived ectodermal cells had a detrimental effect on the growth and development of the chimaera as discussed in chapter 5, whereas ES-derived mesodermal cells showed a similar integration pattern and kidney marker expression profile to kidney progenitor cells. The difference in the behaviour of those two cell types, Bry- and Bry+, could be most likely due to different lineage commitment which developed during the cell differentiation process; i.e., commitment to ectodermal lineage or mesodermal lineage. This is well known from normal mouse development (Rivera-Perez, 2005; Tam, 1997) and therefore similar cell behaviour can be expected in *in vitro* differentiation. Therefore, the ES-derived mesoderm cells have the potential to become kidney cells and hence are competent to read signals sent by the kidney microenvironment, whereas ES-derived ectoderm cells are committed to become neural cells or surface ectoderm and therefore are not competent to respond to signals sent by the kidney cells. For the same reasons, the undifferentiated ESC did not really integrate: it seemed that although ESCs are pluripotent, the microenvironment of the kidney appeared to be too advanced to enable them to integrate, and many of the ESCs remained undifferentiated. This is possibly due to the fact that UB cells express leukaemia inhibitory factor (LIF) (Yoshino, 2003). In the developing kidney, the normal role of LIF is

to promote condensation of the MM, but LIF also promotes the self-renewal of ESC and inhibits their differentiation (Williams, 1988).

Previous studies showed that although ES-derived mesodermal cells could integrate into neonatal mouse kidneys *in vivo*, they only gave rise to proximal tubule cells and did not generate glomerular, distal tubular cells or ureteric bud derivatives (Vigneau, 2007). In contrast, the current study showed that ES-derived mesodermal cells were able to integrate into ureteric bud, proximal tubules and glomeruli (podocytes) (Tab.7.1).

Tab. 7.1 Comparison of findings by Vigneau et al. and current study.

	Vigneau et al. 2007		**Current study**	
Cell type Cell line	Mouse ESC Rosa26-Lac Z		Mouse ESC Bry-GFP	
Study type	• *Ex vivo* (kidney rudiment) • *In vivo* (neonatal mice kidneys)		• *Ex vivo* (kidney rudiment)	
Differentiation method	EB assay, induced with activin A		EB assay, induced with high FCS concentration	
Injection method	Bolus injection		Re-aggregation method	
Cell selection marker	*Wt1, Wnt4, Pax2* positive	*Wt1, Wnt4, Pax2* negative	*T* positive	*T* negative
Integration	Proximal tubules	Distal tubules, Ureteric bud	Proximal tubules, ureteric bud, glomeruli (podocytes)	Detrimental effect
Functionality	Not shown	Not shown	Proximal tubular cells	N/A

The capacity of these cells to integrate and develop distal tubule cells and other cells of the glomerulus (mesangial cells) have not been investigated, and therefore the possibility that the aforementioned cell type (Bry+) could

generate these cells must not be excluded and should be investigated. Very contradictory results were obtained as well in the case of ES-derived ectoderm cells (Bry-), which were showed by Wilson's group to integrate into distal tubules and UB structures (Vigneau, 2007), whereas in the current study, Bry- cells had a negative effect on kidney rudiment growth. These dissimilarities could arise as an effect of the different differentiation methods used. It is known that activin A is inducing the dorsoanterior-like mesoderm, whereas BMP4 induces the posteroventral-like mesoderm (Johansson, 1995), and the latter was reported to support intermediate mesoderm induction (James, 2005a). Therefore supplementation of the media with only activin A (Vigneau, 2007) might have induced only one type of mesoderm, whereas the use of FCS (current study), which contains both activin A and BMP4 (Kodaira, 2006; Sakai, 1992), induced both mesoderm types, and supported intermediate mesoderm differentiation, which is known to give rise to kidney. This could influence the ability of cells to integrate into kidney structures. The other factor that could influence the difference in the results is the integration method used. Bolus injection of cells into intact kidney rudiment/neonatal kidney (Vigneau, 2007) can limit the motility of exogenous cells as well as adversely affect the rudiment. The method of kidney disaggregation (Unbekandt, 2010), used in the current study, allowed the inhibitory effect of intact epithelium borders on the integration of exogenous cells to be minimised (removal of basement membranes) and permitted improved cell integration (e.g. into

glomeruli). On the other hand, due to disaggregation, kidney cells became more sensitive to the effect of exogenous cells and therefore, the negative effect of Bry- cells could be observed.

Kidney functions

Properly organized kidney structures (i.e., nephrons beginning with glomerulus and connecting to the collecting duct), should display appropriate kidney functions. Investigation of cell functionality is very important, as cells differentiated towards specific lineage and expressing tissue-specific markers, may not display normal tissue functions (Sipione, 2004). Therefore, the next step was to investigate if ES-derived mesodermal cells which integrated into kidney structures were able to function. This thesis is the first to report that ES-derived mesodermal cells display proximal tubule cell secretory function *ex vivo.*

Due to the fact that kidney rudiment chimaeras do not have a blood supply, some kidney functions, such as reabsorption, cannot be investigated *ex vivo*. However, future experiments could address this by using a rudiment transplantation assay, where the kidney rudiments are injected under the kidney capsule of neonatal or adult rodents (Hammerman, 2007; Rogers, 1998). Kidney primordia transplants were shown to be provided with a blood supply from the host and in some cases improved renal function, following one-sided nephrectomy (Hammerman, 2007; Rogers, 1998). Therefore, similar results could be expected to take place in the case of

rudiment chimaera transplants, hence allowing for investigation of the contribution of exogenous cells to glomerular filtration with administration of FITC-dextrans (Woolf, 1990), and to proximal tubule reabsorption, by administration of FITC-myoglobin (Gburek, 2003).

Future directions

In regard of stem cell based therapies, results contained herein, suggest that undifferentiated ESC, although pluripotent, would not be a good source of stem cells to be used directly in kidney failure patients. Firstly, due to the fact that ESC showed weak integration with kidney rudiments and secondly, and more importantly, due to their failure to down-regulate Oct4. This raises important questions about safety in terms of use of the undifferentiated ESC in cell therapies. It was shown that Oct4 is expressed in human tissue cancers (Jones, 2004; Karoubi, 2009) and the significance of Oct4 in tumour diagnosis is growing (Teng, 2005), and therefore cells increasing the risk of cancerogenesis would have to be rejected from therapies (Stojkovic, 2005; Thomson, 1998; Yamamoto, 2006).

In the current study, differentiation of ESC into the first stage of kidney development (mesoderm), showed significant improvement in the ability of cells to integrate into kidney rudiments and down-regulate Oct4. Furthermore, these cells showed proximal tubule functions *ex vivo*. Therefore, this kind of cell differentiation is bearing great hope for stem cell-based therapies. However, there is a risk, that these cells can be

rejected by the patient. Therefore, another source of cells - induced pluripotent stem cells (iPSC) can help to overcome this problem. iPSC can be derived from patients' fibroblast, and reprogrammed to become pluripotent (Okita, 2007; Takahashi, 2006; Wernig, 2007). Such cells could be differentiated towards the kidney lineage and then used to treat kidney failure in patients, at the same time, minimising the risk of graft rejection.

Although the use of ESC and iPSC derivatives in human patients raises safety concerns because of the risk of undifferentiated cells being transplanted and the associated risk of tumour formation, it is worth noting that clinical trials using hESC to treat age related macular degeneration (AGM) are due to take place soon in the UK (Coffey, 2009; Vugler, 2008). If these initial trials are successful and the patients do not experience adverse effects, it is likely that other ESC-based therapies will be developed for various other diseases, including renal disease.

Although the ex vivo model used here has shown the potential of mESC-derived mesoderm for generating functional renal cells, the real nephrogenic potential of all appropriate cells can be truly investigated only in animal models of kidney diseases, such as glomerulosclerosis, glomerulonephritis, rhabdomyolysis or pigmented nephropathy (Gburek, 2003; Gburek, 2002; Nordstrand, 1998; Sugimoto, 2007). Animal studies should focus on investigating kidney morphology and functional improvement following stem cells injection as well as preventing

progression of chronic renal failure. This would allow evaluating the cells real potential use in stem cell-based therapies.

In conclusion, differentiation of ESC into mesoderm improved the ability of these cells to integrate into the developing kidney rudiment ex vivo. ES-derived mesodermal cells showed integration into kidney structures, kidney marker up-regulation and proximal tubule cell functions which was similar to that of kidney progenitor cells. These cells down-regulated the expression of the pluripotency marker, Oct4, and in this regard reduced the potential risk of tumourogenesis. All these attributes of ES-derived mesodermal cells makes them very attractive for future stem cell therapy for kidney disease.

BIBLIOGRAPHY

ASASHIMA, M., NAKANO, H., SHIMADA, K., KINISHITA, K., ISHII, K., SHIBAI, H., UENO, N. (1990). Mesodermal induction in early embryos by Activin A (erythroid differentiation factor). *Roux's Archives of Developmental Biology* **198,** 330-335.

ATLASI, Y., MOWLA, S., ZIAEE, S., GOKHALE, P., ANDREWS, P. (2008). Oct4 splieced variants are differentially expressed in human pluripotent and nonpluripotent cells. *Stem Cells* **26,** 3068-3074.

BAICU, S., TAYLOR, M. (2002). Acid-base buffering in organ preservation solution as a function of temperature: new parameters for comparing buffer capacity and efficiency. *Cryobiology* **45,** 33-48.

BARASCH, J., YANG, J., WARE, C., TAGA, T., YOSHIDA, K., ERDJUMENT-BROMAGE, H., TEMPST, P., PARRAVICINI, E., MALACH, S., ARANOFF, T., OLIVER, J., . (1999). Mesenchymal to Epithelial Conversion in Rat Metanephros Is Induced by LIF. *Cell* **99,** 377-386.

BAXTER, M., CAMARASA, M., BATES, N., SMALL, F., MURRAY, P., EDGAR, D., KIMBER, S.,. (2009). Analysis of the distinct functions of growth factors and tissue culture substrates necessary for the long-term self-renewal of human embryonic stem cell lines. *Stem Cell Research* **3,** 28-38.

BLOMER, U., NALDINI, L., KAFRI, T., TRONO, D., VERMA, I., GAGE, F., . (1997). Highly efficient and sustained gene transfer in adult neurons with a lentivirus vector. *Journal of Virology* **71,** 6641-6649.

BOSSOLASCO, P., MONTEMURRO, T., COVA, L., ZANGROSSI, S., CALZAROSSA, C., BUIATIOTIS, S., SOLIGO,D., BOSARI, S., SILANI, V., DELILIERS, G., REBULLA, P., LAZZARI, L. . (2006). Molecular and phenotypic characterization of human amniotic fluid cells and their differentiation potential. *Cell Research* **16,** 329-336.

BOUCHARD, M., PFEFFER, P., BUSSLINGER, M. (2000). Functional equivalence of the transcription factors Pax2 and Pax5 in mouse development. *Development* **127,** 3703-3713.

BOUCHARD, M., SOUABNI, A., MANDLER, M., NEUBÜSER, A., BUSSLINGER, M. (2002). Nephric lineage specification by Pax2 and Pax8. *Genes and Development* **16,** 2958-2970.

BOYLE, S., DE CAESTECKER, M. (2006). Role of transcriptional networks in coordinating early events during kidney development. *American Journal of Physiology Renal Physiology* **291,** 1-8.

BRENNER, B. (2000). *Brenner and Rector's The Kidney*. W.B. Saunders Company, Philadelphia-London-Toronto-Montreal-Sydney-Tokyo.

BURDON, T., SMITH, A., SAVATIER, P. (2002). Signalling, cell cycle and pluripotency in embryonic stem cells. *Trends in Cell Biology* **12,** 432-438.

BUSSOLATI, B. B., S., GRANGE, C., BUTTIGLIERI, S., DEREGIBUS, M., CANTINO, D., CAMUSSI, G. (2005). Isolation of renal progenitor cells from adult human kidney. *American Journal of Pathology* **166,** 545-555.

BUTLER, D. (2005). Wartime tactic doubles power of scarce bird-flu drug. *Nature* **438,** 6.

CHAPMAN, D., AGULNIK, I., HANCOCK, S., SILVER, L., PAPAIOANNOU, V. (1996). Tbx6, a mouse T-box gene implicated in paraxial mesoderm formation at gastrulation. *Developmental Biology* **180,** 534-542.

CHAUDHRY, M., BOWEN, B., PIRET, J., . (2009). Culture pH and osmolality influence proliferation and embryoid body yields of murine embryonic stem cells. *Biochemical Engineering Journal* **45,** 126-135.

COFFEY, P. (2009). Stemming vision loss with stem cells: seeing is believing. *Regenerative Medicine* **4,** 505-507.

COLE, L., COLEMAN, J., KEARNS, A., MORGAN, G., HAWES, C. (1991). The organic anion transport inhibitor, probenecid, inhibits the transport of Lucifer Yellow at the plasma membrane and the tonoplast in suspensioncultured plant cells. *Journal of Cell Science* **99,** 545-555.

COUCOUVANIS E., M. G. (1995). Signals for death and survival: two-step mechanism for cavitation in the vertebrate embryo. *Cell* **83,** 279-283.

DE COPPI, P., BARTSCH, G., SIDDIQUI, M., XU, T., SANTOS, C., PERIN, L., MOSTOSLAVSKY, G., SERRE, A., SNYDER, E., YOO, J., FURTH, M., SOKER, S., ATALA, A. . (2007). Isolation of amniotic fluid stem cell lines with a potential for therapy. *Nature Biotechnology* **25,** 100-106.

DEKEL, B., SHEZEN, E., EVEN-TOV-FRIEDMAN, S., KATCHMAN, H., MARGALIT, R., NAGLER, A., REISNER, Y.,. (2006a). Transplantation of Human Hematopoietic Stem Cells into Ischemic and Growing Kidneys Suggests a Role in Vasculogenesis but Not Tubulogenesis. *Stem Cells* **24,** 1185-1193.

DEKEL, B., ZANGI, L., SHEZEN, E., REICH-ZELIGER, S., EVENTOW-FRIEDMAN, S., KATCHMAN, H., JACOB-HIRSCH, J., AMARIGLIO, N., RECHAVI, G., MARGALIT, R., REISNER, Y. (2006b). Isolation and characterisation of nontubular Sca-1^{+} Lin^{-} multipotent stem/progenitor cells from adult mouse kidney. *Journal of the American Society of Nephrology* **17,** 3300-3314.

DERFUS, A., CHAN, W., BHATIA, S.,. (2004). Probing the cytotixicity of semiconductor quantum dots. *Nano Letters* **4,** 11-18.

DIAZ-FLORES JR. L., M., J., GUTIERREZ, R., VARELA, H., VALLADARES, F., ALVAREZ-ARGUELLES, H., DIAZ-FLORES, L.,. (2006). Review: Aduld stem and transit-amplifying cell location. *Histol Histopathol***,** 995-1027.

DONOVAN, M., NATOLI, T., SAINIO, K., AMSTUTZ, A., JAENISH, R., SARIOLA, H., KREIDBERG, J. (1999). Initial differentiation of the metanephric mesenchyme is independent of WT1 and the ureteric bud. *Development and Genetics* **24,** 252-262.

DRESSLER, G., DEUTSCH, U., CHOWDHURY, K., NORNES, H., GRUSS, P. (1990). Pax2, a new murine paired-box-containing gene and its expression in the developing excretory system. *Development* **109,** 787-795.

DUDLEY, A., GODIN, R., ROBERTSON, E. (1999). Interaction between FGF and BMP signaling pathways regulates development of metanephric mesenchyme. *Genes and Development* **13,** 1601-1613.

EL-SHEIK, A. A. K., MASEREEUW, R., RUSSEL, F.G.M. (2008). Mechanisms of renal anionic drug transport. *European Journal of Pharmacology* **585,** 245-255.

EVANS, M., KAUFMAN, M. (1981). Establishment in culture of pluripotent cells from mouse embryos. *Nature* **292,** 154-156.

FEHLING, H., LACAUD, G., KUBO, A., KENNEDY, M., ROBERTSON, S., KELLER, G., KAUSKOFF, V. (2003). Tracking mesoderm induction and its specification to the hemangioblast during embryonic stem cell differentiation. *Development* **130,** 4217-4227.

FERRARI, A., VELIGODSKIY, A., BERGE, U., LUCAS, M., KROSCHEWSKI, R.,. (2008). ROCK-mediated contractility, tight junctions and channels contribute to the conversion of a preapical patch into apical surface during isochoric lumen initiation. *Journal of Cell Science* **121,** 3649-3662.

FOX, S. (2008). *Human physiology*. McGraw-Hill companies Inc.,, New York.

FUJIWARA, H., HAYASHI, Y., SAZEN, N., KOBAYASHI, R., WEBER, C., EMOTO, T., FUTAKI, S., NIWA, H., MURRAY, P., EDGAR, D., SEKIGUCHI, K. (2007). Regulation of mesodermal differentiation of mouse embryonic stem cells by basement membrane. *Journal of Biological Chemistry* **282,** 29701-29711.

GAO, X., CUI, Y., LEVENSON, R., CHUNG, L., NIE, S., . (2004). In vivo cancer targeting and imaging with semiconductor quantum dots. *Nature Biotechnology* **22,** 969-976.

GAO, X., YANG, L., PETROS, J., MARSHALL, F., SIMONS, J., NIE, S.,. (2005). In vivo molecular and cellular imaging with quantum dots *Current Opinion in Biotechnology* **16**

63-72.

GBUREK, J., BIRN, H., VERROUST, P., GOJ, B., JACOBSEN, C., MOESTUP, S., WILLNOW, T., CHRISTENSEN, E., . (2003). Renal uptake of

myoglobin is mediated by the endocytic receptors megalin and cubilin. *American Journal of Physiology Renal Physiology* **282,** F451-F458.

GBUREK, J. V., P., WILLNOW, T., FYFE, J., NOWACKI, W., JACOBSEN, C., MOESTRUP, S., CHRISTENSEN, E., . (2002). Megalin and Cubilin are Endocytic Receptors Involved in Renal Clearance of Hemoglobin. *Journal of the American Society of Nephrology* **13,** 423-430.

GILBERT, S. (2006). *Developmental biology*. Sinauer Associates Inc, Massachusetts, USA.

GOODWIN, J., KENWORTHY, A.,. (2005). Photbleaching aproaches to investigate diffusinal mobility and trafficking of RAS in living cells. *Methods* **37,** 154-164.

GRATSCH, T., O'SHEA, K. . (2002). Noggin and chordin have distinct activities in promoting lineage commitment of mouse embryonic stem (ES) cells. . *Developmental Biology* **245,** 83-94.

GRIESHAMMER, U., MA, L., PLUMP, A., WANG, F., TESSIER-LAVIGNE, M., MARTIN, G., . (2004). SLIT2-Mediated ROBO2 Signaling Restricts Kidney Induction to a Single Site. *Developmental Cell* **6,** 709-718.

GROTE, D., SOUABNI, A., BUSSLINGER, M., BOUCHARD, M.,. (2005). Pax2/8-regulates Gata3 expression is necessary for morphogenesis and guidance of the nephric duct in the developing kidney. *Development* **133,** 53-61.

GUILLAUME, R., BRESSAN, M., HERZLINGER, D. (2009). Paraxial mesoderm contributes stromal cells to the developing kidney. *Developemntal Biology* **329,** 169-175.

GUO, J., CHENG, E., WANG, L., SWENSON, E., ARDITO, T., KASHGARIAN, M., CANTLEY, L., KRAUSE, D., . (2007). The commonly used b-actin-GFP transgenic mouse strain develops a distinct type of glomerulosclerosis. *Transgenic Research* **16,** 829-834.

GUPTA, S., VERFAILLIE, C., CHMIELEWSKI, D., KREN, S., EIDMAN, K., CONNAIRE, J., HEREMANS, Y., LUND, T., BLACKSTAD, M., JIANG, Y., LUTTUN, A., ROSENBERG, M. (2006). Isolation and characterization of kidney-derived stem cells. *Journal of the American Society of Nephrology* **17,** 3028-3040.

HAMMERMAN, M. (2007). Transplantation of renal primordia: renal organogenesis. *Pediatric Nephrology* **22,** 1991-1998.

HERRERA, M., BUSSOLATI, B., BRUNO, S., FONSATO, V., ROMANAZZI, G., CAMUSSI, G. (2004). Mesenchymal stem cells contribute to the renal repair of acute tubular epithelil injury. *International Journal of Molecular Medicine* **14,** 1035-1041.

HOHENSTEIN, P., HASTIE, N. (2006). The many facets of the Wilms' tumour gene, WT-1. *Human Molecular Genetics* **15,** R196-R201.

HOSHINO, A., FUJIOKA, K., OKU, T., SUGA, M., SASAKI, Y., OHTA, T., YASUHARA, M., SUZUKI, K., YAMAMOTO, K., . (2004). Physicochemical properties oand cellular toxicity of nanocrystal

qduantum dots depend on their surface modification. *Nano Letters* **4,** 2163-2169.

HSYU, P., GISCLON, L., HUI, A., GIACOMINI, K.,. (1988). Interactions of organic anions with the organic cation transporter in renal BBMV. *American Journal of Physiology* **254,** F56-F61.

HUMPHREY, R., BEATTIE, G., LOPEZ, A., BUCAY, N., KING, C., FIRPO, M., ROSE-JOHN, S., HAYEK, A. (2004). Maintenance if pluripotency in human embryonic stem cells is a STAT3 independent. *Stem Cell* **22,** 522-530.

HUMPHREYS, B., VALERIUS, T., KOBAYASHI, A., MUGFORD, J., SOEUNG, S., DUFFIELD, J., MCMAHON, A., BONVENTRE, J., . (2008). Intrinsic Epithelial Cells Repair the Kidney after Injury. *Cell Stem Cell* **2,** 284-291.

ICHIKAWA, I., KUWUYAMA, F., POPEIV, J., STEPHENS, F., MIYAZAKI, Y., . (2002). Paradigm shift from classic anatomic theories to contemporary cell biological vews of CACUT. *Kidney International* **61,** 889-898.

IHCWORLD. (2009). **http://www.ihcworld.com/index.htm**.

ITO, T., SUZUKI, A., IMAI, E., OKABE, M., HORI, M. (2001). Bone marrow is a reservoir of repopulating mesangial cells during glomerular remodeling. *Journal of the American Society of Nephrology* **12,** 2625-2635.

JAMES, R., KAMEI, C., WANG, Q., JIANG, R., SCHULTHEISS, T. (2006). Odd-skipped related 1 is required for development of the metanephric kidney and regulates formation and differentiation of kidney precursor cells. *Development* **133,** 2995-3004.

JAMES, R., SCHULTHEISS, T. (2005a). Bmp signaling promotes intermediate mesoderm gene expression in a dose-dependent, cell-autonomous and translation - dependent manner. *Developmental Biology* **288,** 113-125.

JAMES, R., SCHULTHEISS, T. (2005b). Bmp signaling promotes intermediate mesoderm gene expression in a dose-dependent, cell-autonomous and translation - dependent manner. *Developmental Biology* **288,** 113-125.

JOHANSSON, B., WILES, M. (1995). Evidence for involvement of Activin A and Bone Morfogenetic Protein 4 in mammalian mesoderm and hematopoietic development. *Molecular and Cellular Biology* **15,** 141-151.

JONES, T. D., ULBRIGHT, T. M., EBLE, J. N., BALDRIDGE, L. A., CHENG, L. (2004). OCT4 staining in testicular tumors: a sensitive and specific marker for seminoma and embryonal carcinoma. *American Journal of Surgical Pathology* **28,** 935-940.

KAROUBI, G., GUGGER, M., SCHMID, R., DUTLY, A. (2009). OCT4 expression in human non-small cell lung cancer: implications for

therapeutic intervention. *Interactive CardioVascular and Thoracid Surgery* **8,** 393-397.

KAUFMANN, E., PAUL, H., FRIEDLE, H., METZ, A., SCHEUCHER, M., CLEMENT, J., KNOCHEL, W.,. (1996). Antagonistic actions of Activin A and BMP-2/4 control dorsal lip-specific activation of the early response gene XFD-1' in Xenopus laevis embryos. *The EMBO Journal* **15,** 6739-6749.

KAWANO, Y., KYPTA, R.,. (2003). Secreted antagonists of the Wnt signalling pathway. *Journal of Cell Science* **116,** 2627-2634.

KAZAMA, I., MAHONEY, Z., MINER, J., GRAF, D., ECONOMIDES, A., KREIDBERG, J., . (2008). Podocyte-Derived BMP7 Is Critical for Nephron Development. *Journal of the American Society of Nephrology* **19,** 2181-2191.

KELLER, G. (2005). Embryonic stem cell differentiation: emergence of a new era in biology and medicine. *Genes and Development* **19,** 1129-1155.

KIM, B., JIANG. W., OREOPOULOS, J., YIP, C., RUTKA, J., CHAN, W.,. (2008). Biodegradable Quantum Dot Nanocomposites Enable Live Cell Labeling and Imaging of Cytoplasmic Targets. *Nano Letters* **8,** 3887-3892.

KIM, D., DRESSLER, G. (2005). Nephrogenic factors promote differentiation of mouse embryonic stem cells into renal epithelia. *Journal of the American Society of Nephrology* **16,** 3527-3534.

KIMURA, H., TAKEDA, M., NARIKAWA, S., ENOMOTO, A., ICHIDA, K., ENDOU, H. (2002). Human Organic Anion Transporters and Human Organic Cation Transporters Mediate Renal Transport of Prostaglandins. *Journal of Pharmacology and Experimental Therapeutics* **301,** 293-298.

KINGSLEY, D. (1994). The TGF-beta superfamily: new members, new receptors, and new genestic tests of function in different organisms. *Genes Development* **8,** 133-146.

KIRCHNER, C., LIEDL, T., KUDERA, S., PELLEGRINO, T., JAVIER, A., GAUB, H., STOLZLE, S., FERTIG, N., PARAK, W.,. (2005). Cytotoxicity of colloidal CdSe and CdSe/ZnS nanoparticles. *Nano Letters* **5,** 331-338.

KOBAYASHI, A., KWAN, K., CARROLL, T., MCMAHN, A., MENDELSON, C., BEHRINGER, R. . (2005a). Distinct and seqential tissue-specific activities of the LIM-class homeobox gene Lim1 for tubular morphogenesis during kidney development, . *Development* **132,** 2809-2823.

KOBAYASHI, A., VALERIUS, M. T., MUGFORD, J. W., CARROLL, T. J., SELF, M., OLIVER, G., MCMAHON, A. P. (2008). Six2 Defines and Regulates a Multipotent Self-Renewing Nephron Progenitor Population throughout Mammalian Kidney Development. *Cell Stem Cell* **3,** 169-181.

KOBAYASHI, Y., OHBAYASHI, M., KOHYAMA, N., YAMAMOTO, T. (2005b). Mouse organic anion transporter 2 and 3 (mOAT2/3[Slc22a7/8]) mediates the renal transport of bumetanide *European Journal of Pharmacology* **524,** 44-48.

KODAIRA, K., IMADA, M., GOTO, M., TOMOYASU, A., FUKUDA, T., KAMIJO, R., SUDA, T., HIGASHIO, K., KATAGIRI, T. (2006). Purification and identification of a BMP-like factor from bovine serum. *Biochemical and Biophysical Research Communications* **345,** 1224-1231.

KOESTENBAUER, S., ZECH, N., JUCH, H., VANDERZWALMEN, P., SCHOONJANS, L., DOHR, G. (2006). Embryonic stem cells: similarities and differences between human and murine embryonic stem cells. *American Journal of Reproductive Immunology* **52,** 169-180.

KOSHMAN, Y., WATERS, S., WALKER, L., LOS, T., DE TOMBE, P., GOLDSPINK, P., RUSSELL, B.,. (2008). Delivery and visualization of proteins conjugated to quantum dots in cardiac myocytes. *Journal of Molecular and Cellular Cardiology* **45,** 853-856.

KRAMER, J., STEINHOFF, J., KLINGER, M., FRICKE, L., ROHWEDEL, J., . (2006). Cells differentiated from mouse embryonic stem cells via embryoid bodies express renal marker molecules. *Differentiation* **74,** 91-104.

KREIDBERG, J., SARIOLA, H., LORING, J., MAEDA, M., PELLETIER, J., HOUSMAN, D., JAENISH, R.,. (1993). WT-1 is required for early kidney development. *Cell* **74,** 679-691.

KUBO, A., SHINOZAKI, K., SHANNON, J., KOUSKOFF, V., KENNEDY, M., WOO, S., FEHLING, H., KELLER, G.,. (2004). Development of definitive endoderm from embryonic stem cells in culture. *Development and disease* **131,** 1651-1662.

KUME, T., DENG, K., HOGAN, B. (2000a). Murine forkhead/winged helix FoxC1 (Mf1) and FoxC2 (Mfh1) are required for the early organogenesis of the kidney and urinary tract. *Development* **127,** 1387-1395.

KUME, T., DENG, K., HOGAN, B. (2000b). Murine forkhead/winged helix genes FoxC1 (Mf1) and FoxC2 (Mfh1) are required for the early organogenesis of the kidney and urinary tract. *Development* **127,** 1387-1395.

KUNTER, U., RONG, S., BOOR, P., EITNER, F., MU¨ LLER-NEWEN, G., DJURIC, Z., VAN ROEYEN, C., KONIECZNY, A., OSTENDORF, T., VILLA, L., MILOVANCEVA-POPOVSKA, M., KERJASCHKI, D., FLOEGE, J.,. (2007). Mesenchymal Stem Cells Prevent Progressive Experimental Renal Failure but Maldifferentiate into Glomerular Adipocytes. *Journal of the American Society of Nephrology* **18,** 1754-1764.

LI, X., MENG, G., KRAWETZ, R., LIU, S., RANCOURT, D.,. (2008). The ROCK Inhibitor Y-27632 Enhances the Survival Rate of Human Embryonic Stem Cells Following Cryopreservation. *Stem Cells and Development* **17,** 1079-1086.

LIDKE, D., NAGY, P., HEINTZMAN, R., ARNDT-JOVIN, D., POST, J., GRECCO, H., JARES-ERIJMAN, E., JOVIN, T.,. (2004). Quantum dots ligands provide new insight into erb/HEB receptor-mediated signal transduction. *Nature Biotechnology* **22,** 198-203.

LIEDTKE, S., ENCZMANN, J., WACLAWCZYK, S., WERNET, P., KOGEL, G., . (2007). Oct4 and its pseudogenes confuse stem cell research. *Cell* **1,** 364-366.

LIN, F., CORDES, K., LI, L., HOOD, L., COUSER, W., SHANKLAND, S., IGARASHI, P. (2003). Hematopoietic stem cells contribute to the regeneration of renal tubules after ischemia-reperfusion injury in mice. *Journal of the American Society of Nephrology* **14,** 1188-1199.

LIN, S., XIE, X., PATEL, M., YANG, Y., LI, Z., CAO, F., GHEYSENS, O., ZHANG, Y., GAMBHIR, S., RAO, J., WU, . (2007). Quantum dot imaging for embryonic stem cells. *BMC Biotechnology* **7**.

LINDSLEY, C., GILL, J., KYBA, M., MURPHY, T., MURPHY, K. (2006). Canonical Wnt signalling is required for development of embryonic stem cell - derived mesoderm. *Development* **133,** 3787-3796.

LYONS, B. (2000). Analysing cell division in vivo and in vitro using flow cytometric measurement of CFSE dye dilution. *Journal of Immunological Methods* **243** 147-154.

MAESHIMA, A., SAKURAI, H., NIGAM, S. (2006). Adult kidney tubular cell population showing phenotypic plasticity, tubulogenic capacity, and integration capability into developing kidney. *Journal of the American Society of Nephrology* **17,** 188-198.

MAHERALI, M., SRIDHARAN, R., XIE, W., UTIKAL, J., EMINLI, S., ARNOLD, K., STADTFELD, M., YACHECHKO, R., TCHIEU, J., JAENISH, R., PLATH, K., HOCHEDLINGER, K. (2007). Directly reprogrammed fribroblasts show global epigenetic remodeling and widespread tissue contribution. *Cell Stem Cell* **1,** 55-70.

MAHLAPUU, M., ORMESTAD, M., ENERBACK, S., CARLSON, P. (2001). The forkhead transcription factor FoxF1 is required for differentiation of extraembryonic and lateral plate mesoderm. *Development* **128,** 155-166.

MAJUMDAR, A., VAINIO, S., KISPERT, A., MCMAHON, J., MCMAHON, A.P.,. (2003). Wnt11 and Ret/GDNF pathways cooperete in regulating ureteric bud branching during matanephric kidney development. *Development* **130,** 3175-3185.

MAKHULI, M. J., POLKOWSKI, C.A, GRASSL, S.M. (1995). Organic anion transport in rabbit renal basolateral membrane vesicles. *Journal of Pharmacology and Experimental Therapeutics* **273,** 146-153.

MALIN, D., KIM, I., BOETTICHER, E., KALIN, T., RAMARISHNA, S., MELITON, L., USTIYAN, V., ZHU, X., KALINICHENKI, V. (2007). Forkhead box F1 is essential for migration od mesenchymeal cells and directly induces integrin-beta3 expression. *Molecular and Cellular Biology* **27,** 2486-2498.

MANSERGH, F., DALY, C., HURLEY, A., WRIDE, M., HUNTER, S., EVANS, M. (2009). Gene expression profiles during early differentiation of mouse embryonic stem cells. *BMC Developmental Biology* **9**.

MARTIN, G. (1981). Isolation of a pluripotent cell line from early mouse embryos cultured in medium conditioned by teratocarcinoma stem cells. *Proceedings of the National Academy of Sciences* **78,** 7634-7638.

MASEREEUW, R., RUSSEL, F.,. (2001). Mechanisms and clinical implications of renal drug excretion. *Drug Metabolism Reviews* **33,** 299-351.

MAUCH, T., YANG, G., WRIGHT, M., SMITH, D., SCHOENWOLF, G.,. (2000). Signals from trunk paraxial mesoderm induce pronephrons formation in chick intermediate mesoderm. *Developmental Biology* **220,** 62-75.

MCADAMS, T., MILLER, W., PAPOUTSAKIS, T.,. (1996). Variations in culture pH affect the clonning efficiency and differentiation of progenitor cells in *ex vivo* haemopoiesis. *British Journal of Haematology* **97,** 889-895.

MISTELI, T., SPECTOR, D., . (1997). Applications of the green fluorescent protein in cell biology and biotechnology. *Nature Biotechnology* **15,** 961 - 964.

MOORE, A., MCINNES, L., KREIDBERG, J., HASTIE, N., SCHEDL, A. (1999). YAC complementation shows a requirement for WT-1 in the development of epicardium, adrenal gland and throughout nephrogenesis. *Development* **126,** 1845-1857.

MORIGI, M., IMBERTI, B., ZOJA, C., CORNA, D., TOMASONI, S., ABBATE, M., ROTTOLI, D., ANGIOLETTI, S., BENIGNI, A., PERICO, N., ALISON, M., REMUZZI, G.,. (2004). Mesenchymal stem cells are retinotrpic, helping to repaire the kidney and improve function in acute renal failure. *Journal of the American Society of Nephrology* **15,** 1794-1804.

MORIGI, M., ROTA, C., MONTEMURRO, T., MONTELATICI, E., LO CICERO V., IMBERTI, B., ABBATE, M., ZOJA, C., CASSIS, P., LONGARETTI, L., REBULLA, P., INTRONA, M., CAPELLI, C., BENIGNI, A., REMUZZI, G., LAZZARI, L.,. (2010). Life-Sparing Effect of Human Cord-Blood Mesenchymal Stem Cells in Experimental Acute Kidney Injury. *Stem Cells* **28,** 513-522.

MURRAY, P., EDGAR, D.,. (2000). Regulation of programmed cell death by basement membranes in embryonic development. *The Journal of Cell Biology* **150,** 1215-1221.

MURRAY, P., EDGAR, D.,. (2004). The topographical regulation of embryonic stem cell differentiation. *Philosophical Transactions of the Royal Society B* **359,** 1009-1020.

NAGY, A., GERTSENSTEIN, M., VINTERSTEN, K., BEHRINGER, R. (2003). *Manipulating the mouse embryo; a laboratory manual.* Cold Spring Harbor Laboratory Press, New York.

NAGY, A., ROSSANT, J., NAGY, R., ABRAMOW-NEWERLY, W., RODER, J.C. (1993). Derivation of completely cell culture-derived mice from early-passage embryonic stem cells. *Proceedings of the National Academy of Sciences* **90,** 8424-8428.

NICHOLS, J., SILVA, J., ROODE, M., SMITH, A. (2009a). Suppression of Erk signalling promotes ground state pluripotency in the mouse embryo. *Development* **136,** 3215-3222.

NICHOLS, J., SMITH, A. (2009b). Naive and primed pluripotent state *Cell Stem Cell* **4,** 487-492.

NIKSIC, M., SLIGHT, J., SANFORD, J., CACERES, J., HASTIE, D.,. (2004). The Wilms' tumour protein (WT1) shuttles between nucleus and cytoplasm and is present in functional polysomes. *Human Molecular Genetics* **13,** 463-471.

NISHINAKAMURA, R., MATSUMOTO, Y., NAKAO, K., NAKAMURA, K., SATO, A., COPELAND, N., GILBERT, D., JENKINS, N., SCULLY, S., LACEY, D., KATSUKI, M., ASASHIMA, M., YOKOTA, T. . (2001). Murine homolog of Sall1 is essential for ureteric bud invasion in kidney development. *Development* **128,** 3105-3115.

NORDSTRAND, A., NORGREN, M., FERRETTI, J., HOLM S., . (1998). Streptokinase as a mediator of acute post-streptococcal glomerulonephritis in an experimental mouse model. *Infection and Immunity* **66,** 315-321.

NOTARIANI, E., EVANS, M. (2006). Embryonic Stem Cells - practical approach. *Oxford University Press, New York,* 334.

OKITA, K., ICHISAKA, T., YAMANAKA, S. (2007). Generation of germline-competent induced pluripotent stem cells. *Nature* **448,** 313-318.

OLIVER, J., BARACH, J., YANG, J., HERZLINGER, D., AL-AWQATI, Q. (2002). Metanephric mesenchhyme contains embryonic renal stem cells. *American Journal of Physiology Renal Physiology* **283,** F799-F809.

OLIVER, J., MAAROUF, O., CHEEMA, F.H., MARTENS, T.P., AL-AWQATI, Q.,. (2004). The renal papila is a niche for adult kidney stem cells. *Journal of Clinical Investigation* **114,** 795-804.

OVITT, C., SCHO¨LER, H.,. (1998). The molecular biology of Oct-4 in the early mouse embryo. *Molecular Human Reproduction* **4,** 1021-1031.

PARISH, C. (1999). Fluorescent dyes for lymphocyte migration and proliferation studies. *Immunology and Cell Biology* **77,** 499-508.

PARK, J., VALERIUS, M., MCMAHON, P. (2007). Wnt/B-catenin signaling regulates nephron induction during mouse kidney development. *Development* **134,** 2533-2539.

PARKASH, V., LEPPA¨NEN, V., VIRTANEN, H., JURVANSUU, J., BESPALOV, M., SIDOROVA J., RUNEBERG-ROOS, P., SAARMA, M., GOLDMAN, A.,. (2008). The Structure of the Glial Cell Line-derived Neurotrophic Factor-Coreceptor Complex INSIGHTS INTO RET SIGNALING AND HEPARIN BINDING. *Journal of Biological Chemistry* **283,** 35164-35172.

PERIN, L., GIULIANI, S., JIN, D., SEDRAKYAN, S., CARRARO, G., HABIBIAN, R., WARBURTON, D., ATALA, A., DE FELIPPO, R. (2007). Renal differentiation of amniotic fluid stem cells. *Cell Proliferation* **40,** 936-948.

PFEFFER, P., PAYER, B., REIM, G., DI MAGLIANO, P., BUSSLINGER, M. . (2002). The activation and maintainance of Pax2 expression at the mid-hindbrain boundary is controlled by separate enhancers. *Development* **129,** 307-318.

POESCHLA, E., WONG-STAAL, F., LOONEY, D.,. (1998). Efficient transduction of nondividing human cells by feline immunodeficiency virus lentiviral vectors. *Nature Medicine* **4,** 354 - 357.

POULSOM, R., FORBES, S., HODIVALA-DILKE, K., RYAN, E., WYLES, S., NAVARATNARASAH, S., JEFFERY, R., HUNT, T., ALISON, M., COOK, T., PUSEY, C., WRIGHT, N. . (2001). Bone marrow contributes to renal parenchymal turnover and regeneration. *Journal of Pathology* **195,** 229-235.

PRITCHARD-JONES, K. (1999). The Wilms tumour gene, Wt-1, in normal and abnormal nephrogenesis. *Pediatric Nephrology* **13,** 620-625.

PRODROMIDI, E., POULSOM, R., JEFFERY, R., ROUFOSSE, C., POLLARD, P., PUSEY, C., COOK, T. (2006). Bone marrow-derived cells contribute to podocyte regeneration and amelioration of renal disease in mouse model of Alport Syndrome. *Stem Cells* **24,** 2448-2455.

PRUSA, A., MARTON, E., ROSNER, M., BERNASCHEK, G., HENGSTSCHLAGER, M., . (2003). Oct-4 -expressing cells in human amniotic fluid: a new source for stem cells research? *Human Reproduction* **18,** 1489-1493.

QIAO, J., UZZO, R., OBARA-ISHIHARA, T., DEGENSTEIN, L., FUCHS, E., HERZLINGER, D. (1999). FGF-7 modulates ureteric bud growth and nephron number in the developing kidney. *Development* **126,** 547-554.

RAGNARSON, B., BENGTSSON, L., HAEGERSTRAND, A.,. (1992). Labeling with fluorescent carbocyanine dyes of cultured endothelial and smooth muscle cells by growth in dye-containing medium. *Histochemistry and Cell Biology* **97,** 329-333.

RAZINKOV, V., MELIKYAN, G., COHEN, F. (1999). Hemifusion between Cells Expressing Hemagglutinin of Influenza Virus and Planar Membranes Can Precede the Formation of Fusion Pores that Subsequently Fully Enlarge. *Biophysical Journal* **77,** 3144-3151.

RIVERA-PEREZ, J., MAGNUSON, T. (2005). Primitive streak formation in mice is preceded by localized activation of Brachyury and Wnt3. *Developmental Biology* **288,** 363-371.

ROBERTSON, E. (1987). *Embryo-derived stem cell lines. In teratocarcinomas and embryonic stem cells; a protocal approach*. IRL Press Limited, Oxford.

ROGERS, S., LOWELL,J., HAMMERMAN, N., HAMMERMAN, M.,. (1998). Transplantation of developing metanephroi into adult rats. *Kidney International* **54,** 27-37.

RONCONI, E., SAGRINATI, C., ANGELOTTI, M. L., LAZZERI, E., MAZZINGHI, B., BALLERINI, L., PARENTE, E., BECHERUCCI, F., GACCI, M., CARINI, M., MAGGI, E., SERIO, M., VANNELLI, G. B., LASAGNI, L., ROMAGNANI, S., ROMAGNANI, P. (2009). Regeneration of glomerular podocytes by human renal progenitors. *Journal of the American Society of Nephrology* **20,** 322-332.

ROSEN, A., KELLY, D., SCHULDT, A., LU, J., POTAPOVA, I., DORONIN, S., ROBICHAUD, K., ROBINSON, R., ROSEN, M., BRINK, P., GAUDETTE, G., COHEN, I. (2007). Finding Fluorescent Needles in the Cardiac Haystack: Tracking Human Mesenchymal Stem Cells Labeled with Quantum Dots for Quantitative In Vivo Three-Dimensional Fluorescence Analysis. *Stem Cells* **25,** 2128-2138.

ROSINES, E., SAMPOGNA, R., JOHKURA, K., VAUGHN, D., CHOI, Y., SAKURAI, H., SHAH, M., NIGAM, S. (2007). Staged in vitro reconstitution and implantation of engineered rat kidney tissue. *Proceedings of the National Academy of Sciences* **104,** 20938-20943.

RUSSEL, F., MASEREEUW, R., VAN AUBEL R. (2002). Molecular aspect of renal anionic drug transport. *Annual Review of Physiology* **64**.

SAGRINATI, C., NETTI, S., MAZZINGHI, B., LAZZERI, E., LIOTTA, F., FROSALI, F., RONCONI, E., MEINI, C., GACCI, M., SQUECCO, R., CARINI, M., GESUALDO, L., FRANCINI, F., MAGGI, E., ANNUNZIATO, F., LASAGNI, L., SERIO, M., ROMAGNANI, S., ROMAGNANI, P.,. (2006). Isolation and characterisation of multipotent progenitor cells from the Bowman's capule of adult human kidney. *Journal of the American Society of Nephrology* **17,** 2443-2456.

SAJITHLAL, G., ZOU, D., SILVIUS, D., XU, P. . (2005). Eya1 acts as a critical regulator for specifying the metanephric mesenchyme. *Developmental Biology* **284,** 323-336.

SAKAI, R., SHIOZAKI, M., TABUCHI, M., ETO, Y. (1992). The measurement of activin/EDF in mouse serum: evidence for extragonadal

production. *Biochemical and Biophysical Research Communications* **188,** 921-926.

SASAKI, H., HOGAN, B. (1993). Differential expression of multiple fork head related genes during gastrulation and axial pattern formation in the mouse embryo. *Development* **118,** 47-59.

SAXEN, L. (1987). *Organogenesis of the kidney*. Cambridge University Press Cambridge-London_New York-Melbourne-Sydney

SECHRIST, J., COULOMBE, J., BRONNER-FRASER, M.,. (1989). Combined Vital Dye Labelling and Catecholamine Histofluorescence of Transplanted Ciliary Ganglion Cells. *Journal of Neural Transplantation* **1,** 113-128.

SIEBERTA, K., LORENZENB, M., BROWNC, S., PARKA, Y., BEEMAN, R., . (2008). Tubulin superfamily genes in Tribolium castaneum and the use of a Tubulin promoter to drive transgene expression *Insect Biochemistry and Molecular Biology* **38,** 749- 755.

SILVA, J., BARRANDON, O., NICHOLS, J., KAWAGUCHI, J., THEUNISSEN, T., SMITH, A., . (2008). Promotion of Reprogramming to Ground State Pluripotency by Signal Inhibition. *Public Library of Science: Biology* **6,** 2238-2247.

SIPIONE, S., ESHPETER, A., LYON, J., KORBUTT, G., BLEACKLEY, R.,. (2004). Insulin expressing cells from differentiated embryonic stem cells are not beta cells. *Diabetologia* **47,** 499-508.

SMYTH, N., VATANSEVER, S., MURRAY, P., MEYER, M., FRIE, C., PAULSSON, M., EDGAR, D., . (1999). Absence of basement membranes after targetting the *LAMC1* gene results in embryonic lethality due to failure of endoderm differentiation. *The Journal of Cell Biology* **144,** 151-160.

SOLANKI, A., KIM, J., LEE, K., . (2008). Nanotechnology for regenerative medicine: nanomaterials for stem cell imaging. *Nanomedicine* **3,** 567-578.

STARK, K., VAINIO, S., VASSILEVA, G., MCMAHON, A., . (1994). Epithelial transformation of metanephric mesenchyme in the developing kidney regulated by Wnt-4. *Nature* **372,** 679-683.

STAVRIDIS, M., SMITH, A.,. (2003). Neural differentiation of mouse embryonic stem cells. *Biochemical Society Transactions* **31,** 45-49.

STEENHARD, B., ISOM, K., CAZCARRO, P., DUNMORE, J., GODWIN, A., ST. JOHN, P., ABRAHAMSON, D. (2005). Integration of embryonic stem cells in metanephric kidney organ culture. *Journal of the American Society of Nephrology* **16,** 1623-1631.

STOJKOVIC, P., LAKO, M., PRZYBORSKI, S., STEWART, R., ARMSTRONG, L., EVANS, J., ZHANG, X., STOJKOVIC, M., . (2005). Human-serum matrix supports undifferentiated growth of human embryonic stem cells. *Stem Cells* **23,** 895-902.

STRACK, L., STRONGIN, D., BHATTACHARYYA, D., TAO, W., BERMAN, A., BROXMEYER, H., KEENAN, R., GLICK, B., . (2008). A noncytotoxic DsRed variant for whole-cell labeling. *Nature Methods* **5,** 955.

STRICKER, S., BRIESKE, N., HAUPT, J., MUNDLOS, S. (2006). Comparative expression pattern of Odd-skipped related genes Osr1 and Osr2 in chick embryonic development. . *Genes expression patterns* **6,** 826-834.

STRYER, L. (1995). *Biochemistry*. W.H.Freemann and Company, New York.

SUGIMOTO, H., GRAHOVAC, G., ZEISBERG, M., KALLURI, R., . (2007). Renal Fibrosis and Glomerulosclerosis in a New Mouse Model of Diabetic Nephropathy and Its Regression by Bone Morphogenic Protein-7 and Advanced Glycation End Product Inhibitors *Diabetes* **56,** 1825-1833.

SWEET, D., BUSH, K., NIGAM, S. (2001). The organic anion transporter family: from physiology to ontogeny and the clinics. *American Journal of Physiology Renal Physiology* **281,** F197-F205.

SWEET, D., CHAN, M., WALDEN, R., YANG, X., MILLER, D., PRITCHARD J.B.,. (2003). Organic anion transporter 3 (Slc22a8) is a dicarboxylate exchanger indirectly coupled to the Na+ gradient. *American Journal of Physiology Renal Physiology* **284,** F763-F769.

SWEET, D., ERALY, S., VAUGHN, D., BUSH, K., NIGAM, S. (2006). Organic anion and cation transporter expression and function during embryonic kidney development and in organ culture models. *Kidney International* **69,** 837-845.

SWEET, D., MILLER, D., PRITCHARD, J. (1999). Localization of an organic anion transporter-GFP fusion construct (rROAT1-GFP) in intact proximal tubules. *American Journal of Physiology Renal Physiology* **276,** 864-873.

TAGHIZADEH, R., SHERLEY, J.,. (2008). CFP and YFP, but Not GFP, Provide Stable Fluorescent Marking of Rat Hepatic Adult StemCells. *Journal of Biomedicine and Biotechnology*.

TAHARA, H., KUSUHARA, H., MAEDA, K., KOEPSELL, H., FUSE, E., SUGIYAMA, Y.,. (2006). Inhibition of OAT 3-mediated renal uptake as a mechanism for drug-drug interaction between fexofenadine and probenecid. *Drug Metabolism and Disposition* **34,** 743-747.

TAKAHASHI, K., YAMANAKA, S. (2006). Induction of pluripotent stem cells from mouse embryonic and adult fibroblast cultures by defined factors. *Cell* **126,** 663-676.

TAKASATO, M., OSAFUNE, K., MATSUMOTO, Y., KATAOKA, Y., YOSHIDA, N., MEGURO, H., ABURATANI, H., ASASHIMA, M., NISHINAKAMURA, R.,. (2004). Identification of kidney mesenchymal genes by a combination of micriarray analysis and Sall1-GFP knockin mice. *Mechanisms of Development* **121,** p: 547-557.

TAM, P., BEHRINGER, R. (1997). Mouse gastrulation:formation of a mammalian body plan. *Mechanisms of Development* **68,** 3-25.

TENG, L. H., LU, D. H., XU, Q. Z., FU, Y. J., YANG, H., HE, Z. L. (2005). Expression and diagnostic significance of OCT4, CD117 and CD30 in germ cell tumors. *Zhonghua Bing Li Xue Za Zhi.* **34,** 711-715.

TESAR, P., CHENOWETH, J., BROOK, F., DAVIES, T., EVANS, E., MACK, D., GARDNER, R., MCKAY, R. (2007). New cell lines from mouse epiblast share defining features with human embryonic stem cells. *Nature* **448,** 196-199.

THAKUR, A., FRADIN, C.,. (2005). Characterization of quantum dot behaviour in live mammalian cells. *Canadian Undergraduate Physics Journal* **3,** 7-12.

THOMSON, J., ITSKOVITZ-ELDOR, J., SHAPIRO, S., WAKNITZ, M., SWIERGIEL, J., MARSHAL, V., JONES, J., . (1998). Embryonic stem cell lines derived from human blastocysts. *Science* **282,** 1145-1147.

TONEGAWA, A., TAKAHASHI, Y.,. (1998). Somitogenesis controlled by Noggin. *Developmental Biology* **202,** 172-182.

TSAI, M., LEE, J., CHANG, Y., HWANG S., . (2004). Isolation of human multipotent mesenchymal stem cells from second-trimester amniotic fluid using a novel two-stage culture protocol. *Human Reproduction* **19,** 1450-1456.

UNBEKANDT, M., DAVIES, J.,. (2010). Dissociation of embryonic kidneys followed by reaggregation allows the formation of renal tissues. *Kidney International* **77,** 407-416.

VALTIN, H., SCHAFER, J.,. (1995). *Renal function* Little, Brown and Company, Boston/New York/Toronto/London.

VIGNEAU, C., POLGAR, K., STRIKER, G., ELLIOTT, J., HYINK, D., WEBER, O., FEHLING, H., KELLER, G., BURROW, C., WILSON, P. (2007). Mouse embryonic stem cell-derived embryoid bodies generate progeniors that integrate long term into renal proximal tubules in vivo. *Journal of the American Society of Nephrology* **18,** 1709-1720.

VIZE, P., SEUFERT, D., CARROLL, T., WALLINGFORD, J. (1997). Review: Model system for the study of kidney development: use of the pronephros in the analysis of organ induction and pattering. *Developmental biology* **188,** 189-204.

VIZE, P., WOOLF, A., BARD, J., . (2003). *The kidney, from normal development to congenital disease*. Academic Press Amsterdam-Tokyo.

VON BARTHELD, C., CUNNINGHAM, D., RUBEL, E. (1990). Neuronal Tracing with DiI: Decalcification, Cryosectioning, and Photoconversion for Light and Electron Microscopic Analysis. *The Journal of Histochemistry and Cytochemistry* **38,** 725-733.

VUGLER, A., CARR, A., LAWRENCE, J., CHEN, L., BURRELL, K., WRIGHT, A., LUNDH, P., SEMO, M., AHMADO, A., GIAS, C., DA CRUZ, L., MOORE,

H., ANDREWS, P., WALSH, J., COFFEY, P.,. (2008). Elucidating the phenomenon of HESC-derived RPE: Anatomy of cell genesis, expansion and retinal transplantation. *Experimental Neurology* **214,** 347-361.

WANG, Q., LAN, Y., CHO, E., MALTBY, K., JIANG, R. (2005a). Odd-skipped related (Odd1) is an essential regulator of heart and urogenital development. *Developmental Biology* **288,** 582-594.

WANG, Q., LAN, Y., CHO, E., MALTBY, K., JIANG, R., . (2005b). Odd-skipped related (Odd1) is an essential regulator of heart and urogenital development *Developmental Biology* **288** 582-594.

WANG, X., DUAN, X., LIU, L., FANG, Y., TAN, Y.,. (2005c). Carboxyfluorescein diacetate succinimidyl ester fluorescent dye for cell labeling. *Acta Biochim Biophys Sin (Shanghai)* **37,** 379-385.

WANG, Y., TAYLOR, D., . (1989). *Methods in cell biology*. Academic Press, , San Diego, California.

WATANABE, K., UENO, M., KAMIYA, D., NISHIYAMA, A., MATSUMURA, M., WATAYA, T., TAKAHASHI, J., NISHIKAWA, S., NISHIKAWA, S., MUGURUMA, K., SASAI, Y.,. (2007). A ROCK inhibitor permits survival of dissociated human embryonic stem cells. *Nature Biotechnology* **25,** 681-686.

WELLIK, D., HAWKES, P., CAPECCHI, M. (2002). Hox11 paralogus genes are essential for metanephric kidney induction. *Genes and Development* **16,** 1423-1432.

WERNIG, M., MEISSNER, A., FOREMAN, R., BRAMBRINK, T., KU, M., HOCHEDLINGER, K., BERNSTEIN, B., JAENISH, R. (2007). In vitro reprogramming of fibroblasts into a pluripotent ES-cell-like state. *Nature* **448,** 318-325.

WILLIAMS, L., HILTON, D., PEASE, S., WILLSON, T., STEWARD, C., GEARING, D., WAGNER, E., METCALF, D., NICOLA, N., GOUGH, N. (1988). Myeloid leukemia inhibitory factor maintains the developmental potential of embryonic stem cells. *Nature* **336,** 684-686.

WILM, B., JAMES, R., SCHULTHEISS, T., HOGAN, B.,. (2004). The forkhead genes, Foxc1 and Foxc2, regulates paraxial versus intermediate mesoderm cell fate. *Developmental Biology* **271,** 176-189.

WOOLF, A., PALMER, S., SNOW, M., FINE, L.,. (1990). Creation of functioning chimeric mammalian kidney. *Kidney International* **38,** 991-997.

XU, C., ROSLER, E., JIANG, J., LEBKOWSKI, J., GOLD, J., O'SULLIVAN, C., DELAVAN-BOORSMA, K., MOK, M., BRONSTEIN, A., CARPENTER, M.,. (2005). Basic Fibroblast Growth Factor Supports Undifferentiated Human Embryonic Stem Cell Growth Without Conditioned Medium. *Stem Cells* **23,** 315-323.

XU, P., ADAMS, J., PETERS, H., BROWN, M., HEANEY, S., MAAS, R.,. (1999). Eya1-deficient mice lack ears and kidneys and show abnormal apoptosis of organ primordia. *Nature Genetics* **23,** 113-117.

XU, P., WEIMING, Z., HUANG, L., MAIRE, P., LACLEF, C., SILVIUS, D. (2003). Six1 is required for the early organogenesis of mammalian kidney. *Development* **130,** 3085-3094.

YAMAMOTO, M., CUI, L., JOHKURA, K., ASANUMA, K., OKOUCHI, Y., OGIWARA, N., SASAKI, K. (2006). Branching ducts similar to mesonephric ducts or ureteric buds in teratomas originating from mouse embryonic stem cells. *American Journal of Physiology Renal Physiology* **290,** 52-60.

YANG, J., BLUM, A., NOVAL, T., LEVINSON, R., LAI, E., BARASCH, J. (2002). An epithelial precursor is regulated by the ureteric bud and by the renal stroma. *Developemntal Biology* **246,** 296-310.

YASUNAGA, M., TADA, S., TORIKAI-NISHIKAWA, S., NAKANO, Y., OKADA, M., JAKT, L., NISHIKAWA, S., CHIBA, T., ERA, T., NISHIKAWA, S. . (2005). Induction and monitoring of definitive and visceral endoderm differentiation of mouse ES cells. *Nature Biotechnology* **23,** 1542-1550.

YING, Q., STAVRIDIS, M., GRIFFITHS, D., LI, M., SMITH, A.,. (2003). Conversion of embryonic stem cells into neuroectodermal precursors in adherent monoculture. *Nature Biotechnology* **21,** 183-186.

YOKOO, T., OHASHI, T., SHEN, J., SAKURAI, K., MIYAZAKI, Y., UTSUNOMIYA, Y., TAKAHASHI, M., TERADA, Y., ETO, Y., KAWAMURA, T., OSUMI, N., HOSOYA, T. (2005). Human mesenchymal stem cells in rodent whole-embryo culture are reprogrammed to contribute to kidney tissues. *Proceedings of the National Academy of Sciences* **102,** 3296-3300.

YOSHINO, J., MONKAWA, T., TSUJI, M., HAYASHI, M., SARUTA, T.,. (2003). Leukemia Inhibitory Factor Is Involved in Tubular Regeneration after Experimental Acute Renal Failure. *Journal of the American Society of Nephrology* **14,** 3090-3101.

YU, J., MCMAHON, A., VALERIUS, T. (2004). Recent genetic studies of mouse kidney development. *Genetics and Development***,** 550-557.

YU, Z., QUINN, P.,. (1994). Dimethyl Sulphoxide: A review of its applications in cell biology. *Bioscience Reports* **14,** 259-281.

ZHANG, P., LI, J., TAN, Z., WANG, C., LIU, T., CHEN, L., YONG, J., JIANG, W., SUN, X., DU, L., DING, M., DENG, H. (2008). Short-term MBP4 treatment initiates induction in human embryonic stem cells. *Blood* **111,** 1933-1941.

ZHOU, J., YU, Z., ZHAO, S., HU, L., ZHENG, J., YANG, D., BOUVET, M., HOFFMAN, R.,. (2009). Lentivirus-Based DsRed-2-Transfected Pancreatic Cancer Cells for Deep In Vivo Imaging of Metastatic Disease. *Journal of Surgical Research***,** 1-8.

ZIMMERBERG, J., CHERNOMORDIK, L.,. (1999). Membrane fusion. *Advanced Drug Delivery Reviews* **38,** 197-205.